Order Number 9029991

A quantitative analysis of linear and nonlinear response characteristics of ganglion cells in the frog

Zaleski, Patricia Ann, Ph.D.

City University of New York, 1990

U·M·I
300 N. Zeeb Rd.
Ann Arbor, MI 48106

A QUANTITATIVE ANALYSIS OF LINEAR AND NONLINEAR RESPONSE CHARACTERISTICS OF GANGLION CELLS IN THE FROG

by

PATRICIA A. ZALESKI

A dissertation submitted to the Graduate Faculty in Psychology in partial fulfillment of the requirements for the degree of Doctor of Philosophy, The City University of New York.

1990

This manuscript has been read and accepted for the Graduate Faculty in Psychology in satisfaction of the dissertation requirement for the degree of Doctor of Philosophy.

4/24/90
date

Chairman of Examining Committee

4/27/90
date

Executive Officer

Dr. James Gordon

Dr. Stanley Novak

Dr. Richard L. Chappell

Dr. Daniel Tranchina

Dr. Vance Zemon

Supervisory Committee

The City University of New York

Abstract

A QUANTITATIVE ANALYSIS OF LINEAR AND NONLINEAR RESPONSE CHARACTERISTICS OF GANGLION CELLS IN THE FROG

by

Patricia A. Zaleski

Adviser: Professor James Gordon

The present study examined the functional properties of frog (Rana pipiens) ganglion cells, classified as X, Y and $\overline{X}$ (W-like) based upon criteria used in the cat. Extracellular recordings were obtained from 75 ganglion cells in the isolated eyecup preparation. These cells' responses, to a variety of spatial sinusoids, were Fourier analyzed into linear and nonlinear components.

While X, Y, and $\overline{X}$ cells in the frog displayed a number of essential similarities, regarding spatial summation, to their counterparts in the cat specific differences were noted. (1) Most frog X cells lacked the surround inhibition typical of cat X cells. (2) Unlike cat Y cells, frog Y cells did not produce frequency doubled responses until moderately high spatial frequencies were examined during the null test. (3) Frog Y cells could be further subdivided into two groups : Y1 and Y2. Y1 cells were characterized

by a nonlinear summating mechanism widely distributed throughout a large, homogeneous receptive field. The receptive fields of Y2 cells consisted of mutually antagonistic center and flanking regions with nonlinear components restricted to receptive field centers. A number of additional properties served to further distinguish between these subgroups.

Contrast dependent enhancement of responses to high temporal frequencies was observed in Y cells and, to a lesser degree, X cells suggesting the operation of a mechanism similar to the contrast gain control described in the cat. The form of this enhancement was, however, not identical to that observed in the cat. At low spatial frequencies, high contrasts typically produced shifts in the response's temporal phase without concomitantly affecting response amplitude. Only at high spatial frequencies did high contrasts affect both phase and amplitude response components.

The implications of these differences in terms of known functional and structural differences between cat and frog are discussed.

**This is dedicated to the memory of my mother,
Harriet Zaleski.**

Her unfailing belief that I could accomplish anything and everything, always made it impossible to ever consider 'giving up' a viable alternative.

ACKNOWLEDGEMENTS

The Dissertation - from the first experiment to the final draft of the thesis - is probably unlike any other experience a scientist will have in his or her career. This first, formal scientific endeavor is like an intellectual, emotional and physical roller coaster ride. There were times when one experiences the utmost satisfaction - often downright bliss - in one's work. The first day I successfully isolated a ganglion cell was such a time. There are few words to describe my excitement when I heard a cell firing in time to the stimulus and wateched as successive action potentials appeared on the oscilloscope. Then, there are times when one thinks that all is lost, that perhaps one doesn't have what it takes to be a scientist. Throughout all of this, there was always someone ready to help, give advice or provide moral support. These individuals softened the blows and accentuated the successes and, in general, affirmed that I was doing the right thing.

There was Jim Gordon, my thesis advisor, who transformed empty rooms into an electrophysiology lab, a frog colony, and a tadpole 'nursery' so that I could do my research. He gave me the freedom to learn at my own pace and to make the inevitable mistakes which always teach the most enduring lessons.

Then there were the other members of my committee: Stan Novack, Richard Chappell, Vance Zemon, and Dan Tranchina. They all had a very short time to read my thesis prior to the defense, yet each one graciously consented to doing so and each took great care to provide helpful feedback even though pressed for time.

There was Norman Milkman who was less than a phone call away when equipment problems reared their nasty little heads. I will always think of Norman as a knight in shining armor masquerading as a technical genius. Dirk Houben, always ready to patiently help me with programming glitches, equipment problems, and any other snafu that popped up, also provided a wise and sympathetic ear on many occassions. There was Robert L. Thompson - the modern Renaissance man - who could make me laugh when I didn't feel like it and make me think when I was convinced I had nothing left with which to think.

George Gourevitch - who had been a member of my original thesis committee until his death in 1987 - deserves a special mention. He always knew how to provide a healthy boost to my ego. I will miss his zest for life, the characteristically "George" mannerisms, and his Continental charm.

There were my friends Rosa Abreu, Su Boatright, Mary Conte, Linda Goodloe, Myra Joyce, and Molly Laird. Rosa, the best friend I could ever have more like a sister to me

than a friend, she was my most vocal cheerleader. Su Boatright who lovingly tended to my tadpoles when I was in Pennsylvania on 'weekend leave'. Mary Conte - one of the most competent scientists I have met and the only person I know who is as compulsive and neurotic as me - it was Mary who succeeded in convincing me of the worth of my research. Linda Goodloe and Molly Laird who generously provided me with homes away from home and who made the week seem to pass a little more quickly. Myra Joyce who frequently kept me sane by letting me go insane for a few minutes.

I would also like to thank Alan Rosenquist for being so patient and understanding while I finished my dissertation research before starting my postdoc with him.

A special thank you must go to my parents. All that I am is the result of their upbringing. They taught me that hard work and persistence had their benefits and this Dissertation is proof of that.

And then there is my husband, Kevin Kramer. How do I begin to thank him? Even though he was experiencing his own ups and downs of Internship and Residency he relished my highs and suffered my lows as strongly as though they were his own. He sat through innumerable 'mock defenses', read and reread what seemed like a thousand different versions of this manuscript, made special dinners for my arrival home on Friday nights and never waivered in his conviction that my research was worth any sacrifice. He

never once complained when I wasn't home for days on end. He always encouraged me, never letting me quit or even speak of it. I could not have asked for a more patient, understanding and loving husband. There is no doubt in my mind that the completion of my thesis could not have been done without him in my life.

TABLE OF CONTENTS

LIST OF FIGURES

LIST OF TABLES

1 INTRODUCTION

1.1 The Vertebrate Retinal Network

In vertebrates, information regarding light distribution present at the photoreceptor level is ultimately conveyed to the ganglion cells via a complicated process in which the direct chain of information transferal through bipolar cells interacts with signals provided by the laterally integrating horizontal and amacrine cells. Given the complexity of the cellular influences which ultimately impinge upon a single ganglion cell, it is intuitively apparent that such a network does not simply function to passively transmit a faithful reproduction of the light- dark pattern present at the photoreceptor mosaic. Analyses of optic nerve fiber responses to various stimuli substantiate this intuition. Indeed, even the activity of the optic nerve as a whole reveals that not all aspects of a stimulus are responded to with equal vigor; variation in the light array elicits maximal responsiveness whereas constant levels of illumination are poorly represented in the nerve's pattern of activity (Adrian and

Matthews, 1927).

The retinal network thus serves not only to transduce photic energy into neural impulses but also to encode it within a highly transformed message. How the retina accomplishes its highly specific transformation of visual stimuli is, essentially, a question of sensory coding. Barlow (1961, 1966) has suggested that sensory coding may function to reduce the redundancy present in the stimulus. More specifically, given a limited information capacity in sensory channels, these channels must reduce their responsiveness to aspects of the stimulus which represent redundancy in order to 'clear' the channels for non-redundant, and therefore, crucial features of the visual stimulus. Adrian's and Matthews' (1927) observation suggests that 'redundancy' may lie in the static features of the visual environment whereas changing components may signal crucial features.

Analyses of single ganglion cell responses have revealed numerous manifestations of selective responding reflecting this redundancy reduction mechanism. The earliest analyses of single optic nerve fibers in the vertebrate revealed a functional segregation into three classes: 'on', 'off', and 'on-off' ganglion cells (Hartline, 1938). These functional classes of ganglion cells appear to be, to a major extent, characteristic of the vertebrate retina in general (Kuffler, 1953; Hubel and

Wiesel, 1960). It should be noted that, disregarding the specific differences among the three cell types, all three reflect the same common principle of sensitivity to temporal change. The highest rate of responding occurs at either stimulus onset, offset, or both while, in general, the extended presence of the stimulus is signaled by a lower rate of sustained activity.

Over the last 20 years a much wider range of response properties than suggested by the distinction between 'on', 'off' and 'on-off' responses has been found (Enroth-Cugell and Robson, 1966; Hochstein and Shapley, 1976a; Stone and Hoffman, 1972). Much of this recent advance can be attributed to a particular set of analytic techniques and their underlying theoretical framework which emphasizes a quantitative examination of the input-output functions of a particular ganglion cell. These input-output functions are determined on the basis of the form of spatial summation (linear vs. nonlinear) exhibited by a cell. The most extensive application of these techniques has been in the study of the cat's retinal ganglion cells. It would seem natural, therefore, that these techniques be applied in the analysis of anuran ganglion cells since much of our understanding of general principles of the vertebrate retina was derived from studies in the frog (Hartline, 1938, 1940a, 1940b). Quantitative analyses of spatial summation in the frog are, however, at a preliminary stage

(Gordon and Shapley, 1978). One major reason for the paucity of comparative data in the frog stems from the viewpoint that frog ganglion cells function in a manner qualitatively different from that in mammals (Barlow, 1961, 1966). This opinion was based almost entirely upon the findings reported by Lettvin, Maturana, McCulloch, and Pitts (1959) who advanced the idea of "feature detectors" in the frog's retina. Although it has been suggested that the difference between frog and cat is most likely quantitative in nature (Kuffler, 1953), Lettvin et al.'s findings have had a tremendous impact upon subsequent studies of the anuran retina by determining, in effect, the techniques most of these studies would use to examine frog ganglion cells.

The research presented herein involves quantitative analyses of spatial summation in frog ganglion cells. In order to provide some background information so that the findings obtained in this study can be properly evaluated, relevant studies from diverse areas must be discussed. Firstly, much of what is known about functional properties of frog ganglion cells comes from studies utilizing the feature detector approach of Lettvin, Maturana, McCulloch and Pitts (1959). Thus, while these studies supply little information into the linearity of integration processes in the frog retina, they do provide a great deal of insight into the specifics of anuran retinal physiology. Secondly,

the techniques, and the utility of a quantitative approach must be discussed. Finally, the discussion of linear vs nonlinear spatial summation, and related response characteristics, will draw almost exclusively upon studies conducted in the cat. As a general introduction to these more specific aspects of this project, the following discussion is presented to summarize the nature of sensory encoding in the vertebrate retina.

1.2 The Anuran Retina

Many of the early findings regarding the operational characteristics of single retinal ganglion cells in the vertebrate were obtained in frogs (Hartline, 1938, 1940a, 1940b; Barlow, 1953a, 1953b). The Hartline classes of 'on', 'off', and 'on-off' fibers provide just one example of the comparative generality of retinal operations across vertebrate classes. A number of investigators, however, have chosen to focus upon the differences between mammalian and anuran retinal functions in their examination of response properties of anuran ganglion cells (Lettvin, Maturana, McCulloch, and Pitts, 1959; Lettvin, Maturana, Pitts, and McCulloch, 1961; Pomeranz, 1972; Pomeranz and Chung, 1970). Consequently, it has been proposed that the operations performed by the frog's retinal network are designed to transmit highly specific visual information -

passwords or features - whereas the mammalian retina is seen to be more flexible in its operation, which can be characterized by the redundancy reduction mechanism described earlier (Barlow, 1961, 1966). This view, that the frog's eye is doing something quite different from that of the cat, found its greatest advocacy in the work of Lettvin and his colleagues.

Although the qualitative differences between anurans and mammals, proposed by Barlow and suggested by the findings of Lettvin et al., belie the lack of qualitative differences in retinal anatomy the analysis of anuran visual functions in the years following Lettvin et al.'s influential paper has been almost exclusively limited to the examination of operations considered to be peculiar to frogs. Such a view tends, unfortunately, to militate against the examination of response properties in the frog according to classification schemes initially developed in the mammal such as the distinction between linear and nonlinear spatial summation.

1.2.1 Anuran Retinal Anatomy

The frog's retina, in terms of both cytoarchitectural organization and diversity of cell types, reflects the general structural arrangement present in all vertebrate retinae. While anuran modifications upon this basic scheme are not sufficiently extreme that they would render the

frog an unsuitable subject in an analysis which seeks principles of some comparative generality, quantitative differences from most other vertebrates do exist. These anatomical differences may, in turn, be manifested as functional differences. It should be noted that a comparative approach which emphasizes differences, in structure, function or both, as reflecting quantitative variations upon a basic theme provides a more fruitful approach to the determination of the structure/function relationship than does an approach which emphasizes a high degree of similarity (Bullock, 1984). If these differences, however, are not viewed as part of a comparative continuum which arises from evolutionary 'relatedness' and, therefore, as quantitative, but rather as reflecting qualitative differences among the vertebrate classes, the possibility of examining the full range of the structure-function relationship is essentially precluded.

As it is not the purpose of this dissertation to supply a comprehensive review of the literature regarding anuran retinal morphology, what follows is a brief review of observations which bear particular relevance to the evaluation of the question of comparative differences in the functional organization of the ganglion cell receptive field and its structural correlates. For additional information regarding the frog's retinal anatomy, excellent reviews by Dowling (1976) and Gordon and Hood (1976) are

recommended.

Early studies had suggested that the most notable difference between frogs and other vertebrates, in terms of retinal anatomy, was based upon differences in the inner plexiform layer (IPL) (Dowling, 1968; Dubin, 1970). The IPL in the frog, as in all other vertebrates, is thicker than the outer plexiform layer (OPL); in the frog, however, this increased thickness was found to be more pronounced than in most other vertebrates (Dubin, 1970). Dubin's electron micrographic analysis revealed that such gross differences in the IPL among vertebrates were traceable to quantitative variations in the synaptology of this layer across vertebrates. The exceptional thickness of the frog's IPL, therefore, reflected a higher number of synapses per unit area and an exceptionally robust amacrine cell participation as compared to other vertebrates.

This greater amacrine cell participation in the frog is apparently manifested in the following ways. Firstly, the transfer of information from bipolar to ganglion cell, in frogs, most frequently occurs indirectly, through an intervening amacrine cell. According to Dubin (1970) these indirect contacts accounted for 90% of the synapses examined in the frog whereas these synaptic arrangements comprised 70% of the cat's IPL synapses. Secondly, the presence of extensive serial synapses involving amacrines suggests that a high level of additional lateral processing

in the IPL exists in the frog (Dowling, 1968). These observations led both Dubin and Dowling to conclude that the IPL of the frog was more synaptically complex than that of the majority of mammals and that, furthermore, this anatomical complexity might provide the basis for the greater functional complexity in the anuran retina suggested by the findings of Lettvin and colleagues (1959). Recently a number of studies (Kolb and Famiglietti, 1974; Kolb and Nelson, 1981; Kolb, Nelson, and Mariani, 1981) have revealed that the IPL of the cat is not as simple, in terms of structure, as the earlier studies might suggest. Kolb, Nelson and Mariani, for example, have reported the existence of 22 different types of amacrine cell and 23 classes of ganglion cell in the cat retina. While this study does not suggest that Dubin had underestimated the number of amacrine mediated synapses in the cat, it does emphasize that the role of amacrines in retinal processing in the cat is much more complex than indicated by comparing the ratio of direct to indirect synapses across vertebrates. These recent findings also indicate that the term 'complexity', when used in a comparative sense, must be used carefully since different forms of structural complexity may be hallmarks of different vertebrate classes.

1.2.2 Functional Properties of Frog Ganglion Cells

For the past 35 years, it was believed that the mutual center/surround antagonism, characteristic of the mammalian ganglion cell's receptive field (RF) organization (Kuffler, 1953), was absent in the frog (Barlow, 1953b). Instead, the surround component of the RF of frog ganglion cells was considered to function in a purely suppressive way. Stimulation of the surround inhibited center elicited activity but did not result in surround generated impulses as in mammals; hence, the term 'silent surround' was used to characterize this RF component in frogs. To clarify discussions regarding the RF organization of anuran ganglion cells, the center is often referred to as the excitatory RF (ERF) and the silent surround is termed the inhibitory RF (IRF) to emphasize the purely inhibitory effects of the latter in frogs (Grusser and Grusser-Cornehls, 1976). This difference in RF organization between cat and frog was cited by Kuffler (1953), perhaps prematurely, as indicative of wider flexibility in the encoding operations performed by mammalian ganglion cells as compared to those of amphibians. This view was based on the fact that, given mutual center/surround antagonism, the entire range of Hartline response types can be elicited within a single ganglion cell in the cat depending upon the locus of stimulation. In an on-center cell, for example,

'on' and 'off' responses will be evoked by stimulation of the center and surround regions, respectively, and 'on-off' responses will be elicited when the center/surround boundary is stimulated.

Recent studies (Donner and Gronholm, 1984; Stirling and Merrill,1987), however, have revealed that a responsive surround is, in fact, characteristic of a substantial number of frog ganglion cells. Keating and Gaze (1970) had earlier found that responses could be elicited from the surrounds of a few 'off' cells but could not entirely rule out the possibility that light scatter may have inadvertently stimulated the center. By carefully compensating for light scatter and using narrow annuli to stimulate the surround, the RF organization of frog ganglion cells proves to be exceptionally complex (Donner and Gronholm, 1984). A number of observations made by Donner and Gronholm led them to conclude that two, independent surround mechanisms may exist within a single RF: a responsive surround as well as the classic IRF or purely suppressive surround. Because these two surround components are spatially coextensive, inhibition from the IRF, which has a wider spatial extent than the responsive surround, would completely suppress the responsive surround when a large stimulus is used to map the RF. This would account for the fact that surround responses were not observed in previous studies which employed large annuli or

spots of increasing diameters to examine surround mediated effects.

The RF organizations of both frog and mammalian ganglion cells, therefore, suggest comparable flexibility at the level of the individual ganglion cell. Other functional properties of the RF in the frog display a number of similarities to those reported in the cat. For example, the extent of the RF of a given ganglion cell in the frog is dynamically related to a number of factors: level of adaptation, stimulus size, and stimulus intensity (Hartline, 1938). These factors display similar influences upon RF size in mammals (Kuffler, 1953; Barlow, Fitzhugh, and Kuffler, 1957; Kaplan, Marcus, and So, 1979).

'On-off' ganglion cells in the frog retina have no direct parallel in the mammalian retina given Kuffler's model of the RF. In the frog, both 'on' and 'off' response components result from stimulation of the center of the RF (Barlow, 1953b). The 'on' and 'off' components are aligned within the center although they differ slightly in their spatial extent. Thus, the relative strength of the two response components depends somewhat upon the specific region of the center which is stimulated by a small spot of light. In the cat, 'on-off' responses were initially considered to result solely as a combination of antagonistic center and surround responses (Kuffler, 1953). More recently, however, a class of cat ganglion cells, the

phasic 'on-off' W cells (Stone and Fukada, 1974), were found which are analogous to frog 'on-off' cells in terms of the RF components responsible for generating 'on' and 'off' responses. W cells will be discussed in greater detail in a subsequent section (1.5).

Differences in the level of spontaneous discharge also serve to distinguish between frog and cat retinal ganglion cells. Frog retinal ganglion cells are typically characterized by a low rate of spontaneous activity (Barlow, 1953b). Mammalian ganglion cells, on the other hand, have a high level of spontaneous discharge (Kuffler, 1953).

1.2.3 Feature Detectors

As noted earlier, Barlow's (1961, 1966) position that anuran retinal operations may be qualitatively different from those in mammals was based upon the work of Lettvin et al. (1959). Lettvin and his colleagues suggested that frog ganglion cells were even more selective in their response properties than suggested by Hartline's 'on', 'off', 'on-off' classification. Adopting an approach which emphasized the relationship between sensory selectivity and the ecology of the frog, Lettvin et al. recorded the response of optic nerve fibers in the frog to various stimuli chosen on the basis of their similarity to objects which might be of some relevance to the frog's survival. The authors

found that at least four classes, or operations, (and an additional unspecified group of cells) could be distinguished according to differences in responsiveness to relatively complex aspects or features of a stimulus.

In the discussion which follows, the terms used in Lettvin et al.'s original paper to describe these operations are maintained. However, as somewhat different terms were employed in subsequent papers (Maturana, Lettvin, McCulloch and Pitts, 1960, 1961), the latter ones are provided in parentheses in order to avoid any confusion.

Class I fibers, the 'sustained contrast detectors' (boundary detectors), responded best to an edge lying in sharp contrast to its background, and were unresponsive to changes in ambient illumination. The response was sustained for the duration of the stimulus. The sharpness of the boundary between the object and the background, rather than amount of contrast, appeared to be the most critical factor in determining the response.

The class II optic fibers, labelled 'net convexity detectors' (movement-gated, dark convex boundary detectors), were similarly unresponsive to variations in ambient illumination. The specific feature for these cells appeared to be the amount of convexity possessed by the object; thus, corners as opposed to straight edges elicited the highest rate of discharge. Movement was also an

important variable in determining rate of discharge. "Jerky" movements along a centripitally oriented path were especially effective. These cells also responded best to small objects less than three degrees in extent.

Class III fibers responded best to edges moved across their RF, hence the term 'moving edge detectors' (moving or changing contrast detector) was used to characterize these cells. According to Lettvin et al., these cells were identical to Hartline's 'on-off' cells which Barlow (1953b) had earlier noted as being especially well designed to detect movement.

The last well defined class, the class IV or 'net dimming detectors', possessed RFs much larger than those of the first three classes. Discharge from these cells was proportionally, but inversely, related to illumination. These cells thus appear identical to Hartline's 'off' cells.

There was also a fifth group of cells, left unclassified, which appeared to transmit information regarding the absolute level of 'darkness' over a large area.

While classes III and IV are easily identified with two of Hartline's classes, neither class I nor II cells are so clearly related. Furthermore, no cells were observed which could be identified as Hartline's 'on' cells. It is possible that recording from optic fiber terminations in

the tectum, as Lettvin et al. did in the majority of their tests, may have precluded recording from 'on' cells which presumably project to diencephalic structures (Muntz, 1962). This explanation, however, does not account for the absence of typical 'on' responses in the few optic nerve recordings reported by Lettvin et al. nor does it explain the absence of an anatomical group of cells which might correspond to 'on' cells in subsequent histological analyses performed by Lettvin et al. (1961).

In 1961, Lettvin et al. proposed that each of their functional classes could be related to one of five anatomical types of ganglion cells, which by virtue of differences in the stratification of their dendritic arbors, might differ in terms of bipolar input. Cajal (1893), using criteria similar to those later employed by Lettvin and his colleagues as well as additional guidelines, had earlier identified 11 different structural classes of ganglion cells. This suggests that, if a clear anatomical-functional relationship exists, not only are there more structural classes than proposed by Lettvin et al. but there should also be a much larger range of response types than simply four or five feature detector operations.

1.2.4 Wavelength Sensitivity

Experiments which analyze the response of ganglion cells in the frog to various wavelengths of light reveal a wider response range within a single ganglion cell than that suggested by studies using black or white stimuli. For example, the Lettvin et al. class IV cells, corresponding to Hartline's 'off' cells, revealed 'on' responses to short wavelengths and 'off' at longer wavelengths thus suggesting that these cells are actually 'on-off' cells with an opponent color organization (Backstrom and Reuter, 1975; Reuter and Virtanen, 1972). The presence of spectral opponency in the response of class IV fibers is also substantiated by the observation that the 'chromatic response curve' of a class IV neuron is typical of a neuron which possesses an opponent color organization (Grusser-Cornehls and Saunders, 1981). This observation regarding class IV fibers does not reflect an isolated occurrence; rather, it appears that a large number of ganglion cells in the frog possess some form of the chromatic antagonism observed in the ganglion cells of other vertebrates (Reuter and Virtanen, 1972).

Consideration of spectral opponency also reveals the existence of subclasses, based upon differences among their spectral response curves, within at least the first three of the Lettvin et al. classes (Grusser-Cornehls and

Saunders, 1981). This suggests that the number of functional cell types, in the frog, may better correspond to the range of morphological types identified by Cajal.

1.2.5 Movement Sensitivity

Finally, some brief mention of directional selectivity in frog retinal ganglion cells should be made. While the form of directional selectivity in anurans is not as finely tuned as that seen in pigeons (Maturana and Frenk, 1963), a substantial fraction of both class I and II cells in Rana temporaria display directional selectivity (Backstrom, Hemila, and Reuter, 1978). Some class III cells in Rana pipiens have also demonstrated directional selectivity (Lettvin, Maturana, McCulloch, and Pitts, 1959). For cells which exhibit directional selectivity, there exists an optimal direction of movement; trajectories along directions other than this elicit little or no activity from these cells. Backstrom et al. have proposed that such directional selectivity in the frog may result from anisotropies in an amacrine mediated IRF.

Both chromatic opponency and directional selectivity reveal additional properties of the responsiveness of the frog's ganglion cell. It is difficult, therefore, to reconcile a purely qualitative distinction, based upon relatively simple stimulus features, among ganglion cells in the frog with the wide range of stimulus parameters

which affect the activity of a ganglion cell. This point will be further explored in the next section.

1.3 Feature Detection in the Anuran Retina A Reevaluation

Statements that class II fibers are well designed to detect flies or that class IV cells may serve to detect large predators (Lettvin, Maturana, McCulloch, and Pitts, 1959; Ingle, 1968, 1971) have suggested a correspondence, which may not be justified, between the function of a ganglion cell and its response properties. Such statements typify a feature detector approach which suggests that frog ganglion cells are sharply tuned and function to detect and transmit 'password' information. The following critical examination of the literature therefore addresses the utility of a feature detector approach, in general, and of the Lettvin et al. classification scheme, in particular, as a method of analyzing the functional characteristics of the frog's retinal network.

By expressing a sensory cell's function in terms of some "optimal" stimulus - whereby "optimal" is based upon the stimulus' ability to elicit a maximal firing rate - very little insight has been gained into the encoding operations performed by that cell. Does, for example, the labelling of a cell as a 'convex edge' detector indicate that the cell functions solely to signal the presence of

such a stimulus? A number of observations suggest that such labels represent a gross oversimplification of the function of retinal ganglion cells in anura. Firstly, Grusser and Grusser-Cornehls (1968) have found that a wide range of stimuli can elicit some activity from each cell class, thereby suggesting that none of these cell classes are as sharply tuned as their feature labels imply. Furthermore, quantitative analyses performed upon each of the Lettvin et al. classes reveals that, for any given stimulus, a vast range of parameters, in addition to their 'feature', will affect the responsiveness of frog ganglion cells (Grusser and Grusser-Cornehls, 1976). It is, in fact, naive to assume that the information transmission characteristics of a single cell are so limited that only a high rate of firing is used as the 'message'. The information potential in a single anuran ganglion cell may be carried not only by the number of impulses emitted but also by their temporal distribution (Chung, Raymond and Lettvin, 1970).

The notion of specific features or passwords further suggests that ganglion cells in the frog pass specific information which would be used to choose an appropriate response from the frog's relatively limited behavioral repertoire. While there is a general indication that activity, for example, in class II fibers tends to result in feeding behaviors (Ingle, 1968), Grusser and Grusser-

Cornehls (1968), as noted previously, have demonstrated a less than clear cut relationship between activity within ganglion cell classes and stimuli representing various ecologically relevant objects. Indeed, careful examination of the behavioral data, according to Muntz (1977), reveals that "In many cases behavior patterns depend on the characteristics of the stimulus in ways that are much more complex than would be expected from our knowledge of the retinal ganglion cells" (p.286).

Given these considerations, it is apparent that the information transmitted by a single class of frog ganglion cells cannot be described according to a simple, qualitative or password terminology. As Gordon and Hood (1976) have noted, a view that different ganglion cells are performing qualitatively different operations is completely dependent upon a high degree of mutual exclusiveness among these cell classes in terms of their sensitivity to stimuli. Are the Lettvin et al. classes mutually exclusive? Gordon and Hood suggest that they are not. Less than clear cut differences are observed, for example, between class I and II fibers in terms of optimal stimuli (Gaze and Jacobsen, 1963). Furthermore, all classes, according to Gordon and Hood, are especially sensitive to a single stimulus feature - a change in contrast - suggesting that the specific sensitivities of each class represent a continuum of responses to contrast variation. In fact, as

the full range of response types in frog ganglion cells is explored through the examination of chromatic properties (Grusser-Cornehls and Saunders, 1981), determinations of velocity functions (Grusser, Grusser-Cornehls, and Licker, 1968), and quantitative analyses of the relative contributions of the ERF and IRF to responding (Grusser-Cornehls, Grusser, and Bullock, 1963), the operations performed at the level of the retina in the frog appear more commensurate with the type of retinal function observed in mammals. As seen earlier, all vertebrate optic fibers are highly sensitive to change, a fact which corresponds well to Barlow's notion of redundancy reduction in the mammalian retina. Given Gordon and Hood's view, that change in contrast supplies the crucial determinant of responding in all frog ganglion cells, it appears that the frog's retina is performing a characteristically 'mammalian' operation of reducing redundancy, although perhaps in a somewhat modified fashion.

The qualitative functional distinctions assumed in Lettvin et al.'s classification also possess little utility in terms of generating hypotheses regarding possible mechanisms which might underly the differences in responsiveness among cells. In their 1960 paper, Maturana, Lettvin, McCulloch and Pitts, perhaps in anticipation of this criticism, recognized and defended the lack of predictive utility in their classification scheme. They

admit that quantitative analyses are required in order to examine underlying synaptic mechanisms, but aver that quantitative distinctions among ganglion cells, rather than the qualitative distinctions upon which their groupings are based, " is, at present, likely to be misleading and to miss the biological point" (p.160).

While the "biological point" refers to the importance of understanding unique species adaptations the very lack of viable hypothesis regarding structural or physiological mechanisms militates against understanding the manner in which retinal mechanisms in the frog might differ from other vertebrates. As noted earlier, possible differences between mammals and anura, with regard to retinal structure, are most likely quantitative - a fact which is difficult to reconcile with the notion that the frog's eye does something qualitatively different than that of the cat.

1.4 An Alternative Approach
Analysis of Transformational Properties

An alternative to the feature detector approach, and the approach adopted in this dissertation, examines the input/output function of the retinal network in a quantitative fashion. Such a view assumes that the choice of stimuli is, on one hand, arbitrary and, further, that the effectiveness of a stimulus in evoking a response does

not designate that stimulus as the single, eliciting feature for that cell. The essential task of analysis, therefore, according to this approach is to discover the transformational processes which lie between the input and output poles of the retinal network (Robson, 1975). The continuum of responsiveness, as it depends upon the quantitative variation in stimuli, must therefore be examined.

In the analysis of these transformational 'codes', the only guidelines employed in the choice of the stimulus are based upon practical considerations related to the ease of input/output determinations. Thus, the optimal stimulus is one which is simple in its mathematical characterization. While complex stimuli such as 'buglike objects' when employed according to this approach can be considered arbitrary, these stimuli, like the spots and annuli of light used in other studies, are highly complex, which render input/output determinations herculean tasks of mathematical analyses. What is required, therefore, is a simple stimulus which allows for a precise characterization of the input which, in turn, may be related more easily to the output, thus leading to an elucidation of the transformational rules employed by the ganglion cell. One such stimulus - a sinusoidal modulation of luminance - was the stimulus employed in the present study and therefore is described in detail in the following section.

1.4.1 Sinusoidal Stimulation

In theory, the manner in which light is distributed in the retinal image is, in its simplest form, characterized by a sine wave function (Maffei and Fiorentini, 1973); that is, intensity is sinusoidally modulated as a function of space. Given this it is possible, according to the Fourier theorem, to view any complex pattern of light as being composed of an infinite number of sine waves or sinusoids. Whereas the Fourier theorem has been applied in the analysis of acoustic stimuli in the examination of auditory physiology with excellent results by Helmholtz and successors, the extension of this approach to the analysis of visual physiology has been a relatively recent development (Stark and Sherman, 1957).

A sinusoidal, spatial modulation of intensity appears as a grating pattern in which adjacent dark and bright regions appear to gradually alternate across space. This can be contrasted, for example, with a square wave grating pattern in which spatial alternation occurs as abrupt changes among bright and dark bars.

A sinusoidally modulated stimulus possesses a number of parameters which may be manipulated independently. If the sine wave stimulus is a modulation of intensity in the spatial domain, as in Figure 1, the number of cycles of intensity alternation per visual degree defines the spatial

Figure 1

Sinusoidal variation in intensity as a function of space in millimeters.

Sinusoidal Variation in Intensity As a Function of Space

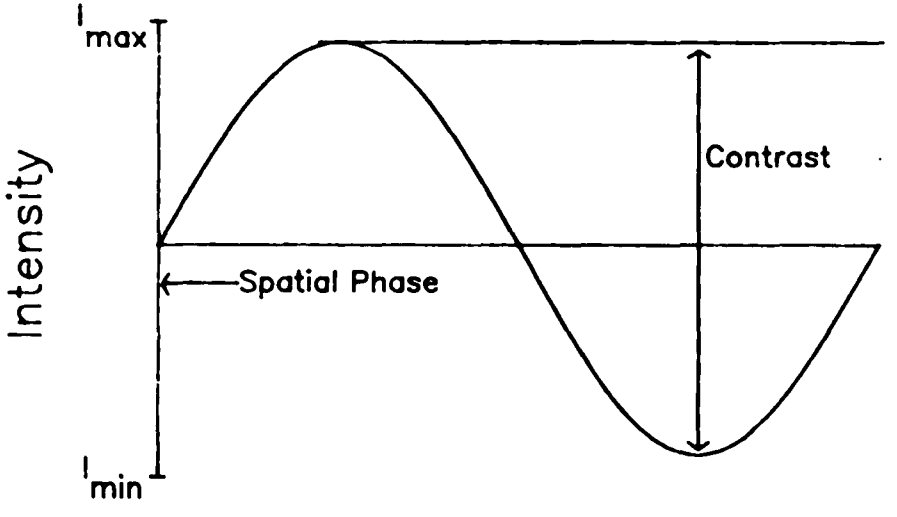

frequency of the stimulus. Sinusoidal modulation of intensity can also be performed in the temporal domain; in this case the number of complete alternations in intensity per second defines the temporal frequency.

The peak to peak modulation of amplitude specifies the contrast which is defined as ((Imax-Imin) / (Imax+Imin)) where Imax and Imin refer to maximal intensity and minimal intensity, respectively. Finally, the position of the grating relative to the RF of a ganglion cell represents the spatial phase angle of the grating. Different phase angles will result in different distributions of intensity across the RF, a fact which lies as the cornerstone of Enroth-Cugell's and Robson's (1966) analysis of linear and nonlinear spatial summation.

The basic sine wave grating pattern may be subjected to a number of additional variations. A sine wave grating may be allowed to drift across a cell's RF at various velocities or temporal frequencies. These drifting gratings, therefore, afford the opportunity to obtain a continuous record of the response of the cell to all phase angles of the grating. The contrast of a stationary grating may be allowed to reverse according to a sinusoidal temporal function producing what is called a 'contrast reversal grating'. During one complete temporal cycle of contrast reversal adjacent bars gradually alternate in intensity. Thus, the mean intensity of the grating is

maintained at a constant value while the spatiotemporal distribution is altered. Contrast can also be temporally modulated according to a square wave function in which case the intensity of adjacent regions alternates in an abrupt fashion.

The facility of determining input/output functions afforded by this stimulus has resulted in its utilization in many different analyses of the functional aspects of the visual system. For example, on- and off-center ganglion cells in the cat have been re-examined in terms of their phase relationship to temporal variations in the stimulus (Hughes and Maffei, 1966). Some researchers have also employed sinusoidal stimuli, according to an approach similar to feature detection, to advance the notion that the visual system operates to detect different spatial frequency components of the stimulus (Campbell and Robson, 1968). While the data suggest that the visual system can perform such analyses, Maffei and Fiorentini (1973) caution that this does not necessarily mean that the visual system actually makes use of this information. Furthermore, such studies run the same inherent problems of interpretation, noted previously, for qualitative distinctions among sensory fibers in feature detection models.

Sinusoidal stimuli are especially efficacious when transformational processes are examined for linear and nonlinear components. A sensory system, as an electrical

circuit, can be analyzed for linear transformations according to how well the transform can be described by linear equations (Kaufman, 1974). To classify a system as linear the system's operation must conform to the principles of superposition and homogeneity. The principle of superposition states that the response of the system to a complex stimulus should be equal to the sum of that system's responses to individually presented components of the complex stimulus. The system must also obey the principle of homogeneity: the amount of change in magnitude of the input or stimulus should result in an equal amount of change in the magnitude of the output or response without causing any additional or fortuitous perturbations in the output. For a more complete discussion of these principles and their implications, the reader is referred to Moore (1982).

If a system operates linearly it will display at its output the frequency of the input sinusoid, i.e., the fundamental or first harmonic. Any nonlinearities in the system will be evidenced by the appearance of frequencies, not present in the input signal, which occur as multiples (or harmonics) of the input frequency. The determination of linearity in response to a complex stimulus is complicated by the presence of a number of frequencies within the input. The utilization of a single sinusoid as the input, therefore, avoids such complexities of analysis.

While the determination of the relationship between input and output, when using a single sinusoid as the stimulus, is theoretically simple, examination of the cell's response for the presence of harmonics requires that the response be subjected to Fourier analysis. Fourier analysis of a ganglion cell's response involves, essentially, an examination of the correspondence between the variation in response amplitude (impulses per second) and the temporal sinusoidal variation in the stimulus.

By plotting the cell's response amplitude as a function of spatial frequency - the modulation transfer function (MTF) - the degree to which a cell can 'transmit' a range of spatial frequencies can be determined. A similar transfer function can be obtained when the variation in input is temporal rather than spatial. Both transfer functions essentially reflect the transformational processes of the cell. If the cell operates in a linear fashion, based on the principle of superposition, it is possible to predict that cell's response to any complex configuration through a process known as convolution. This process involves the analysis of the stimulus into its component sinusoids which are then individually 'adjusted' according to the cell's MTF. The 'adjusted' sinusoids are then recombined and can be used to predict that cell's response to the original stimulus.

As cells with nonlinear summation do not conform to

the principle of superposition, the response to complex stimuli cannot be predicted with the same sort of facility as seen with linear cells. The range of the cell's transformational properties are dependent on both the extent and nature of the nonlinear components of the cell's responsiveness. The quantitative analyses afforded by sinusoidal stimulation and the Fourier theorem provides for a clear exposition of the transformational capacity of cells with nonlinear summation.

1.5 Classification of Cells Based on the Distinction Between Linear and Nonlinear Spatial Summation

Earlier analyses of ganglion cells in which spots of light were employed as stimuli suggested that spatial summation in ganglion cells might, on occasion, deviate from linearity as defined by Ricco's law (Hartline, 1940; Barlow, 1953). The deviations, however, were considered to represent a saturating type of nonlinearity. Linear integration, therefore, was considered the rule. The model proposed by Rodieck and Stone (1965) to describe the functional RF organization of cat retinal ganglion cells, for example, assumes linear summation. Rodieck's and Stone's assumption of linear integration of excitatory and inhibitory processes, however, has proven inadequate to explain the generation of 'on-off' responses (Gordon and Graham, 1973).

In 1966, by using sinusoidal spatial gratings and by defining spatial summation in a less restricted fashion than that embedded in Ricco's law, Enroth-Cugell and Robson demonstrated that nonlinear spatial summation was an essential property of a number of cells. When these gratings were alternately introduced and withdrawn, Enroth-Cugell and Robson observed that two groups of cat retinal ganglion cells could be distinguished based on their mode of response to different phase angles of the grating. These response differences, in turn, reflected the difference between linear and nonlinear spatial summation.

For one group of cells - labelled 'X' cells by the authors - a phase angle could be found such that the presentation of the grating elicited no change in response from baseline activity, i.e., a 'null' response. At this phase angle, the null position, increases and decreases in illuminance are distributed symmetrically about the center of the RF. As no response was obtained at this phase angle the authors concluded that signals opposite in polarity but of equal magnitude summated in a linear fashion thereby cancelling one another. Such an observation reflects a maintenance of the principle of superposition, one requisite for linear performance. If the phase angle of the grating is shifted 90 degrees to either the right or left of this null position, the cell's RF receives either the decreasing portion of the luminance cycle or the

increasing portion. These phase angles resulted in maximal changes in responding from baseline in the X cell and, hence, were referred to as 'peak' positions.

The other group of cells - labelled Y cells - appeared to summate signals in a nonlinear fashion. For Y cells, therefore, no null position could be found. In fact, phase angles that normally resulted in null responses in X cells elicited two bursts of discharges from Y cells: the first to the introduction of the grating and the second to its withdrawal.

When the responses of X and Y cells were subjected to Fourier analysis (Hochstein and Shapley, 1976a), the X cell's response was found to be dominated by a fundamental (linear) component whereas the Y cell's response possessed both a fundamental and a nonlinear, mostly second harmonic, component. The sensitivity of the fundamental component of both the X and Y cells displayed a sinusoidal dependence upon spatial phase of the grating, a further indication of linear spatial summation. The second harmonic component of the Y cell, however, was insensitive to the grating's phase, thus accounting for the inability to find a null position for the Y cell.

When a contrast reversal grating was employed (Hochstein and Shapley, 1976a, 1976b) in a modified version of Enroth-Cugell's and Robson's null test, a continuous record was obtained of the Y cell's response to changes in

the spatiotemporal distribution of the light. Thus, both the nature and extent of the nonlinear component of the Y cell, over some period of time, could be fully examined. At a phase angle that would normally constitute a null position for X cells, the Y cell produced two bursts of impulses during one temporal cycle of the grating's alternation. Thus the Y cell's response occurred at a frequency twice that of the temporal variation in the stimulus - a second harmonic. With low spatial frequency gratings, the Y cell's response to peak positions appeared identical to that of the X cells; but, when the grating's spatial frequency was increased, frequency doubling occurred at peak as well as null positions. This reveals a dynamic dependency of the Y cell's response components upon spatial frequency of the stimulus.

By plotting the reciprocal of the contrast required to elicit a minimal criterion response from a cell to a drifting grating as a function of spatial frequency, the spatial frequency sensitivity function (SFS), also known as a spatial contrast sensitivity function, can be obtained (Enroth-Cugell and Robson, 1966). This function can be used to predict the cell's sensitivity to other stimulus patterns through a method similar in principle to convolution in Fourier techniques. The predictive utility of this function is necessarily, however, limited to only those systems which reflect a maintenance of the

superposition principle and thereby evince linear spatial summation. The SFS for X cells revealed a gradual decline in sensitivity to spatial frequencies lower than the optimal frequency and a more rapid decline to higher frequencies. A similar determination for Y cells revealed that the fundamental and the second harmonic components of these cells' responses each possess a unique SFS. The second harmonic is more sensitive to higher spatial frequencies than is the fundamental. This difference in the SFS between the fundamental and the second harmonic of the Y cell thus explains the observation that nonlinearities begin to dominate the Y cell's response as higher spatial frequencies are employed.

The differences in spatial summation between X and Y cells also account for the differences in their responses to drifting gratings. X cells modulate their responses according to the rate of drift at moderate drift frequencies (Enroth-Cugell and Robson, 1966). The Y cell's response is typically more complex with modulated discharge occurring at low spatial frequencies and a general increase in mean, unmodulated discharge produced at higher frequencies. According to Hochstein and Shapley (1976a) the modulated response is presumably contributed by the Y cell's fundamental component while the elevation in mean responding is attributable to the activity of the nonlinear mechanism. Other researchers, using the terms "sustained"

and "transient" to identify X and Y cells, respectively, have shown that transient (Y) cells are capable of responding to much higher velocities of a moving stimulus than are the sustained (X) cells (Cleland, Dubin and Levick, 1971). When the mechanisms underlying the differences between X and Y cells are discussed in a subsequent section (1.5.1), it will be shown that the mechanism giving rise to the nonlinear component of Y cells is responsible for their exceptional sensitivity to high velocities.

The nonlinearities observed in Y cells appear to reflect an essential nonlinear mechanism in the retina; that is, the nonlinearities observed do not reflect any form of compressive nonlinearity or 'ceiling effect' often encountered when responsiveness is pushed beyond its optimal level (Hochstein and Shapley, 1976a). Furthermore, it must be emphasized that the terms linear and nonlinear refer only to the cell's process of spatial summation, it is not meant to suggest that the response of a cell is linearly related to widely varying levels of illumination. When response magnitude is related to amount of illumination over a wide range then even X cells are observed to behave in a highly nonlinear fashion. For this reason, the SFS function of a given cell is determined with sensitivity of response rather than absolute rate of response as its dependent measure. If mean levels of

illumination are kept constant, however, and contrast is varied over a limited range so that responding is examined within a linear range, it is possible to use response rate as the dependent measure (Gordon and Shapley, 1978).

In 1972, Stone and Hoffman reported the existence of a third type of ganglion cell in the cat which they labelled 'W' cells. W cells were considered distinct from both X and Y cells, not on the basis of differences in spatial summation but because of differences in conduction velocity. Hence, the label 'W' was applied to these cells to indicate that they had the slowest conducting axons while intermediate and fast conduction velocities were characteristic of X and Y cells, respectively. W cells can also be distinguished from X and Y cells on the basis of response latency. In general, W cells respond more slowly to stimulation than do either X or Y cells (Sur and Sherman, 1982), suggesting that W cells are probably the "sluggish" cells described by Cleland and Levick (1974).

The W class was further divided into cells with phasic responses and those which produced tonic responses (Stone and Fukada, 1974). While both groups of W cells may possess either on- or off- centers, only one subgroup of phasic W cells reveal 'on-off' centers. Phasic W cells are similar to Y cells in that they are 'transient' in their response. Unlike Y cells, however, phasic W cells exhibit poor responsiveness to moving stimuli which is probably related

to the "sluggishness" of their responses (Cleland and Levick, 1974). Tonic W cells share with X cells a 'sustained' aspect of responding but may be distinguished from X cells in that the W cells do not possess the antagonistic center/surround organization of the X cells. Therefore, once a stimulus has elicited the appropriate center response in the W cell, withdrawal of the stimulus does not result in either surround mediated inhibition or excitation. Stone and Fukada suggest that the many different types of W cells represent a continuum of cell types. This conclusion is supported by the quantitative variation in conduction velocity exhibited among W cell subgroups.

Linear/nonlinear spatial summation analyses comparable to those described for X and Y cells reveal that W cells in the cat, at least at the level of the LGN, may be further differentiated into a linear and a nonlinear group (Sur and Sherman, 1982). The nonlinear W cells may be distinguished from Y cells on the basis of the spatial sensitivity of the second harmonic component: the optimum spatial frequency for the second harmonic in W cells is much lower than that in Y cells. Differences in the shape of the SFS serve to distinguish between X cells and linear W cells, the low frequency decline characteristic of the former is absent in the SFS of linear W cells although a high frequency decline is characteristic of both cell groups. As the linear-

nonlinear distinction was applied to geniculate W cells, it is unclear whether these response properties may also typify the retinal W cells which terminate upon the geniculate cells or whether they represent unique geniculate response characteristics. Analyses of individual LGN cells which receive input from either X or Y cells, however, suggest that linear-nonlinear summation properties established at the retinal level are maintained at the geniculate level (Cleland, Dubin, and Levick, 1971; Kaplan and Shapley, 1982).

The question often arises as to whether the W, X, and Y classes represent functionally separate groups of ganglion cells. Firstly, no overlap was found between X and Y cells when a nonlinearity index, based upon the ratio of the relative strengths of fundamental and second harmonic response components, was used (Hochstein and Shapley, 1976a). Secondly, there is evidence that the central visual system differentiates among the three classes; fibers from these classes are kept separate and selectively terminate, for the most part, in different areas of the visual system. In cats, the majority of W cells terminate within the superior colliculus (Fukada and Stone, 1974) although a small portion project to the C-lamina of the LGN (Sur and Sherman, 1982). The vast majority of X cells project to the LGN while Y cell axons bifurcate and innervate both the LGN and the superior

colliculus (Fukada and Stone, 1974). Additional details of the central projections of these three cell classes are fully explored in an extensive review by Lennie (1980).

The three classes can be distinguished according to a number of features in addition to the essential distinction based upon linearity of spatial summation. As seen earlier, axonal conduction velocity differs greatly among the three cell classes. RF size as well as retinal distribution also vary among these cells. X cells possess smaller RFs than do Y cells. This relationship between X and Y cells is maintained at all retinal loci even though RF size, in general, increases as a function of retinal eccentricity (Fukada and Stone, 1974). The RFs of W cells tend to be larger than X cells but, perhaps owing to the wide range of W cell types, W cells' RF size displays a great deal of variability at a given retinal region. The three cell types may also be differentiated by virtue of their retinal distributions. X cells and, to a smaller degree, W cells are most numerous within the area centralis with density falling off sharply as more peripheral regions are sampled (Fukada and Stone, 1974). Y cells, rarely encountered within the central retina (Enroth-Cugell and Robson, 1966), appear to be confined to the peripheral retina (Fukada and Stone, 1974).

1.5.1 Proposed Models

The quantitative analyses performed by Hochstein and Shapley, previously described, have provided sufficient information to enable these authors to devise models of the RF organization of X and Y cells (1976b). The organization of the RF mechanisms underlying the X cell has been assumed to correspond to the model proposed by Rodieck and Stone (1965) which provides an adequate description of a linearly integrating cell.

Hochstein and Shapley propose that the X cell's RF possesses a center region, which summates contributing signals in a linear manner, overlapped by a surround region greater in spatial extent and which linearly summates signals opposite in polarity to those of the center. As suggested by Rodieck and Stone, sensitivity is distributed in a Gaussian fashion in both center and surround regions. The 'goodness of fit' of X cell RF characteristics to the Rodieck and Stone model is provided, in part, by a consideration of the utility of this model in predicting the SFS of X cells (Enroth-Cugell and Robson, 1966; Linsenmeier, Frishman, Jakiela, and Enroth-Cugell, 1982). As Enroth-Cugell and Robson have noted, the gradual low frequency decline of the X cell's SFS is attributable to the inhibitory action of a linearly summating surround region. The spatial extent of the central linear summation

region of Rodieck and Stone's model adequately accounts for the abrupt cut-off of sensitivity to high spatial frequencies exhibited by the X cell's SFS.

The interaction between center and surround components of the X cell is, however, somewhat complex. Attenuation of responsiveness to low spatial frequencies, which results from surround inhibition, is dependent, in many cells, upon the rate at which gratings are drifted across the cell's RF (Derrington and Lennie, 1982; Dawis, Shapley, Kaplan, and Tranchina, 1984). The low frequency decline evident in the SFS is diminished as drift rate is increased. This interaction between spatial and temporal frequencies also characterizes the SFS of many Y cells (Hochstein and Shapley, 1976a). These findings suggest that the temporal dynamics of center and surround components differ. The surround is typically less sensitive than the center to faster temporal frequencies.

Hochstein and Shapley (1976b) examined the SFS functions of both the fundamental and second harmonic components of Y cells and concluded that the mechanism generating second harmonics was capable of integrating information from spatial regions smaller in extent than the region giving rise to the fundamental mechanism. This led, in turn, to the proposition that spatial subunits were responsible for the second harmonic response of Y cells while another RF mechanism, much larger in spatial extent,

was responsible for the fundamental.

In order to discern the spatial relationship between the linear and nonlinear mechanisms, Hochstein and Shapley analyzed the effect of selectively exposing a contrast reversal grating to either the central (window condition) or peripheral (shutter condition) region of the cell's RF upon the fundamental and second harmonic response components. The shutter condition resulted in almost complete obliteration of the fundamental and a moderate but insubstantial diminution of the second harmonic. When the periphery was obscured during the window condition, the fundamental was insignificantly diminished while the second harmonic was greatly attenuated. These results suggest the following organization of the Y cell's RF, shown in Figure 2. The fundamental is produced by a RF mechanism virtually identical to the center-surround X cell organization while the nonlinear spatial subunits are individually small but widely distributed and are, therefore, apparently coextensive with the linear surround region. As the subunits contribute responses of the same polarity as that of the linear center, the extensive distribution of these smaller summating regions may account for the shallow gradient observed when the sensitivity of the Y cell's center region is analyzed by more conventional means which employ spots of light of increasing diameters (Ikeda and Wright, 1972). The absence of a dependence upon stimulus

Figure 2

Proposed model of the receptive field organization of the Y cell according to Hochstein and Shapley (1976b). Linearly summating components are represented by solid lines, nonlinearly summating subunits by dashed lines.

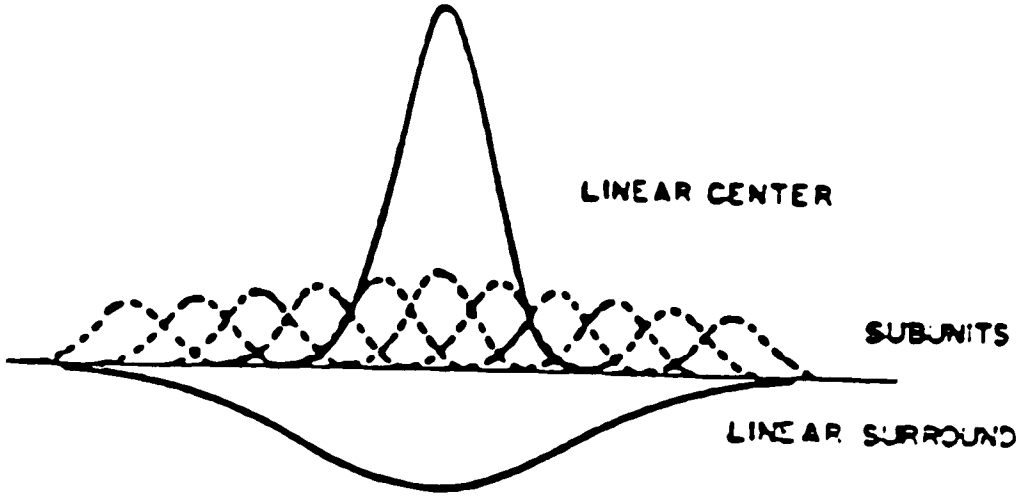
LINEAR CENTER
SUBUNITS
LINEAR SURROUND

phase angle in the nonlinear component of the Y cell response can be similarly attributed to the smaller summating regions of the subunits and their extensive distribution throughout the cell's RF. The activity of subunits also explains the exceptional sensitivity displayed by Y cells to moving stimuli. As the stimulus moves across the RF it successively activates adjacent subunits which individually contribute frequency doubled responses thereby resulting in an overall increase in mean discharge rate as seen in Enroth-Cugell's and Robson's study.

Victor and Shapley (1979) have suggested that the bipolar cell is the structural unit for both the linear center of X and Y cells and the nonlinear subunit specific to Y cells. The basic structural difference between the linear and nonlinear integrating mechanisms concerns the nature of the bipolar cell input. Numerous bipolar cells contribute directly to the linear center while fewer bipolar cells provide input, indirectly, to the subunit. A number of considerations point to the amacrine cell as the intermediate element between bipolar and ganglion cell responsible for generating the nonlinear responses of Y cells. For example, Toyoda (1974) has reported that a number of amacrine cells, in the carp, respond at the second harmonic of the stimulus frequency. Rectification of synaptic input has been suggested as a plausible

mechanism for generating frequency doubled responses (Hochstein and Shapley, 1976a). This rectification must occur at some stage prior to summation at the ganglion cell or else inputs of opposite polarity would cancel each other. There is evidence that conventional synapses, indicating amacrine cell involvement, have a strong tendency to rectify whereas ribbon (bipolar) synapses are more likely candidates for a linear, non-rectified transmission (Katz and Miledi, 1967). The involvement of half-wave rather than full wave rectification in amacrine cell synapses is suggested by the observation that 'on-off' responses in carp amacrine cells appear to be generated by the selective transmission of excitatory post-synaptic potentials (EPSP's) (Toyoda, Hashimoto and Ohtsue, 1973). There is little reason to believe that the nonlinearities can arise from OPL interactions as horizontal cells, in the turtle, appear to be capable of only linear spatial summation (Tranchina, Gordon, Shapley, and Toyoda, 1981). The tremendous sensitivity of the subunits to relatively high temporal rates of drift further decreases the possibility that the horizontal cells, with their characteristic slow, graded responses, could generate the fast transient response required for this sensitivity (Werblin, 1972; Werblin and Copenhagen, 1974; Werblin and Dowling, 1972).

1.6 Contrast Gain Control

Recently, an additional nonlinear mechanism in the retina has been identified and labelled the 'contrast gain control' (Shapley and Victor, 1978, 1979, 1981). This mechanism, essentially "adjusts the sensitivity and dynamic characteristics of the retina contingent on the average contrast of visual stimuli" (p.293). Shapley and Victor examined the responsiveness of the linear summating components in both X and Y cells to various temporal frequencies as stimulus contrast was increased. The stimulus they used was a spatial grating which was modulated simultaneously by a number of incommensurate temporal frequencies i.e., a sum of sinusoids. As contrast was increased the temporal transfer function (TTF), a measure of the cell's sensitivity to a grating's temporal frequency, was shifted to faster temporal frequencies. With increasing contrast, response amplitudes increased more rapidly for fast temporal frequencies than for slow. In fact, response amplitudes for slow temporal frequencies were somewhat suppressed as higher contrasts were used. Furthermore, the relative temporal phase of the response was advanced at higher contrasts to fast but not slow temporal frequencies. It should be emphasized that phase shifts which result from increased contrast represent a marked nonlinearity based on the assumptions underlying the

principle of homogeneity; that is, any change in the output which is not identical to modification in the input indicates a deviation from linearity.

As suggested by the relative insensitivity of this mechanism to the spatial phase of the stimulus, in addition to numerous other similarities, contrast gain control appears to be closely related to the activity of subunits which generate second harmonics in Y cell responses (Shapley and Victor, 1980). X cells' responses, however, were also affected by higher contrasts in a manner similar to but to a lesser degree than responses in Y cells. This observation led Shapley and Victor to conclude that the nonlinear subunits are involved, directly, in the generation of Y cell responses while, through an indirect pathway, modulate X cell responsiveness by varying its gain.

1.7 Extension of the Linear/Nonlinear Distinction to Frogs

That the linear/nonlinear distinction in spatial summation properties may reveal a general principle in the vertebrate retina is suggested by the wide variety of vertebrate species which have been shown to display ganglion cell response characteristics similar to the cell types reported in the cat's retina. Both linear and nonlinear integrating cells have been found in the retina

of the mudpuppy (Tuttle and Scott, 1978). X, Y and W cells have been identified in the goldfish retina (Bilotta and Abramov, 1989). X cells and a class similar to the 'on-off' W cells in the cat, $\overline{X}$ cells, have been observed in the retina of the American eel (Gordon and Shapley, 1978; Shapley and Gordon, 1978). Finally, preliminary findings in the frog indicate that three classes of ganglion cells can be distinguished based on criteria used in the cat: the $\overline{X}$ class, which exhibits W-like characteristics, as well as X and Y classes (Gordon and Shapley, 1978).

In the frog, cells identified as X cells display null responses to appropriate spatial phases of the stimulus and display a sinusoidal dependence of sensitivity on stimulus phase (Gordon and Shapley, 1978). When the responses of these cells are subjected to Fourier analysis no significant nonlinear components are observed. One difference which has been noted between X cells in frogs and those in cats is that, in the frog, off-center X cells do not display a low spatial frequency cutoff in their contrast sensitivity functions. As the lack of this low frequency decline suggests that surround inhibition may be absent, such an observation is in partial agreement with other studies which show that a large number of class IV cells, Hartline's 'off' cells, do not possess an IRF (Grusser-Cornehls, Grusser, and Bullock, 1963). In those class IV cells which do display an inhibitory surround,

however, the IRF is exceptionally large, approximately 15 degrees in extent. It is unclear, at present, whether or not the presence of extensive IRF's in 'off' cells may confer any, as yet, unidentified properties upon the ganglion cell in terms of linear/nonlinear distinctions.

The frog Y cell is also quite similar to that in the cat based on Gordon's and Shapley's findings. A substantial second harmonic is observed, at low spatial frequencies, when the grating is at a 'null' position. The relative strength of this nonlinear component changes as a function of spatial frequency in a manner similar to that reported for the cat Y cell.

A third type of cell observed in the frog, one which displays nonlinear spatial summation and is similar to the 'on-off' phasic W cells in the cat is the $\overline{X}$ cell. Both the $\overline{X}$ and the phasic W cell exhibit poor spatial resolution. $\overline{X}$ cells are similar to the frog's Y cells in that they produce frequency doubled, i.e. second harmonic, responses to null positions and typically fundamental responses to peak positions. Unlike the Y cell, however, the ratio of the second harmonic to the fundamental in the $\overline{X}$ cell ceases to increase at spatial frequencies considerably lower than that which would elicit maximal second harmonic activity in the Y cell. An additional characteristic which serves to distinguish $\overline{X}$ cells from Y cells in the frog is the observation that both the fundamental and second harmonic

of the former are insensitive to spatial phase. Quantitative analyses of the fundamental and second harmonic components of the $\overline{X}$ cell therefore suggest a close correspondence between these ganglion cells in the frog and the nonlinear W cells in the cat's LGN.

With the exception of the frog's off-center X cells, a remarkable similarity exists between frog and cat with regard to the expression of these three cell types. Yet, as indicated earlier, the examination of frog ganglion cells according to the WXY classification is at a preliminary stage. Thus, the observed similarities may be based upon a relatively superficial examination of response properties. As seen earlier the frog's retina, when compared to that of mammals, displays quantitative anatomical differences. While these differences do not necessarily preclude the possibility that similarities between frog and cat X, Y, and W ($\overline{X}$) cells exist, some quantitative differences may be expected. The effect of an increased number of amacrine synapses upon X and Y cell expression in the frog, for example, needs to be determined.

The effect of increased amacrine cell participation in the organization of anuran ganglion cells, however, is not expected to be of a simple, unitary nature. Amacrine cells in the frog do not represent a homogeneous group with regard to either response features or their effect upon

postsynaptic structures. While transient responses appear characteristic of amacrine cells, responding of a more sustained nature may not be uncommon as suggested by studies of the synaptic mechanisms contributing to sustained ganglion cell responses in mudpuppies (Belgum, Dvorak and McReynolds, 1983). Furthermore, different classes of amacrine cells, utilizing different neurotransmitters, may subserve unique functional roles (Gronholm and Reuter, 1981). Speculations regarding the effect of amacrine cell activity upon the nature of X, Y or $\overline{X}$ responding in the frog are, therefore, best reserved until additional quantitative data are obtained.

The basic components of the models proposed for X and Y cells in the cat have been observed, to some extent, in frog ganglion cells. Hartline (1940a) had noted that sensitivity drops off gradually as more peripheral regions of a frog's ganglion cell is stimulated thereby suggesting that the central region of the RF in frogs displays a Gaussian-like distribution of responsiveness. The notion that smaller summating regions within the larger RF area may be responsible for the generation of local 'on-off' responses in the majority of frog ganglion cells (Burkhardt, 1970) is reminiscent of the model proposed for cat Y cells.

A second aspect of the research initiated in the cat which has yet to be examined in frogs is the activity of

the contrast gain control mechanism. Gordon and Shapley (1978) employed relatively low contrasts in their analyses of frog ganglion cells. A wide range of contrasts are required to fully assess the gain in sensitivity to fast temporal changes provided by this mechanism. As this mechanism supposedly arises from the spatial subunits which have been tentatively related to amacrine cell activity, examination of this mechanism in the frog, with its large number of amacrine synapses, may provide additional insight into the cellular processing which underlies this contrast dependent effect.

1.7.1 Comparison of Linear/Nonlinear Cells to Feature Detectors in the Frog Retina

An additional aspect of a linear/nonlinear classification of frog ganglion cells is the problem of determining the extent to which these cells may be related to the Lettvin et al. classes. For example, the X cell distinction, as in cats, cuts across cell types labelled as 'on' or 'off' (Gordon and Shapley, 1978). It is possible, therefore, that the linear/nonlinear distinction may similarly cut across the various Lettvin et al. classes. While the majority of X cells examined in the frog appear similar to Lettvin et al. classes I and II other X cells appear identical to class IV fibers. Henn and Grusser (1968) have provided data which suggest that, according to

a direct test of the principle of superposition, class II fibers do not display linear spatial summation. It is possible, therefore, that two types of cells with different integration processes are grouped under the 'class II' label. An alternative explanation, which cannot be eliminated, is that class II fibers do display linear spatial summation and that Henn's and Grusser's use of response rate, rather than sensitivity, as the dependent measure introduced nonlinearities resulting from saturation of the response.

Citron, Kroeker and McCann (1981), using stimuli and analytical techniques theoretically similar to sinusoidal stimulation and Fourier analyses, suggest that class III cells reveal many nonlinear response characteristics which are suggestive of Y cell behavior in the cat. Although the similarity between the frequency doubling response of Y cells and the 'on-off' responses of class III cells is highly compelling, it might be premature to suggest that Y cells are 'on-off' cells or vice versa.

The difficulty in establishing a firm relationship between Y cells and class III cells stems from numerous sources, the most crucial of which is the difference in stimuli used traditionally to identify these two types. As seen earlier, Y cells are not simple in their characterization: the form of their response is completely dependent upon the spatial frequency of the stimulus.

Nonlinearities are most pronounced when high spatial frequencies are employed. At low spatial frequencies nonlinear spatial summation is apparent only at null positions. In cats, Y cells, when stimulated with low spatial frequencies, may be either 'on' or 'off' based on their responses to peak positions of a grating. Class III cells in the frog, however, are typically identified by virtue of their response to complex stimuli such as spots of light or bug-like shapes which tend to obscure spatial frequency dependent response properties.

Another difficulty in relating the linear/nonlinear distinction to the earlier classification scheme of frog ganglion cells is suggested by Gordon and Shapley's (1978) observation that $\overline{X}$ cells in frogs, like W cells in the cat, may produce 'on-off' responses. This presents the further complication that previously identified 'on-off' cells in the frog may not represent a homogeneous group of cell types. Unfortunately, the Citron et al. (1981) study did not subject the nonlinear class III ganglion cells to analyses which could distinguish between Y and $\overline{X}$ cells. The designation of 'on-off' cells in the frog as either Y or $\overline{X}$ requires Fourier analytic techniques and an examination of the dynamic response properties of the fundamental and second harmonic.

1.8 Issues Addressed in the Present Study

The research described in this dissertation was intended to extend the findings reported by Gordon and Shapley (1978) so that anuran ganglion cells may be fully characterized using quantitative techniques which have proven extremely useful in revealing the full functional complexity of the mammalian retina. One general goal of this research, therefore, was to reveal the extent to which response properties based on the linear/nonlinear distinction represent general functional principles of the vertebrate retina. The specific questions addressed in this research are presented below.

1. Classification of frog ganglion cells according to a linear/nonlinear spatial summation distinction.

a. What is the extent of similarities and/or differences between X, Y and W-like ($\overline{X}$) cells in the frog and those in the cat in terms of RF organization, spatial frequency responsivity, and harmonic components of the response?

b. Are there any ganglion cells which do not fall neatly into X, Y, $\overline{X}$ classes?

c. Do any subclasses exist within the X, Y, $\overline{X}$ categories?

d. How might functional differences, known to exist

between anura and mammals based upon early studies using spots and annuli as stimuli, be expressed as modifications in response properties of X, Y and $\overline{X}$ cells in the frog?

e. How might structural variation in the IPL between frog and cat be manifested as functional differences in X, Y and W-like cells between the two?

2. The effect of high contrasts upon the temporal transfer function of different cell classes.

a. Is the contrast gain control mechanism operable in frogs and, if so, what is its effect on X and Y cells?

b. If the mechanism exists in the frog, are there any differences in its operation from that in the cat which might be related to known functional or structural differences between the two animals?

3. The comparison of the linear/nonlinear distinction to the Lettvin et al. classification.

a. Are properties based on spatial summation differences independent of the Lettvin et al. classes?

2 METHODS

2.1 Subjects

Male and female frogs (Rana pipiens), purchased from West Jersey Biological Supply, were housed in glass aquaria purchased from Carolina Biological and maintained at a temperature of 20 to 25 degrees centigrade. Each tank contained a maximum of 20 frogs. Bricks placed within the aquaria provided the frogs with dry landing and feeding areas and broken clay pots furnished appropriate hiding places required by this species (Orlans, 1977). Mosquito netting, stretched across a wooden frame and placed across the top of the tank, secured the animals inside the tank. The aquaria were filled with tap water to a depth of six inches. Water was changed three times a week and the tanks were cleaned once weekly. Frogs were maintained on a diet consisting chiefly of sowbugs.

2.2 Apparatus

A system, designed by Milkman, Shapley, and Schick (1978) which utilizes a microprocessor to govern the output

of a number of peripheral circuits, was used to generate all of the visual stimuli employed in the analyses described herein. All stimulus patterns were presented on the face of a Tektronix (5103) oscilloscope with a p31 phosphor. As the stimulator has been described in detail by Milkman et al., what follows is a brief description of the capacities of the system.

A raster generator circuit provides the input to the x and y axes of the oscilloscope thereby producing a uniform field of luminance upon the face of the oscilloscope. Modulation of intensity upon this uniform field is accomplished by multiplying the signals of a spatial modulator circuit with those of a temporal modulator and then feeding this composite signal into the z axis of the oscilloscope. The spatial modulator can produce either one of two grating patterns - bar or sinusoidal in profile - or a fixed uniform background. The temporal function generated by the temporal modulator can be chosen from one of three: sinusoidal, square wave or a constant temporal signal. Various combinations of the two modulators' input functions can therefore result in a diverse range of visual patterns. The interfacing of the microprocessor with these modulator circuits allows for ease of selection of each modulator's function with inputs from a keypad or from a separate microcomputer (Radioshack, TRS-80, model III).

For most of the analyses described herein, a spatial

sinusoidal grating was employed. The flexibility afforded by the visual stimulator allows for a number of variations in the sinusoidal grating. The grating may remain stationary and reverse its contrast at one of nine temporal frequencies which range from .125 to 32 Hz or it may be allowed to drift across the oscilloscope screen at any one of these frequencies.

All of the following parameters which define a particular sine wave grating may be independently manipulated by the microprocessor via the TRS-80. 1) Spatial frequency in cycles/mm measured at the level of the retina. 2) The contrast of the grating defined as (Imax - Imin/ Imax + Imin) where Imax and Imin refer, respectively, to the values of the maximum and minimum intensity of the grating. 3) Phase angle which defines the relative position of the grating within a cell's RF. 4) Temporal modulation, in cycles/sec (Hz), of either contrast reversal or drift rate.

The pattern produced upon the oscilloscope was imaged upon the retina with a high-quality photographic lens (Nikon, FL= 85mm, f 1.4) and a first surface mirror. The entire stimulus display, when projected onto the retina, occupied a 5 x 5 mm area. The mean illuminance of the image, on the retina, was 4.8 lumens/m^2. The contrast of all stimuli therefore represent modulation above and below this mean level. The contrast produced on the oscilloscope

was linearly related to contrast input from the stimulator up to the highest value used in these experiments (see Figure 3).

Glass micropipette electrodes, pulled by a Kopf vertical micropipette puller to an approximate tip diameter (about 2 microns) and filled with frog Ringer's solution (yielding a resistance on the order of 5 MŌ) were used to record extracellular potentials from individual ganglion cells. A micropositioner (Nanostepper Model NS1000-A), manufactured by World Precision Instruments, mounted on a Brinkmann Instrument three-dimensional micromanipulator (Model 06-20-02) was used to advance the electrode toward the ganglion cell layer. All extracellular recordings were performed upon a Micro-G vibration isolation table manufactured by Technical Manufacturing Corporation.

Once impulses had been amplified by a high gain, low noise AC amplifier (Rockefeller University electronics shop) they were led to an oscilloscope, an audio monitor and a discriminator circuit. The discriminator circuit emitted a .5msec pulse when an impulse crossed a preset threshold. The discriminator's output (TTL pulse) was then fed to the microprocessor which binned the pulses according to their time of occurrence relative to the stimulus cycle. The number of data bins, per temporal cycle of the stimulus, depended upon the stimulus' temporal frequency. For frequencies up to and including 4Hz there were 64 bins

Figure 3

Input/output function relating contrast signals from visual stimulator to contrast produced on stimulus display oscilloscope. Output contrast - ((Imax-Imin) / (Imax + Imin)) - was measured at the level of the retina. The entire range of contrast signals available from the stimulator are represented on the Y axis. Open and filled circles depict two separate sets of measurements obtained on two different days. The solid line represents the first order polynomial regression calculated for the mean values of the two data sets.

Retinal Contrast as a Function of Signal Input

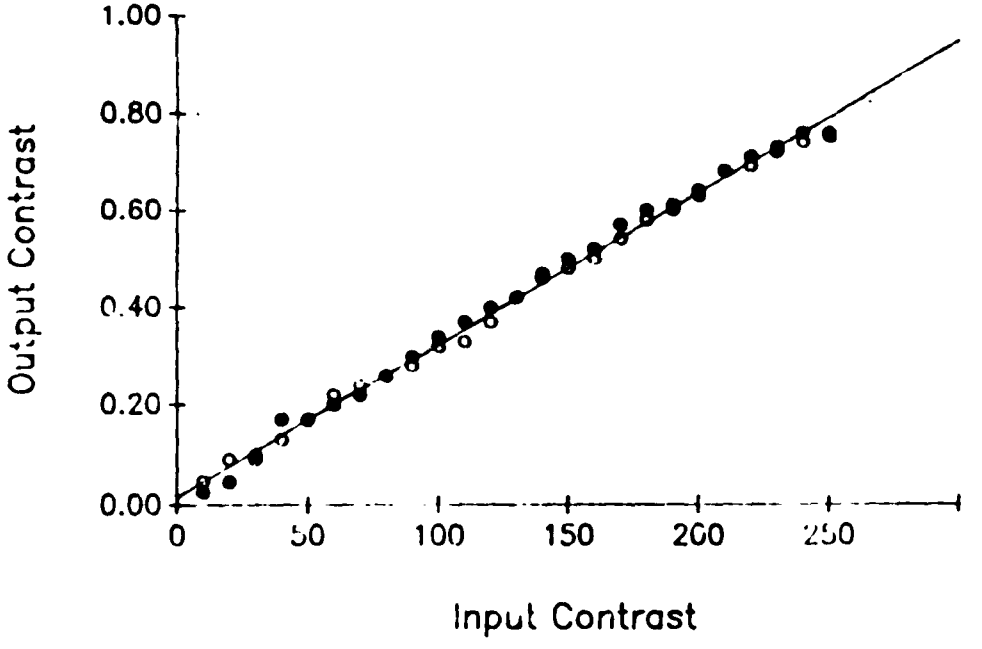

per temporal cycle; the number of bins for frequencies higher than 4 Hz was equal to the number 256 divided by the specific frequency in Hz. At the end of each run, the sums of the bins were fed to the TRS-80 where a Fourier Transform program calculated the magnitudes and relative phases of the first ten harmonic components of the response. Response averaging was also performed by the TRS-80.

2.3 Procedures

2.3.1 Eyecup Preparation and Recording.

Under light adapted conditions the animal was decapitated, double pithed and enucleated. The portion of the eye rostral to the ora serrata was dissected away in order to expose the retina and the vitreous was drained. The eyecup was held in place within an appropriately shaped plastic chamber. This chamber was lined with Ringer moistened Kimwipe and an indifferent electrode (silver-silver chloride rod) contacted the back of the eye through a Ringer-filled hole. Moistened oxygen was blown over the retina. Under these conditions, the retina remained viable for as long as 8 hours. The health of the retina was periodically assessed by examining the ERG for any evidence of a dying retina.

2.3.2 Localization of Single Units

The 'search' pattern used to initially localize a cell was a square wave, .5 Hz, uniform modulation of full field intensity above and below the mean background level. The contrast of this full field stimulation, calculated as previously described for grating stimuli, was .5. The micropipette was advanced along the antero-posterior axis of the eye until a single ganglion cell was isolated.

2.3.3 Determination of Hartline Response Type

The cell was classified as either 'off', 'on', or 'on-off' based initially upon its responses to the search pattern described above. Once the cell had been isolated this search pattern was typically modulated at a number of temporal frequencies, ranging from .125 to 4 Hz., to insure that the response was stable and to obtain a preliminary indication of the cell's temporal responsiveness.

2.3.4 Determination of Linear and Nonlinear Spatial Summation: The Null Test.

Prior to describing the protocol used during the null test in this study, it would be helpful to briefly review the assumptions underlying the utility of the null test in determining linearity of spatial summation. When a grating's intensity is spatially modulated according to a

sinusoidal function, two positions of the grating exist in which the zero crossing of the sine wave function lies approximately within the the cell's RF center. At these positions, increases in intensity in one half of the RF are compensated by decreases occurring in the other half. If the cell's spatial summation is linear no response should be observed at these positions. At positions 90 degrees away from these 'null' positions, whereby maximal changes in intensity are occurring within the cell's RF, contrast reversal of the grating should elicit maximal or 'peak' responding. Any deviation from this dependence upon the position - or spatial phase- of the stimulus indicates that spatial summation is nonlinear.

In the null test, the relative phase angle of a contrast reversal grating was systematically varied, by 45 degree increments, from 0 to 360 degrees. If no definitive null or peak positions could be determined a second test was run in which midpositions (22.5 to 337.5 degrees) of the grating were examined. In a few cells, only the first 180 degrees of the stimulus were explored as long as no ambiguity existed regarding null and peak positions. Because many Y cells' summation processes appear linear when low spatial frequencies are used (Hochstein and Shapley, 1976a), the null test was conducted for each cell over a wide range of spatial frequencies. The temporal frequency used for contrast reversal was dependent upon a

cell's temporal preference as determined by full field stimulation and/or drifting grating experiments (described in section 2.3.5). For a number of cells, the null test was also performed at several temporal frequencies in order to establish whether or not summation properties were temporally dependent. In cells demonstrating responsiveness to the square wave modulated search pattern but none to sinusoidally modulated stimuli, contrast was reversed according to a square wave function during the null test.

An additional requirement for a linear system is that the dominant temporal frequency of the system's output must be the same as that of the input. To establish linearity in the temporal domain, cells' responses were analyzed into their Fourier components. The dominant harmonic of the response indicates the value by which the stimulus frequency must be multiplied in order to obtain the temporal frequency at which responding is modulated. Thus, a dominant first harmonic, also referred to as the fundamental, indicated that a cell's responding was modulated at the stimulus' temporal frequency. Conversely, responses which were modulated at twice the stimulus frequency revealed a dominant second harmonic component.

2.3.5 Spatial Frequency Responsiveness (SFR)

The optimal spatial frequency for a given cell was determined by drifting gratings of various spatial frequencies across the cell's RF. Beginning at .2 cycles/mm, spatial frequency was increased, by full octave increments, up to 3.2 cycles/mm for the majority of cells and as high as 12.8 cycles/mm for a few. Velocity varied inversely as a function of spatial frequency in order to maintain a constant temporal rate of drift. Thus, for all spatial frequencies, at a given drift rate, the number of cycles passing a particular point on the retina was the same. Whenever possible, the SFR of a given cell was determined at each of three drift rates - .125, 1, and 8 Hz - in order to determine if spatio-temporal interactions existed. Grating contrast was typically .5. If time permitted, SFR determinations were repeated at a contrast of .76.

2.3.6 Analysis of Receptive Field Profile

RF profiles were determined by recording responsiveness to a narrow bar placed at various positions, separated by .5 mm, across the retina. For most cells, the intensity of the bar was square wave modulated above and below the mean level of the background. A sinusoidal modulation of the bar was employed for the remaining cells.

The width of the bar used to map the RF of a particular cell depended somewhat upon the responsiveness of the cell to narrow stimuli. For most cells, therefore, a .5 mm width was adequate. A number of cells, however, did not respond to a bar less than 1 mm wide. The temporal frequency at which the bar's contrast was modulated depended upon the cell's temporal responsiveness as measured during full field stimulation. In most cases the contrast of the bar, relative to the background, was .5.

Responding was divided into 'on' and 'off' components by the following method. The total number of impulses occurring during each half of the stimulus cycle - bright bar vs dark bar - were individually averaged to obtain the response rate, in impulses/sec, attributable respectively to 'on' vs 'off' components.

2.3.7 Receptive Field Locations of Linear and Nonlinear Summating Components in Y Cells: Window/Shutter Tests

The window/shutter technique for isolating central and peripheral RF regions, used by Hochstein and Shapley in the cat (1976b), was employed in a modified fashion in a number of frog Y cells to determine the location and spread of nonlinear subunits within the RF. In the window condition, stimuli were confined to the RF center while stimuli were restricted to the periphery of the RF during the shutter condition. Unlike Shapley's and Hochstein's

window 'aperture' which was restricted in two dimensions (height as well as width), only width was restricted in the present study. Thus, stimuli appeared within a vertical band on the display screen. Consequently, stimuli presented in the shutter condition appeared on both sides of this band. The width of the window depended upon the size of the cell's RF as indicated by prior analysis of its RF profile. Similarly, the location of the window was adjusted based upon the relative location of the cell's RF center.

Stimuli were contrast reversal gratings in which relative spatial phase angle was systematically varied as described for the null test. Two spatial frequencies were presented in each condition: a low spatial frequency optimal for the linear summating component and a high spatial frequency optimal for the nonlinear mechanism. These two spatial frequencies were determined individually and were based upon the results obtained on a given cell during the null test.

2.3.8 Determination of Contrast Gain Control.

To test for the existence of this mechanism within the frog's retina it was necessary to use a much larger range of contrasts than those used in the initial examination of anuran X and Y cells conducted by Gordon and Shapley (1978). Contrast reversal gratings, positioned to obtain a peak response, were temporally modulated at each of four

frequencies (.25, 1, 4, and 16 Hz) at a given contrast. Four levels of contrast were employed (.34, .5, .63, and .76). A low spatial frequency, deemed optimal for a given cell on the basis of previous tests, was used for all cells. For a number of cells - mostly Y cells - a high spatial frequency, which had elicited the highest second harmonic magnitudes during the null test, was also employed. This method differed from the sum of sinusoids method utilized frequently by Shapley and Victor (1978, 1979, 1981) in that only one temporal frequency was employed during a given run. It was similar to the Shapley and Victor procedure, however, because it provided an indication of the effect of increasing contrast upon a cell's responsiveness to stimulus' temporal frequency.

3 RESULTS

3.1 Overview

A total of 75 cells were successfully isolated for a sufficient amount of time to determine their spatial summation characteristics. No systematic attempt was made to identify the retinal location of the cells. A cell was classified as X, Y or $\overline{X}$ based upon several aspects of the cell's performance during the null test: linearity of spatial summation, the effect of spatial frequency upon the second/first harmonic ratio, and dependence of harmonic response components upon stimulus spatial phase. Once a cell had been classified, additional analyses, described in detail in the Methods section, were performed in order to further characterize the cell. The percentage of cells, from each class, which could be fully examined was directly related to the length of time a cell could be successfully isolated. Y cells typically provided stable recordings for longer periods of time than did X or $\overline{X}$ cells. As a result of this, more information was obtained for Y cells than either of the other two classes.

3.2 X Cells

Seventeen ganglion cells were identified as X cells. These cells exhibited linear spatial summation, unaffected by increasing spatial frequency, and were therefore identical to X cells in the cat.

3.2.1 Spatial Summation

Responses from a typical X cell to three positions of a contrast reversal grating, for two spatial frequencies, are shown in Figure 4. Peak levels of responding, modulated according to the grating's reversal rate and displaying a 180 degree temporal phase shift, were recorded at stimulus spatial phase angles separated by 180 degrees. At phase angles located 90 degrees away from these peak positions, X cells produced minimal, or null, responding. Increasing the spatial frequuency of the stimulus grating resulted in a progressive diminution in responding without affecting the occurrence of null and peak responses or their relative dependence upon spatial phase.

Fourier analyses of X cells' responses during the null test revealed a dominant fundamental, i.e., first harmonic, component at all stimulus phases and at all spatial frequencies. The relative strength, or power, contributed by each of the first ten harmonics to an X cell's responses, for a low and a high spatial frequency grating,

Figure 4

Averaged response histograms obtained from an X cell to three positions of a contrast reversal grating. Responses to a spatial frequency of .2 cycles/mm are displayed in the top row while the bottom row illustrates responses to .8 cycles/mm. The relative spatial phase angle, in degrees, of the grating is indicated above each histogram. The grating's contrast was sinusoidally modulated at a rate of 1 Hz. The duration of each record represents one temporal cycle of the stimulus. The contrast of the grating was .5 .

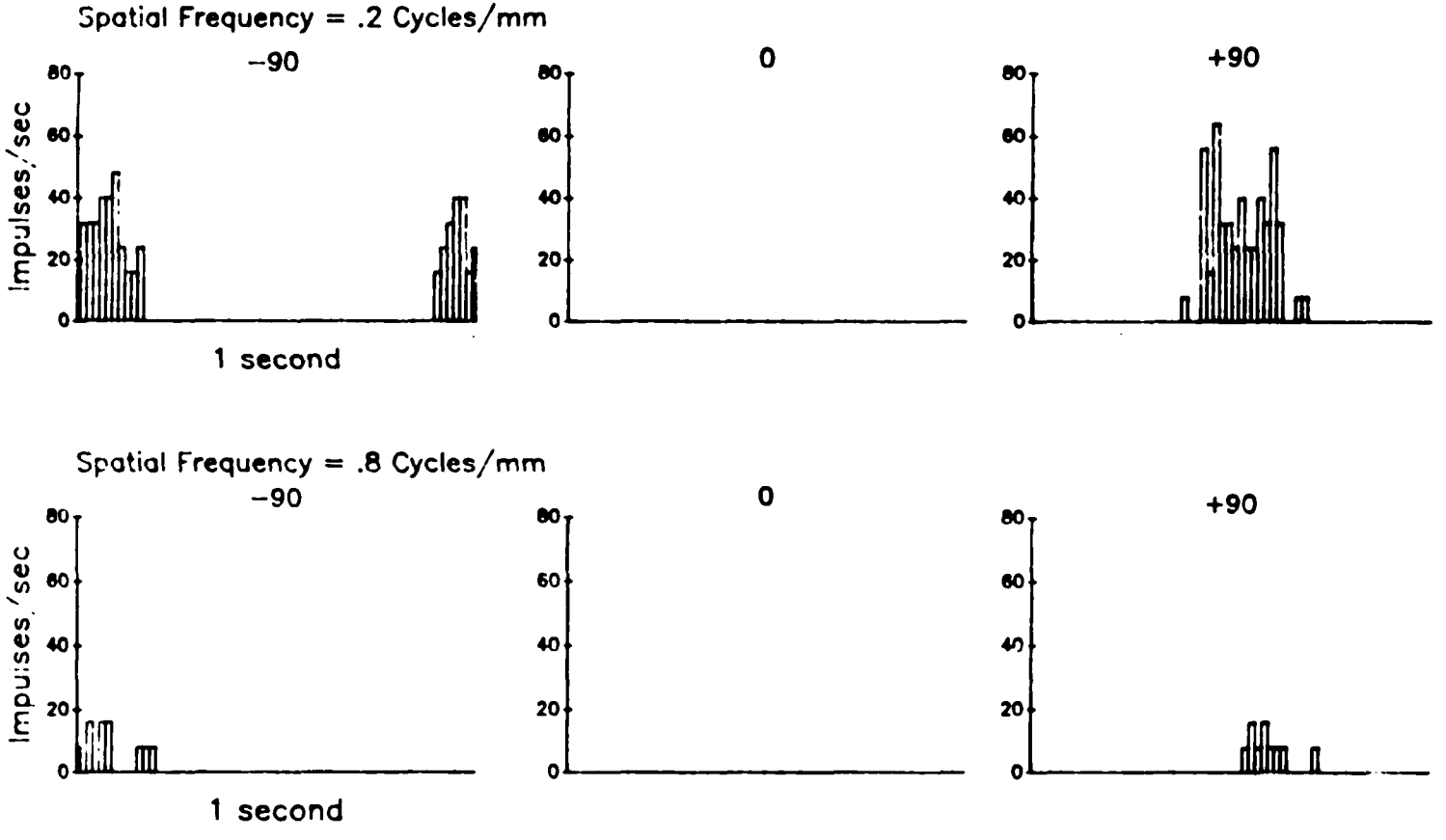
Null Test
X Cell (Pn231)
Spatial Frequency = .2 Cycles/mm
−90
0
+90
Impulses/sec
80
60
40
20
0
1 second
Spatial Frequency = .8 Cycles/mm
−90
0
+90
Impulses/sec
80
60
40
20
0
1 second

is graphically presented in Figure 5. The rectification resulting from a lack of spontaneous activity in most frog ganglion cells, however, often caused an elevation in second and other even harmonics, unrelated to frequency doubled responses, which was rarely greater in magnitude than the fundamental. This fortuitous elevation in second harmonics was most noticeable, as seen in Figure 5, when response rates were very low, for example, at null positions and at high spatial frequencies approaching the limits of a cell's resolution. As a consequence of the latter fact, second/first harmonic ratios calculated for many X cells appeared to increase with spatial frequency in a similar fashion to that observed for Y cells. In order to differentiate, therefore, between genuine and specious high second/first harmonic ratios it was critically important to exclude from consideration spatial frequencies which had elicited negligible responding. Figure 6 shows that, within the spatial frequency range to which X cells were significantly responsive, the second/ first harmonic ratio was rarely greater than 1. Exceptions will be discussed later.

The existence of a dominant fundamental response component satisfies one of the criteria for a linear system; that the predominant temporal frequency of the system's output be the same as that of the input. An additional requirement when considering linearity in the

Figure 5

Fourier analyses of an X cell's peak and null responses. The stimulus was a contrast reversal grating, sinusoidally modulated at 1 Hz. The spatial frequency of the grating was .4 cycles/mm for the power spectra shown in the top row and 3.2 cycles/mm for those in the bottom row. Stimulus contrast was .5.

Fourier Analysis

X Cell (Pn422)

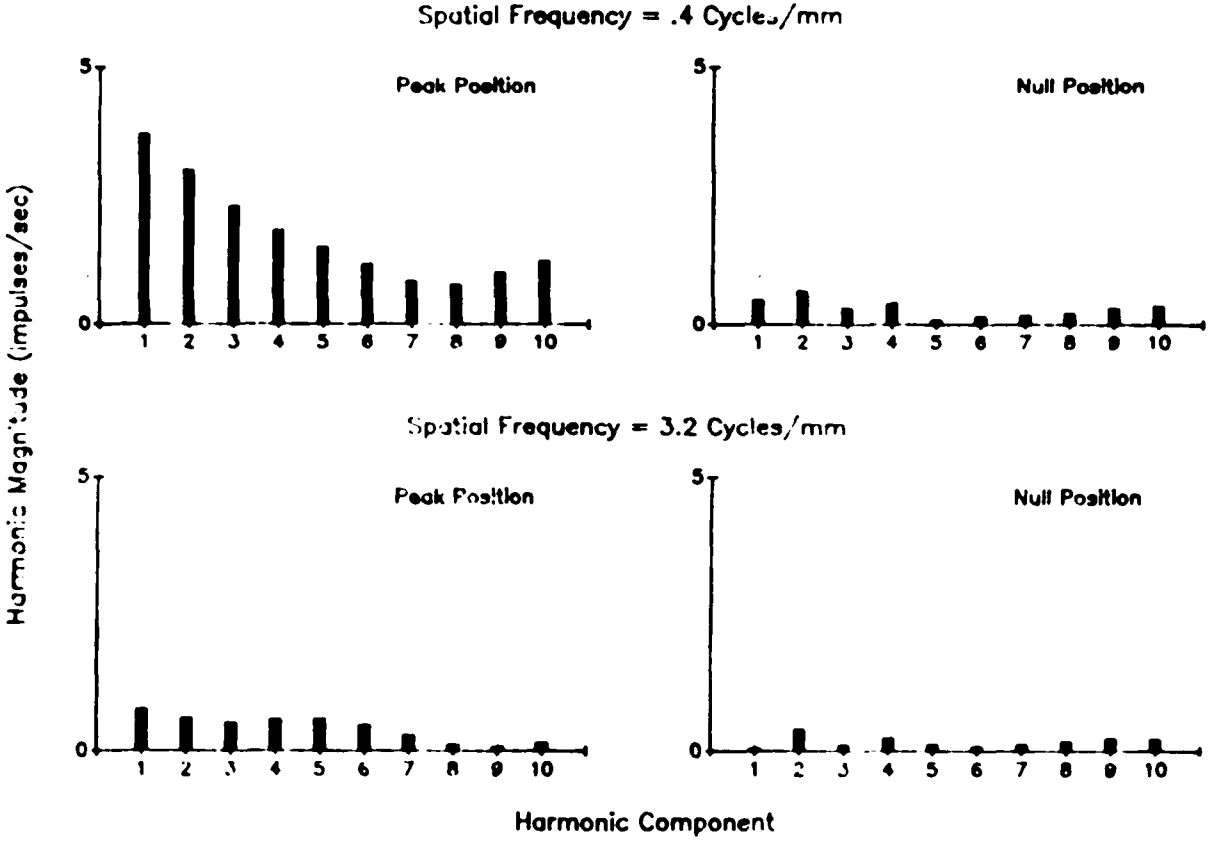

Figure 6

Second/first harmonic ratio and maximum response rate as a function of spatial frequency for two X cells. The harmonic ratio is represented by filled circles, the maximum response rate by open circles. The second/first harmonic ratio for a given spatial frequency was obtained by dividing the mean second harmonic magnitude by the mean first harmonic magnitude. The response rate corresponding to the peak position of the grating, for a given spatial frequency, was designated as the maximum response rate. For both X cells, the stimulus was a contrast reversal grating, with a contrast of .5, sinusoidally modulated at 1 Hz.

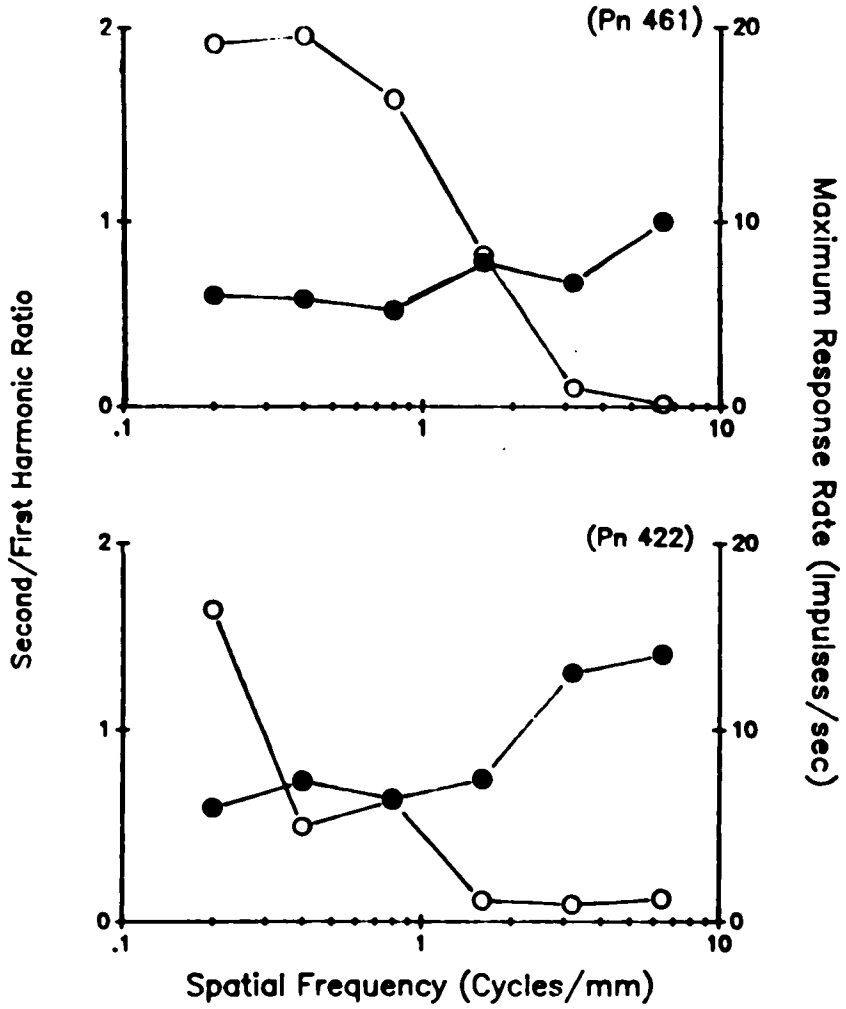

Second/First Harmonic Ratios
X Cells

●—● Second/First Ratio

○—○ Response Rate

spatial domain, is that the cell's response must also vary as a function of the spatial waveform of the stimulus. Figure 7 shows the relationship of the first and second harmonic components of an 'off' X cell's response to the spatial phase of the grating, at each of four spatial frequencies. The first harmonic component displays a sinusoidal dependence upon spatial phase. This dependence was maintained at all spatial frequencies which were within the resolution capabilities of the cell.

Another important feature of a linear system - the dependence of response temporal phase upon stimulus spatial phase - is demonstrated in Figure 8. The temporal phase of an X cell's first and second harmonicc response components are plotted as a function of spatial phase of both a low and high spatial frequency contrast reversed grating. Note that a 180 degree temporal phase difference characterizes first harmonic responses to spatial phases separated by 180 degrees with the temporal phase shift occurring at spatial phase angles corresponding to the cell's null position (0 and 180 degrees). Furthermore, the 180 degree temporal phase shift of the first harmonic is remarkably stable even at a spatial frequency approaching the upper limits of the cell's resolution (Figure 8B). Given that second harmonics in X cells arise from the lack of spontaneous activity, variations in the temporal phase of the second harmonic with spatial phase parallel those of the first harmonic

Figure 7

Magnitudes of the first (filled circles) and second harmonics (open diamonds) of an X cell's response as a function of spatial phase of a contrast reversal grating. By convention, responses occurring during the first half of the grating's temporal cycle (i.e., responses with a temporal phase of less than 180 degrees) are assigned positive values. Responses produced during the second half of the stimulus cycle, thus possessing a temporal phase equal to or greater than 180 degrees, are assigned negative values. The results from four spatial frequencies are shown in (A, B, C, and D). The spatial frequency of the grating is given above each function. Gratings were sinusoidally modulated at 1 Hz and had a contrast of .5. The solid line represents the best fit sinusoid for the first harmonic component.

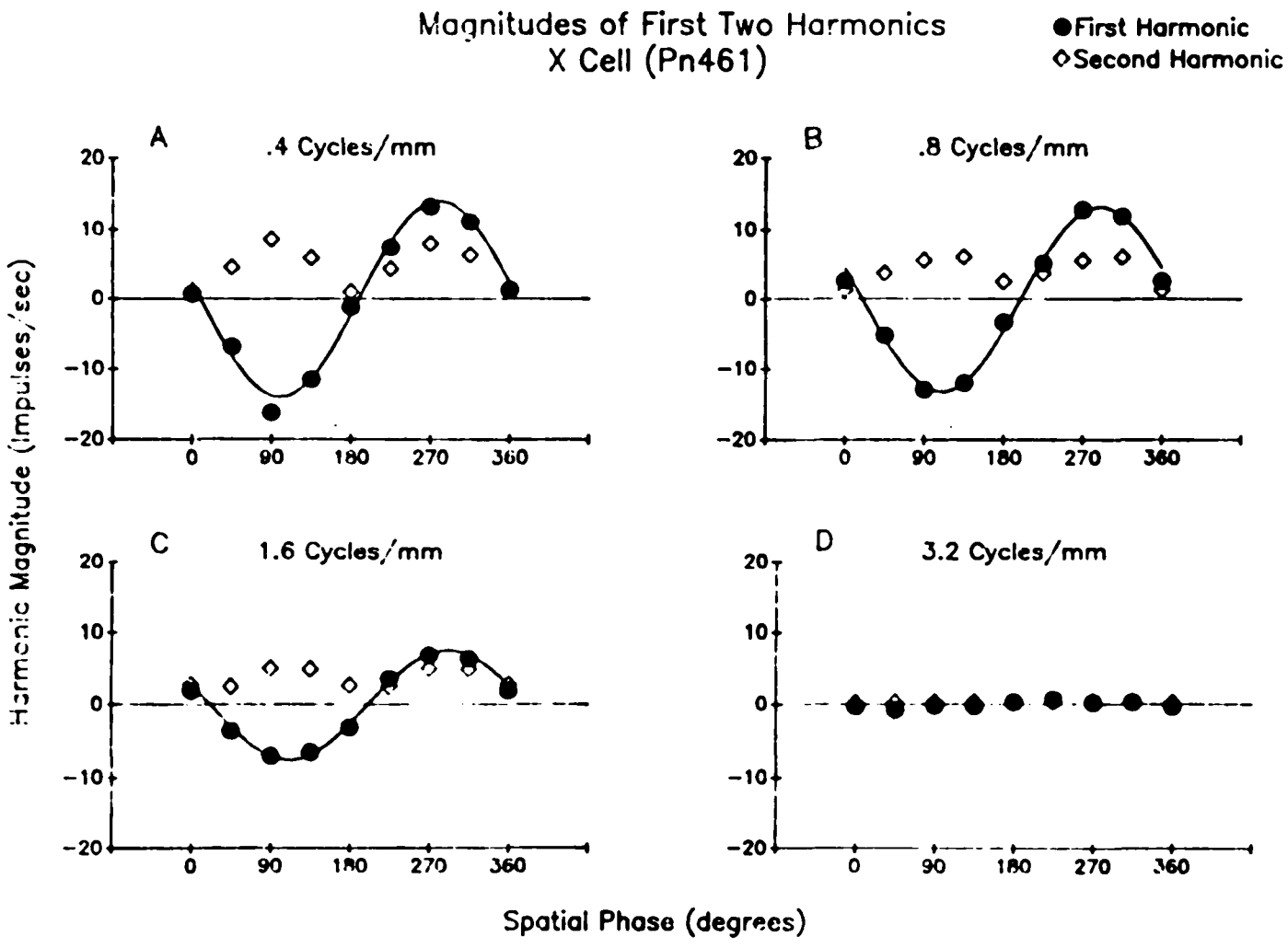
Magnitudes of First Two Harmonics
X Cell (Pn461)
●First Harmonic
◇Second Harmonic
A
.4 Cycles/mm
B
.8 Cycles/mm
C
1.6 Cycles/mm
D
3.2 Cycles/mm
Harmonic Magnitude (Impulses/sec)
Spatial Phase (degrees)
20
10
0
-10
-20
0
90
180
270
360

Figure 8

Temporal phase of first (filled circles) and second (open diamonds) harmonics of an X cell's response as a function of spatial phase of a low (A) and high (B) spatial frequency contrast reversed grating. Temporal phases less than 180 degrees reflect responding during the first half of the stimulus' temporal cycle while phases equal to or greater than 180 degrees indicate responding during the second half of the stimulus cycle. The spatial frequency of the grating is given, in cycles/mm, above each graph. One complete spatial cycle of the grating is represented in each graph. The contrast of the grating was .5 and reversal rate was sinusoidally modulated at 1 Hz.

Response Temporal Phase as a
Function of Stimulus Spatial Phase

X Cell (PN422)

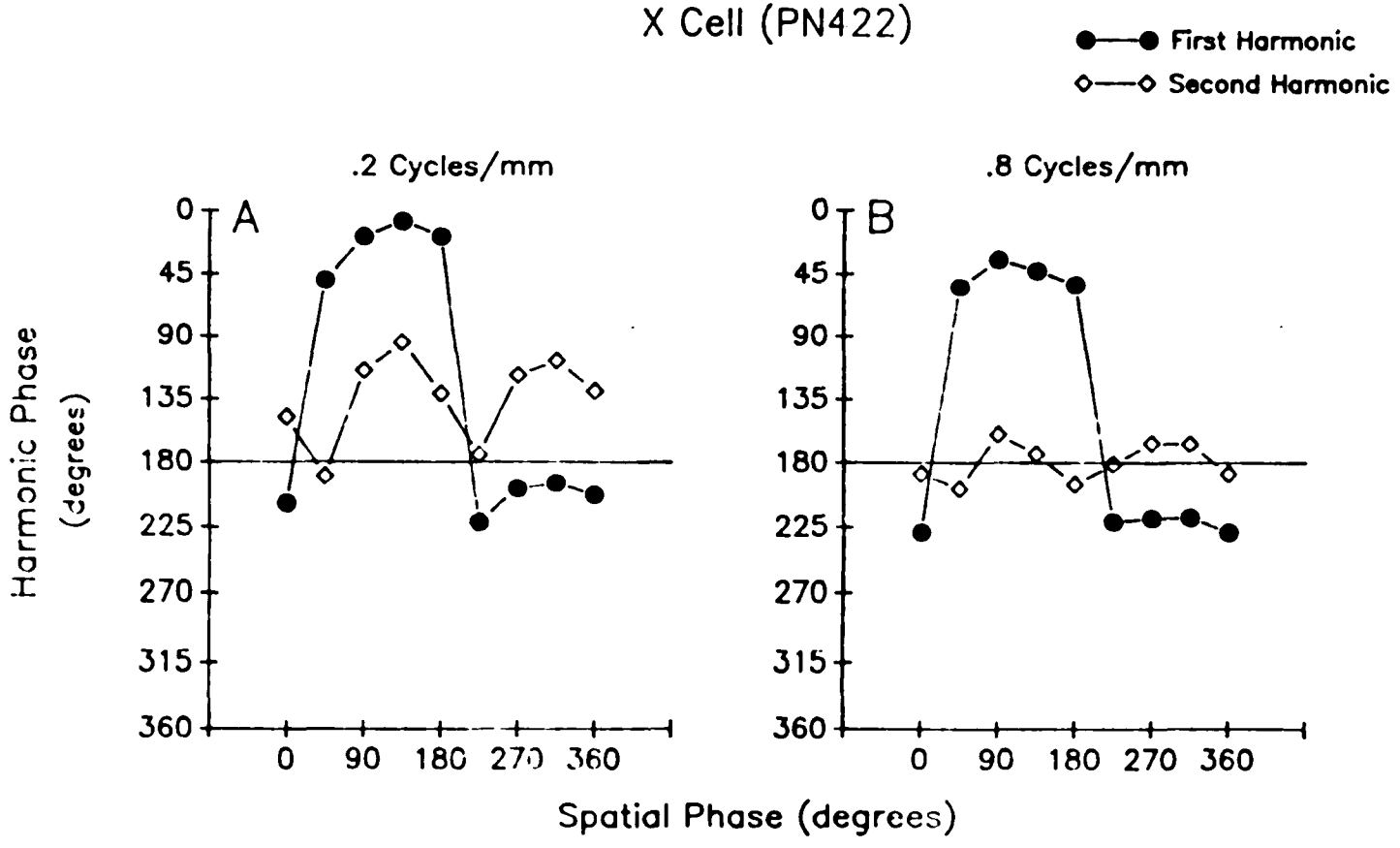

except that the second harmonic never displays a 180 degree phase shift. This fluctuation in the temporal phase of X cell second harmonics, especially at high spatial frequencies (Figure 8B), serves to distinguish them from the frequency doubled responses of Y cells which display no variation in temporal phase with stimulus spatial phase at high spatial frequencies which are optimal for eliciting subunit activity (see Figures 18B and 18C, for example).

With the exception of linear spatial summation, X cells differed considerably with respect to a number of other response features. The X classification cut across Hartline's response categories: 66% were 'off', 17% 'on', and 17% 'on-off'. Givenn the apparent similarity between 'on-off' responses and frequency doubled responses in Y cells, it may seem unusual that the X class in the frog includes 'on-off' cells. It should be emphasized, however, that 'on-off' responses to uniform changes in illumination used to identify Hartline response types can arise from processes unrelated to spatial integration of patterned stimuli. Furthermore, the frequency doubling seen in Y cells (see section 3.3.1) is only evident when patterned stimuli are used.

X cells' responses to a variety of stimuli, similarly, varied widely along a continuum between sustained and transient. It should be emphasized that the use of 'sustained' and 'transient' to describe responses of cells

examined in the present study reflects a broader definition of these terms than that employed by Cleland, Dubin and Levick (1971) when classifying cells based on their responses to standing contrast. As employed herein, 'sustained' will refer to responding which persists throughout most or all of any stimulus' cycle (as in Figure 9C) while 'transient' will be used to delineate a response consisting only of a brief burst of impulses to any stimulus (as in Figure 9D).

Transient X cells were identical to those with more sustained responses in all aspects of spatial summation except with respect to the distribution of power across the first 10 harmonic response components. Figure 9 compares the power spectra from a sustained and a transient X cell. The corresponding response histograms of these two cells are presented in Figures 9C and 9D. For the sustained cell the most power was clearly contained in the first harmonic with progressively less power attributable to higher harmonics. In the transient cell, however, there was an approximate even distribution of power throughout all harmonics. This is as expected given that the width of the power spectrum of any system's response is inversely proportional to the duration of the response (Pickles, 1988). The lack of a clearly dominant first harmonic attests to the absence of sinusoidal modulation in the response profile indicating some nonlinearity in the cell's

Figure 9

Comparisons between a sustained and a transient X cell. The results of Fourier analysis of a sustained cell are shown in (A) and for a transient cell in (B). The response patterns corresponding to the power spectra in (A and B) are presented in (C) for the sustained cell and in (D) for the transient cell. The spatial frequency of the grating was .2 cycles/mm for the sustained cell and .4 cycles/mm for the transient cell. The grating was sinusoidally modulated at a rate of .5 Hz for the sustained cell and 1 Hz for the transient cell. Stimulus contrast was .5.

Comparisons Between Sustained And Transient X Cells

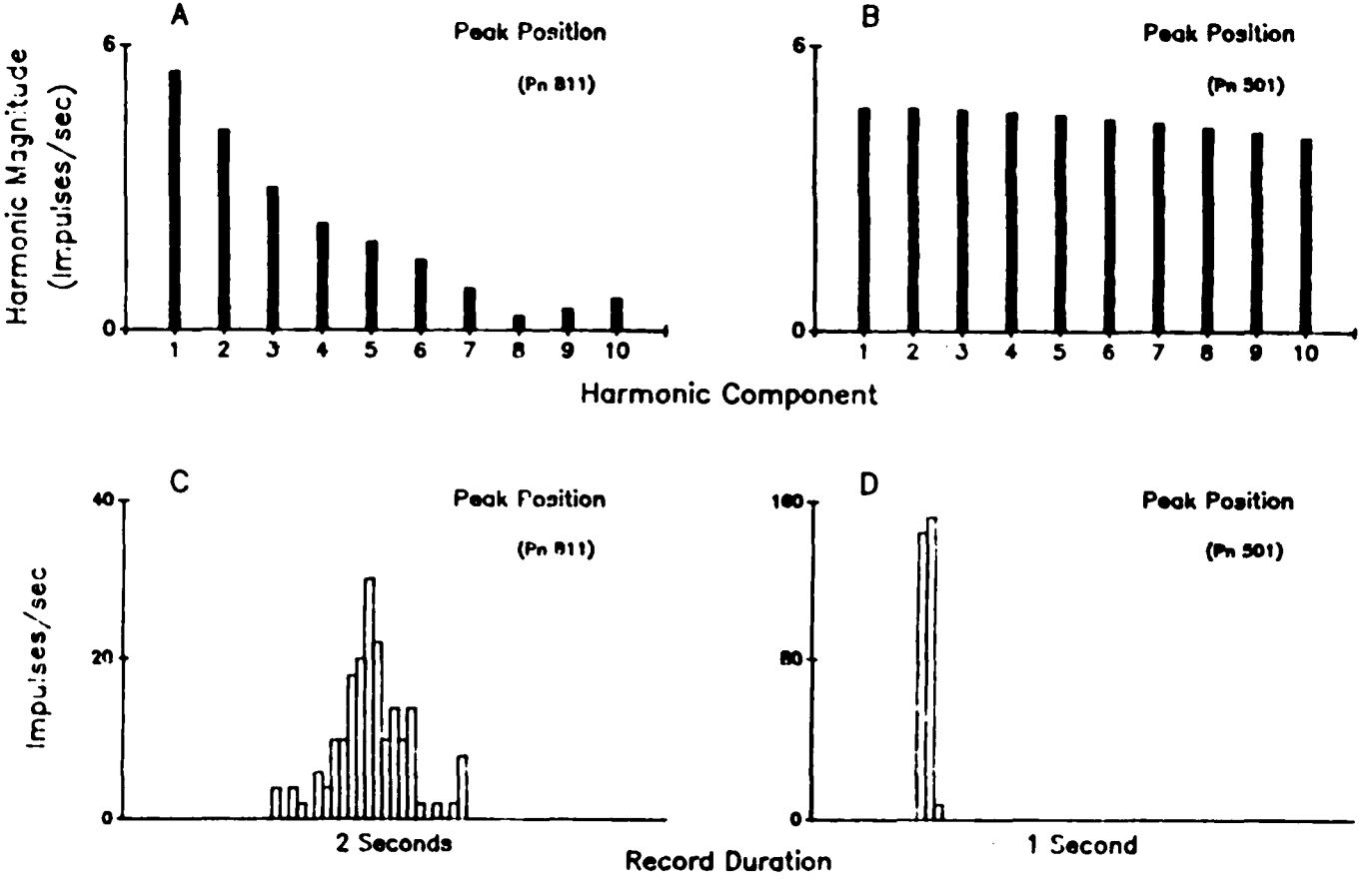

response. The absence of any dominant harmonic, however, indicates that responding in the transient X cell did not occur at a temporal frequency other than that present in the input. Power spectra from transient Y cells, for example, while displaying a similar uniform elevation of all harmonics, do show an increase in even harmonics relative to odd harmonics at high spatial frequencies when responding occurs at twice the input frequency (see Figure 20B).

One unusual X cell, which was 'on-off' to slow changes in full field illumination, deserves special mention. This cell exhibited linear spatial summation over a wide range of spatial frequencies (.2 to 3.2 cycles/mm). Responding had fallen to approximately zero for a spatial frequency of 6.4 cycles/mm. At a very high spatial frequency (25 cycles/mm), however, second harmonic responses appeared which were not as strong as those in Y cells at the same spatial frequency but which were nevertheless clearly evident in response histograms. These second harmonics appeared to be genuine on the basis of subsequent contrast gain determinations (see Figure 56) to be discussed in a later section (3.6.2). High spatial frequency induced second harmonics had also been observed in a few other X cells but were not noteworthy because their magnitudes were extremely low, as was overall responding, and therefore could not be reliably differentiated from noise.

The isolated occurrence of second harmonics at exceptionally high spatial frequencies does not detract from the linearity of integration manifested by frog X cells over a wide range of spatial frequencies. Rather, it may suggest that the mechanism responsible for the essential nonlinearity observed in Y cells' spatial summation is capable of also influencing X cells albeit to a lesser degree. A comparable conclusion was reached by Shapley and Victor (1979) regarding the source of contrast gain control effects in X cells in the cat.

3.2.2 Response to Drifting Gratings

Since they were typically determined at only one contrast, spatial frequency response (SFR) curves are not measures of sensitivity. They do, however, provide a preliminary indication of a cell's spatial frequency preference and its dependence upon drift rate.

The responsiveness of eleven X cells to drifting gratings was examined. Figure 10 demonstrates that X cells' responses to drifting gratings were typically modulated according to the drift rate, even for very high spatial frequencies which elicited very low levels of responding. The SFR obtained from the X cell shown in Figure 10 is presented in Figure 11. Both mean response rate as well as the magnitudes of the first two harmonics are plotted as a function of spatial frequency. The drift

Figure 10

Averaged response histograms from an X cell to drifting gratings ranging in spatial frequency from .2 to 3.2 cycles/mm (A,B,C,D, and E). The spatial frequency, in cycles/mm, is given above each response record. The drift rate of the grating was 1 Hz. The duration of each record represents one temporal cycle of the stimulus. The contrast of the grating was .5.

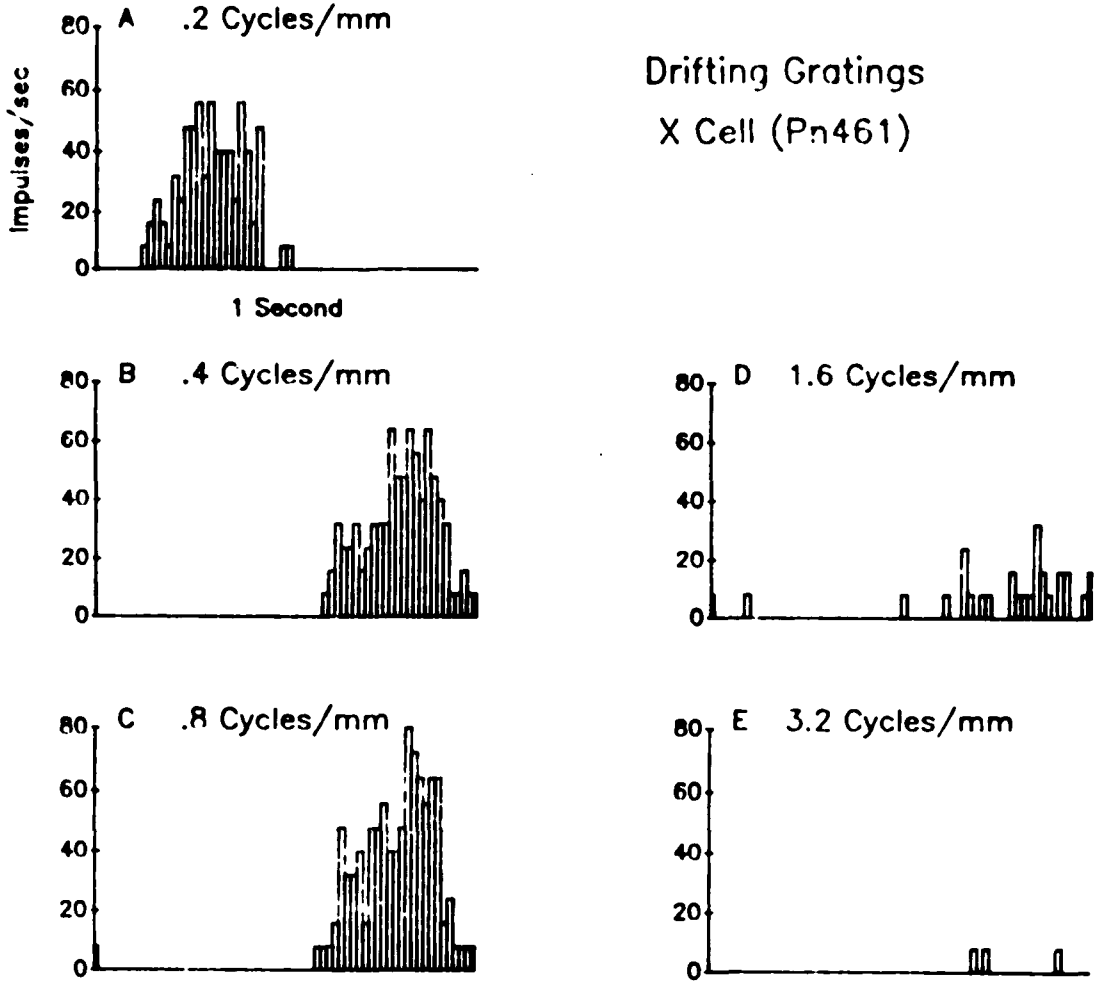

Drifting Gratings

X Cell (Pn461)

Figure 11

SFR, of the X cell in Figure 10, illustrating the correspondence between response rate and harmonic measures. Three response measures are plotted as a function of spatial frequency: mean response rate (filled circles), first harmonic magnitude (filled squares), and second harmonic magnitude (open squares). The drift rate of the grating was 1 Hz and contrast was .5.

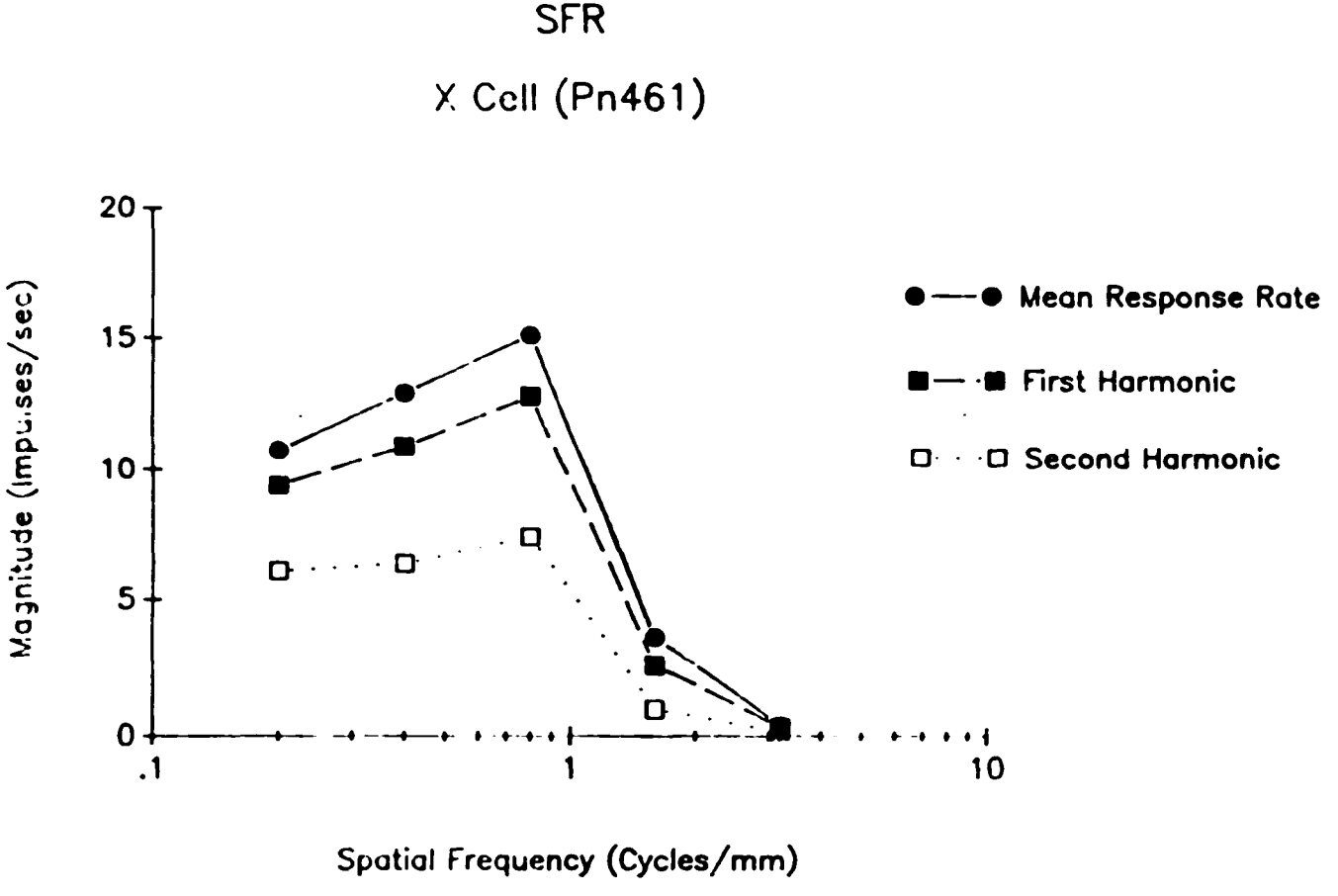
SFR
X Cell (Pn461)
20
15
10
5
0
.1
1
10
Magnitude (Impulses/sec)
Spatial Frequency (Cycles/mm)
Mean Response Rate
First Harmonic
Second Harmonic

rate of the grating, 1 Hz, was optimal for this particular cell. SFR functions obtained at other drift rates for this cell, while revealing comparatively lower response amplitudes, were identical in shape to that shown in Figure 11. Note especially the agreement between response rate and the first harmonic at all spatial frequencies, indicating that even low rates of responding were stimulus modulated.

One X cell, unusual with regard to a number of functional properties, produced frequency doubled responses to low spatial frequency gratings when a fast drift rate (8 Hz) was employed. Figure 12A displays the SFRs obtained at three drift rates (.125, 1, and 8 hz) for this cell with mean response rate plotted as the response measure. The corresponding magnitudes of the first and second harmonic components are shown in Figures 12B, C and D. At slow and moderate drift rates the first harmonic component was dominant. A low spatial frequency decline was evident at a moderate temporal modulation. This was, in fact, the only X cell to exhibit an interaction between optimal spatial frequency and temporal modulation. At 8 Hz, there is a minor attenuation of the first harmonic and a concomitant increase in second harmonic magnitude at a low spatial frequency. An additional feature, unique to this cell, was the striking difference observed between its responses to drifting as opposed to contrast reversed gratings. A

Figure 12

SFRs obtained at three drift rates in an X cell producing frequency doubled responses at a fast drift rate. In (A) mean response rate is plotted as a function of spatial frequency for three drift rates : .125 Hz (filled squares), 1 Hz (open squares), and 8 Hz (open triangles). In (B,C and D) the magnitudes of the first two harmonics are plotted as a function of spatial frequency for each of the three drift rates with drift rate given above each function. Filled circles refer to the first harmonic, open circles to the second harmonic. The contrast of all gratings was .5.

SFR

Frequency Doubled Response
In An X Cell (Pn92)

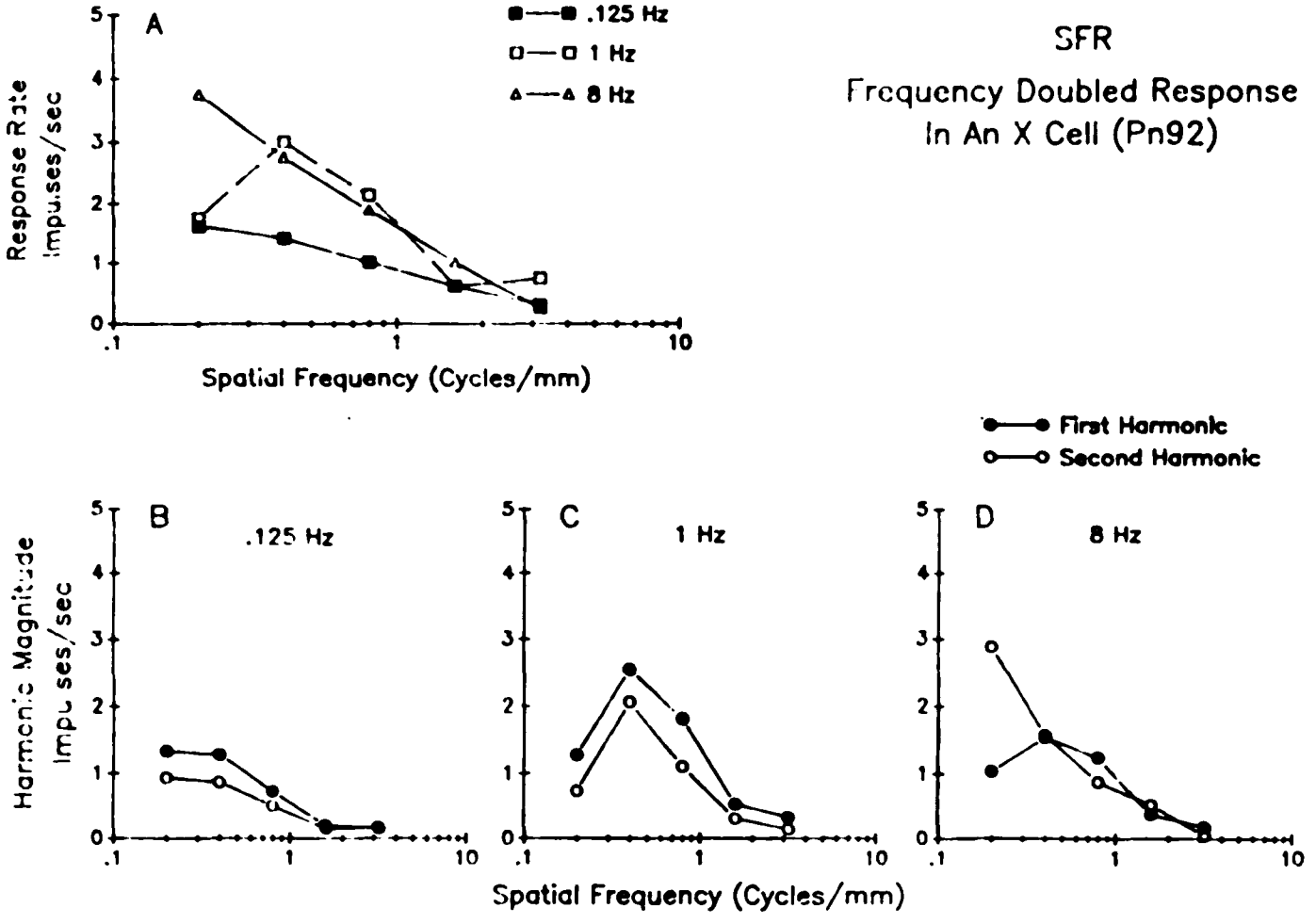

comparison of this cell's SFRs at the three drift rates, in Figure 12A, suggests a broad temporal tuning and a uniformly low responsiveness to drifting gratings. When contrast was reversed, however, at each of these three temporal modulations during the null test (Figure 13A), the cell's responses were finely tuned to the fast reversal rate. No substantial second harmonics were observed at this fast reversal rate (Figure 13D), nor was there any deviation from linear spatial summation at this or the other temporal modulations (Figures 13B, C, and D).

3.2.3 Spatial Frequency Response Curves

The majority of X cells (72%) - seven 'off' and one 'on-off' cell - showed no evidence of diminished responsiveness to the lowest spatial frequency (.2 cycles/mm) employed in these tests. The absence of a low frequency decline in a cell's SFR does not necessarily preclude the existence of a suppressive surround. If the RF center is very large the possibility exists that one-half cycle of the lowest spatial frequency fills the center without encroaching upon the surround as the grating drifts across the cell's RF. If an inhibitory surround exists in cells with exceptionally large RF centers, only uniform changes in illumination would mutually stimulate center and surround regions in an antagonistic manner. Such full field stimulation can be considered therefore as having a

Figure 13

Null test results for the X cell in Figure 12 at three reversal rates. In (A) mean response rate is plotted as a function of spatial phase for each of three reversal rates : .125 Hz (filled squares), 1 Hz (open squares), and 8 Hz (open triangles). In (B,C, and D) the magnitudes of the first (filled circles) and second (open diamonds) harmonics for each of the three reversal rates are plotted as a function of spatial phase. Stimulus reversal rate is given above each function. Responses occurring during the first half of the grating's temporal cycle are plotted as positive values while those produced during the second half of the cycle are plotted as negative values. The solid lines represent the best fit sinusoid for the mean response rate in (A) and for the first harmonic component in (D). The spatial frequency of the grating was .2 cycles/mm. The contrast of the grating was .5.

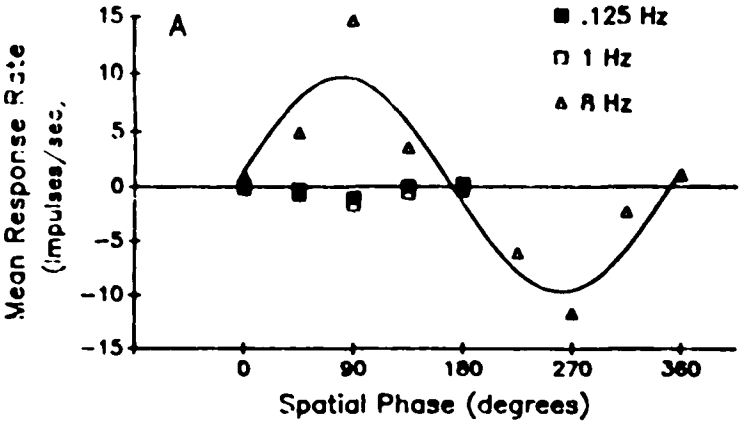

Null Test

Narrow Temporal Tuning
In An X Cell (Pn92)

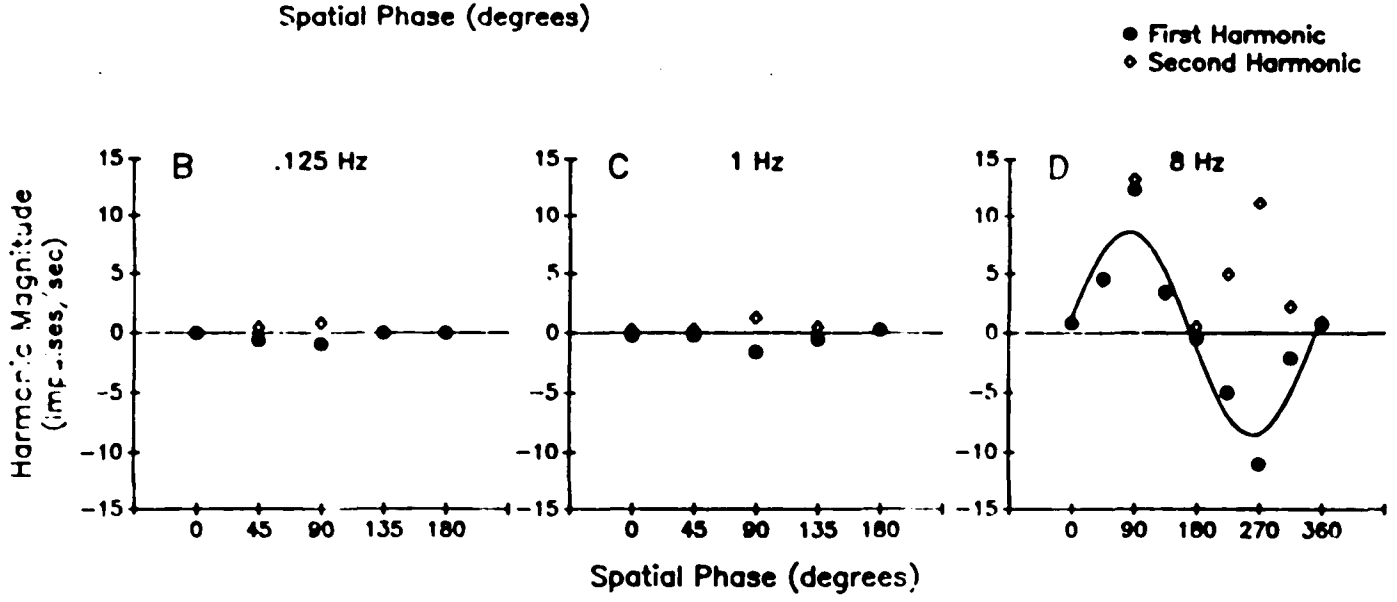

spatial frequency of 0 cycles/mm. Therefore, an inhibitory surround can be demonstrated if responsiveness to full field stimulation is decreased relative to that recorded for the lowest spatial frequency (.2 cycles/mm). A comparison of responsiveness to uniform stimulation vs low spatial frequencies was performed in a few X cells. There was no indication of a suppressive surround in any of these cells (see Figure 14, for example). Of course, the issue of an inhibitory surround remains unresolved in those X cells not similarly examined.

Among X cells not displaying a low frequency decline, a very abrupt high frequency cut-off was typical in most 'off' X cells; only two displayed more moderate high frequency declines. The 'on-off' cell displayed a more gradual high frequency decline . The SFR curves of a representative 'off' cell and the 'on-off' cell are presented for comparison in Figure 14. Because the fundamental is the dominant response component in X cells, the first harmonic's magnitude is the response measure in Figure 14. Responses to full field stimulation (0 cycles/mm) are included.

Only two X cells, one 'on' and one 'off' cell, showed low frequency declines at all drift rates. Figure 15 presents the SFR curves of these two cells. The two cells differed, however, in the rate of decline in responsiveness to high spatial frequencies. Even though the optimum

Figure 14

SFRs of an 'off' and an 'on-off' X cell showing no low frequency declines but differing in the rate of high frequency decline. The relative response measure is the magnitude of the first harmonic plotted as a percentage of the maximal response obtained at the optimal spatial frequency. Full field changes in intensity are plotted on the X axis as 0 cycles/mm. The drift rate of the gratings was 1 Hz. Full field intensity was square wave modulated above and below the mean intensity level at a rate of 1 Hz. The contrast of all stimuli was .5.

SFR
Off vs On–Off X cell

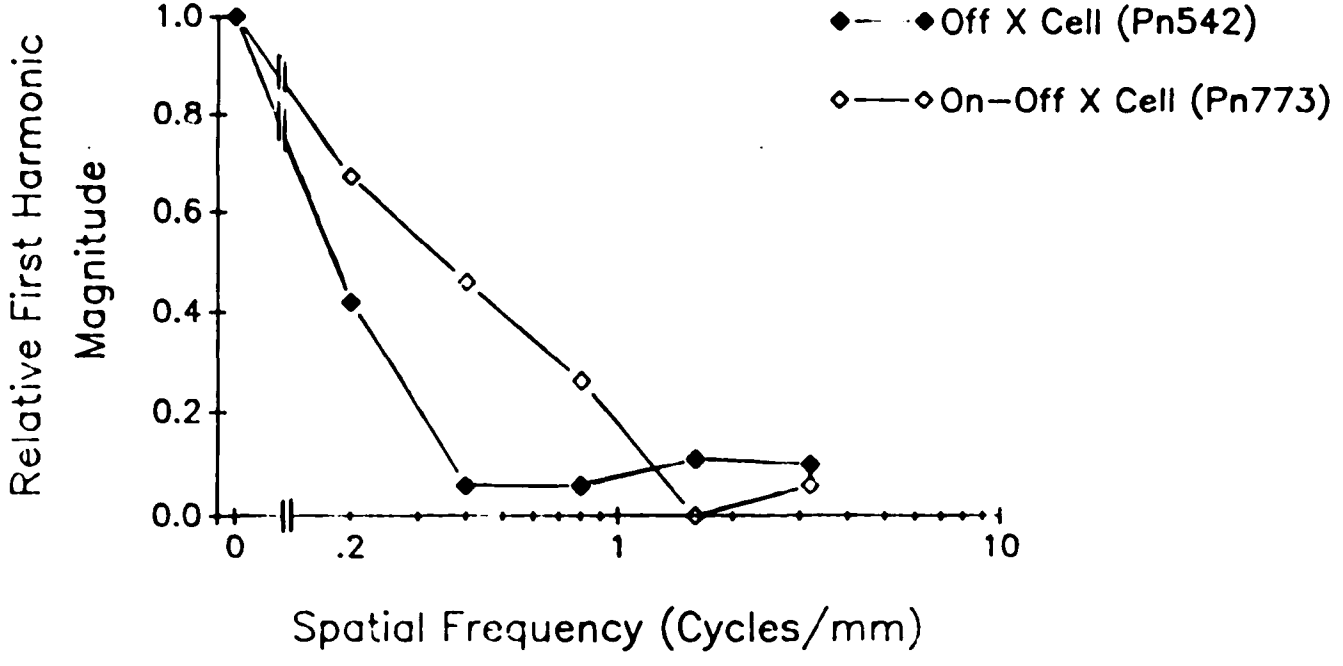

Figure 15

SFRs of an 'on' and an 'off' X cell showing low frequency attenuation but differing in the rate of high frequency decline. The relative response measure is the magnitude of the first harmonic plotted as a percentage of the maximal response obtained at the optimal spatial frequency. The stimulus was a 1 Hz drifting grating with a contrast of .5.

SFR
On vs Off X Cell

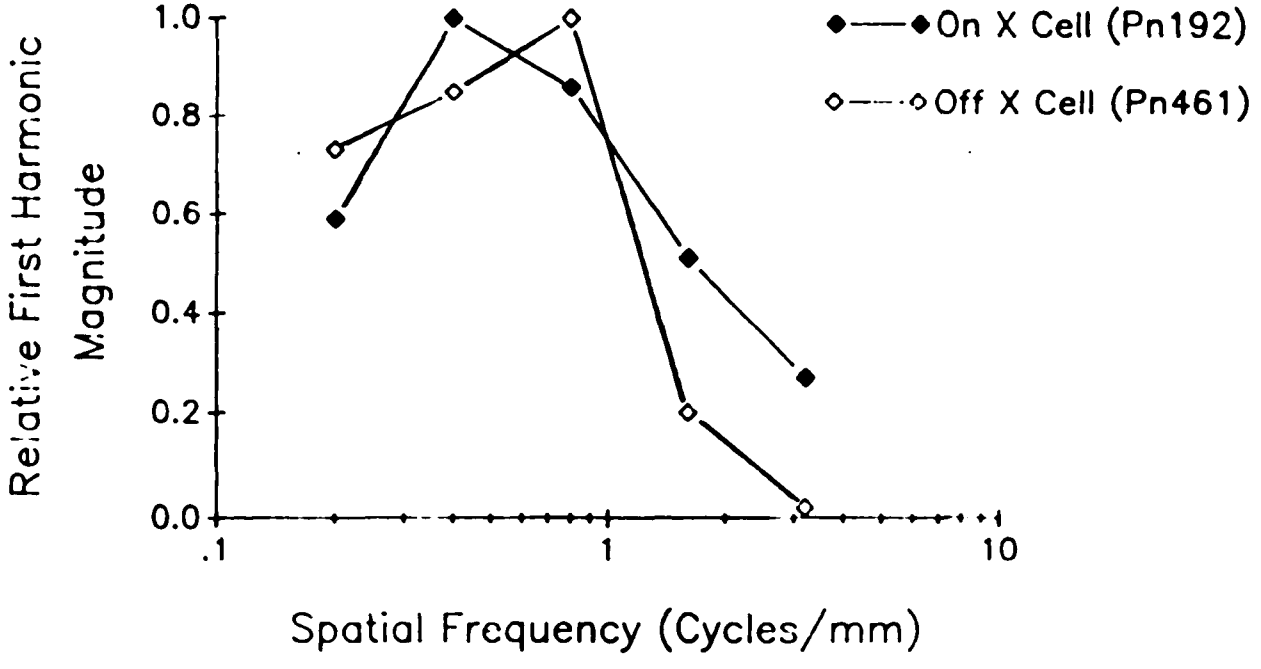

spatial frequency for the 'off' cell was higher than that for the 'on' cell, the 'off' cell's responsiveness decreased much more rapidly to high spatial frequencies.

3.2.4 Receptive Field Profile.

Because most X cells were lost relatively soon after they were isolated, systematic examination of their RF profile could be performed in only a few cells. Because of this small sample it was difficult to draw any general conclusions regarding the RF organization of X cells since it was questionable whether observed differences among cells represented minor or important RF variations. The three 'off' cells examined all possessed extensive RF centers which was expected given the lack of a low frequency decline and the rapid high frequency cut-off in these cells' SFRs. In two of these cells responsiveness was distributed across the RF in a Gaussian-like fashion. The third 'off' cell possessed an unusual RF profile in which responsivity displayed a somewhat skewed distribution. The one 'on-off' cell examined possessed a small 'off' center with a minor 'on' region spread evenly throughout. This was the same 'on-off' cell which had produced second harmonics at a very high spatial frequency.

3.3 Y Cells

Thirty-two cells were clearly identified as Y cells.

The classification of cells as "Y", as for the X class, cut across distinctions based upon Hartline response types. In general, Y cells in the frog displayed close similarity to those described in the cat in terms of the essential nature of their summation processes: frequency doubled responses which were insensitive to spatial phase at moderate to high spatial frequencies. Specific differences, which will be addressed in the following sections, did however exist. One unexpected finding was the existence of at least two clearly distinct groups of Y cells in the frog.

3.3.1 Spatial Summation

Responses from a representative Y cell to three spatial frequencies during the null test are shown in Figure 16. Almost all Y cells examined in this project displayed the progression from linear to nonlinear summation typified by the cell shown in Figure 16. At a low spatial frequency, peak responses were modulated according to the stimulus' temporal frequency and occurred to phase angles 90 degrees away from those resulting in null responses. No frequency doubling was evident at null positions. Y cells' behavior at low spatial frequencies, therefore, was identical to that observed in X cells. Frequency doubling was not evident until higher spatial frequencies were employed, occurring typically to relative stimulus phase angles which, at low spatial frequencies,

Figure 16

Averaged response histograms obtained from a Y cell to three positions of a contrast reversal grating. The spatial frequency of the grating was .2 cycles/mm for the top row, .8 cycles/mm for the middle row, and 3.2 cycles/mm for the bottom row. The relative spatial phase angle, in degrees, of the grating is indicated above each histogram. The grating's contrast was sinusoidally modulated at a rate of 1 Hz. The duration of each response record represents one temporal cycle of the stimulus. The contrast of the grating was .5 .

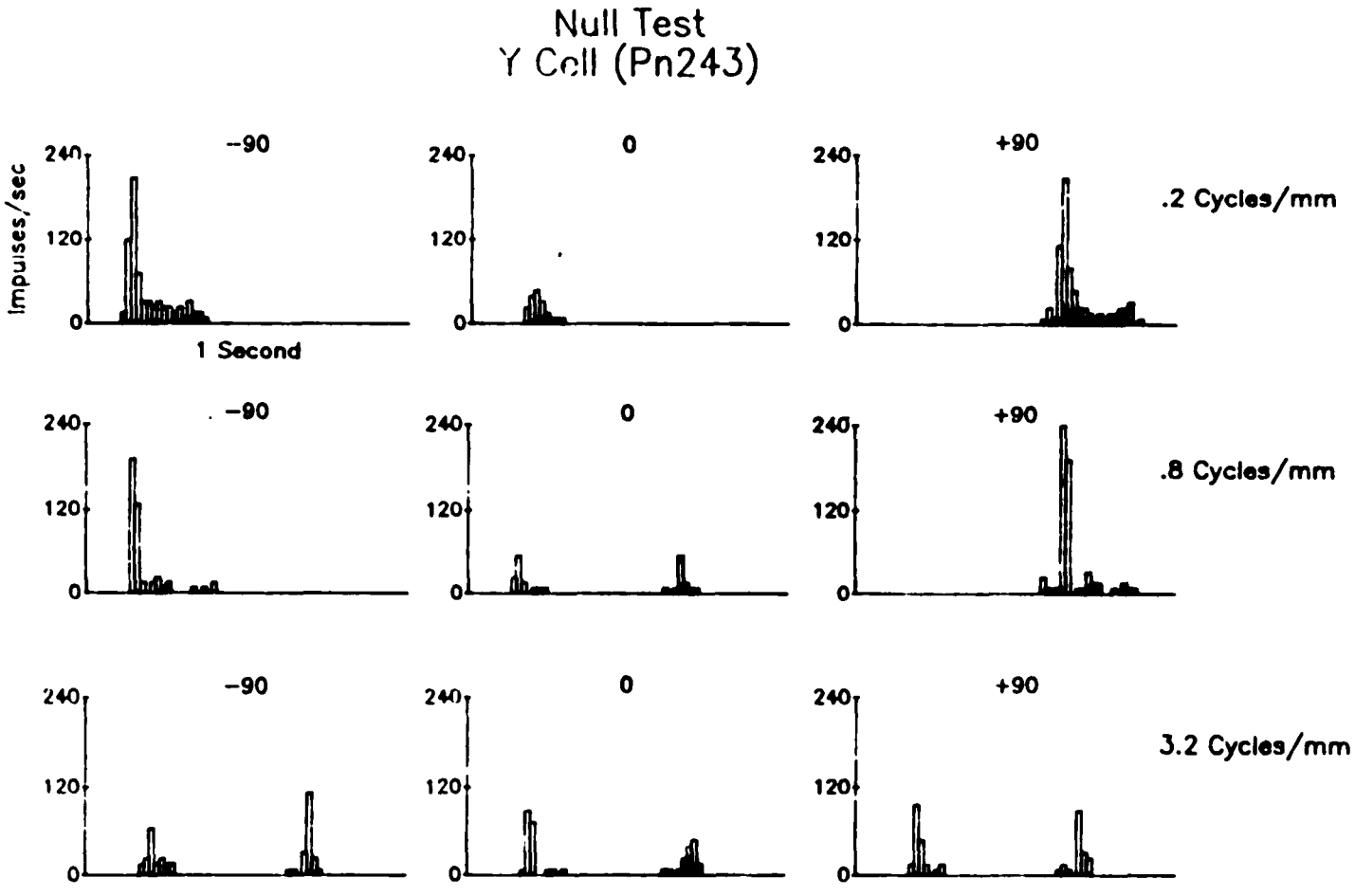
Null Test
Y Cell (Pn243)
Impulses/sec
240
120
0
-90
0
+90
1 Second
.2 Cycles/mm
.8 Cycles/mm
3.2 Cycles/mm

had resulted in null responses. Peak responses continued to be modulated at the stimulus reversal rate. As increasingly finer gratings were presented, frequency doubled responses were produced to all phase angles of the grating. It should be noted that the transient peak responses of the cell shown in Figure 16 were not characteristic of all frog Y cells, the majority of which produced more sustained responses.

Figure 17 presents the first and second harmonic magnitudes of the responses of the cell in Figure 16, as a function of spatial phase, at three spatial frequencies. The first harmonic displays a sinusoidal relationship to stimulus phase at a low spatial frequency and is dominant at all phase angles. At a moderate spatial frequency the first harmonic continues to maintain a sinusoidal dependence upon stimulus phase but the second harmonic now dominates at spatial phases representing null positions for the fundamental. At a high spatial frequency the fundamental's magnitude has decreased to nearly zero while the second harmonic dominates at all phase angles and is insensitive to the spatial phase of the stimulus. These findings correspond to those reported for cat Y cells with one exception: in cat Y cells, second harmonics are evident at null positions for relatively low spatial frequencies. A substantial second harmonic component of Y cell responses in the frog, however, was not observed until

Figure 17

The magnitudes of the first and second harmonics of a Y cell's response as a function of spatial phase of a contrast reversal grating. By convention, responses occurring during the first half of the grating's temporal cycle (i.e., responses with a temporal phase of less than 180 degrees) are assigned positive values. Responses produced during the second half of the stimulus cycle, thus possessing a temporal phase equal to or greater than 180 degrees, are assigned negative values. The results from three spatial frequencies are shown in (A,B, and C). The spatial frequency of the grating is indicated above each function. The first harmonic component is represented by filled circles, the second harmonic component by open diamonds. The reversal rate of the grating was 1 Hz and the contrast was .5 . The solid line represents the best fit sinusoid for the first harmonic response component.

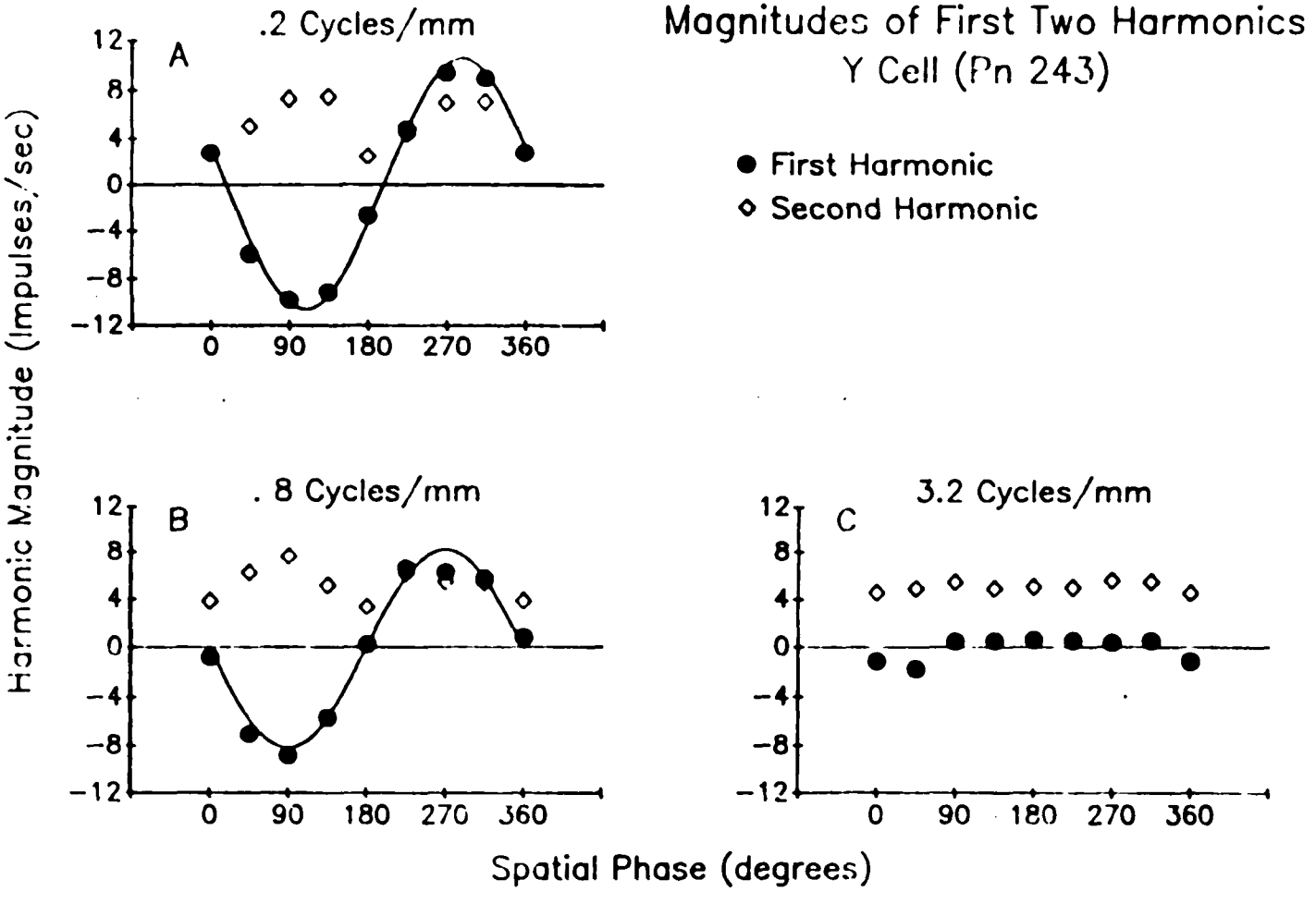
Magnitudes of First Two Harmonics
Y Cell (Pn 243)
● First Harmonic
◇ Second Harmonic
A
.2 Cycles/mm
B
. 8 Cycles/mm
C
3.2 Cycles/mm
Harmonic Magnitude (Impulses/sec)
12
8
4
0
-4
-8
-12
0
90
180
270
360
Spatial Phase (degrees)

moderate spatial frequencies were employed. The implications of this difference will be explored in the Discussion.

Figure 18 presents the temporal phases of the first and second harmonic components of a Y cell's response plotted as a function of a contrast reversed grating's spatial phase. As with X cells, the temporal phase of the first harmonic component of Y cells shifts by 180 degrees at spatial phases of the grating corresponding to the cell's null position (0 and 180 degrees) so that temporal phases of responses to stimulus spatial phase angles 180 degrees apart are themselves separated by 180 degrees. This spatial phase dependent temporal phase shift in the first harmonic is maintained with increasing spatial frequency until the frequency is above the spatial resolution of the Y cell's linear mechanism (Figure 18C). At a low spatial frequency the second harmonic component of the frog Y cell is essentially due to the rectification produced by the lack of spontaneous activity. Thus, in Y cells, the fluctuation in temporal phase of the second harmonic across spatial phase at low spatial frequencies is similar to that seen in X cells (see Figure 8 for example). It is only when higher spatial frequencies are used that the spatial phases insensitivity of the temporal phase of the second harmonic is seen in frog Y cells.

The change from linear to nonlinear summation does not

Figure 18

Temporal phase of first (filled circles) and second (open diamonds) harmonics of a Y cell's response as a function of spatial phase of a low (A), moderate (B) and high (C) spatial frequency contrast reversed grating. Temporal phases less than 180 degrees reflect responding during the first half of the stimulus' temporal cycle while phases equal to or greater than 180 degrees indicate responding during the second half of the stimulus cycle. The spatial frequency of the grating is given, in cycles/mm, above each graph. One complete spatial cycle of the grating is represented in each graph. The contrast of the grating was .5 and reversal rate was sinusoidally modulated at 1 Hz.

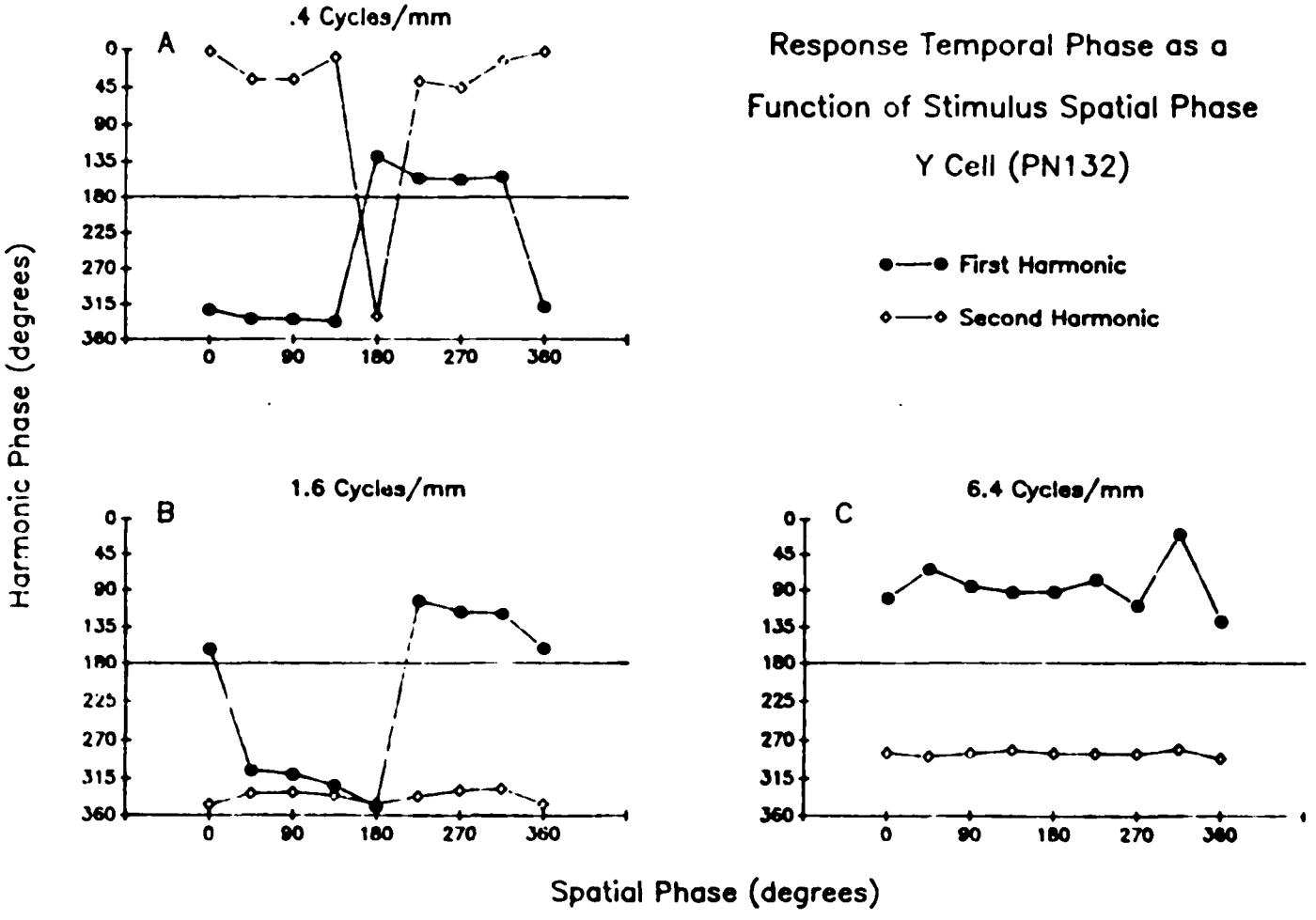
Response Temporal Phase as a
Function of Stimulus Spatial Phase
Y Cell (PN132)
First Harmonic
Second Harmonic
.4 Cycles/mm
A
1.6 Cycles/mm
B
6.4 Cycles/mm
C
Harmonic Phase (degrees)
Spatial Phase (degrees)
0
45
90
135
180
225
270
315
360

simply reflect a shift in strength from the first to second harmonic. There is a global shift in the distribution of power among all harmonics. Two power spectra, showing the magnitudes of the fundamental and the next nine harmonics for a Y cell at a peak position for a low and a high spatial frequency, are presented in Figures 19A and 19B, respectively). For comparison, two power spectra of an X cell's peak responses, at the same spatial frequencies, are shown in Figures 19C and 19D.

While the most power is contained within the first harmonic when Y cell summation is linear at a low spatial frequency, all odd harmonics reveal a slight elevation relative to even harmonics. Similarly, second harmonic dominance, at a high spatial frequency, is mirrored by relative increases in all even harmonics. Compare this to the power distribution for the X cell at the same high spatial frequency in which a uniform decrease in power but no shift in dominance from the fundamental or other odd harmonics is seen. The power spectra shown in Figures 19A and 19B were obtained from a Y cell producing sustained peak responses. Transient Y cells, like transient X cells described in the previous section, differ only in terms of the general shape of their power spectra (Figure 20). A comparison between Figures 20A and 20B reveals that the power spectra of a transient Y cell's responses still display the shift to elevated second and other even order

Figure 19

Fourier analyses of a Y and an X cell's peak responses at low and high spatial frequencies. The Y cell's power spectra are shown in (A), for a spatial frequency of .4 cycles/mm, and in (B), for 1.6 cycles/mm. The power spectra of the X cell at .4 and 1.6 cycles/mm are shown in (C) and (D), respectively. The stimulus was a contrast reversal grating, with a contrast of .5, which was sinusoidally modulated at .5 Hz for the X cell and at 1 Hz for the Y cell.

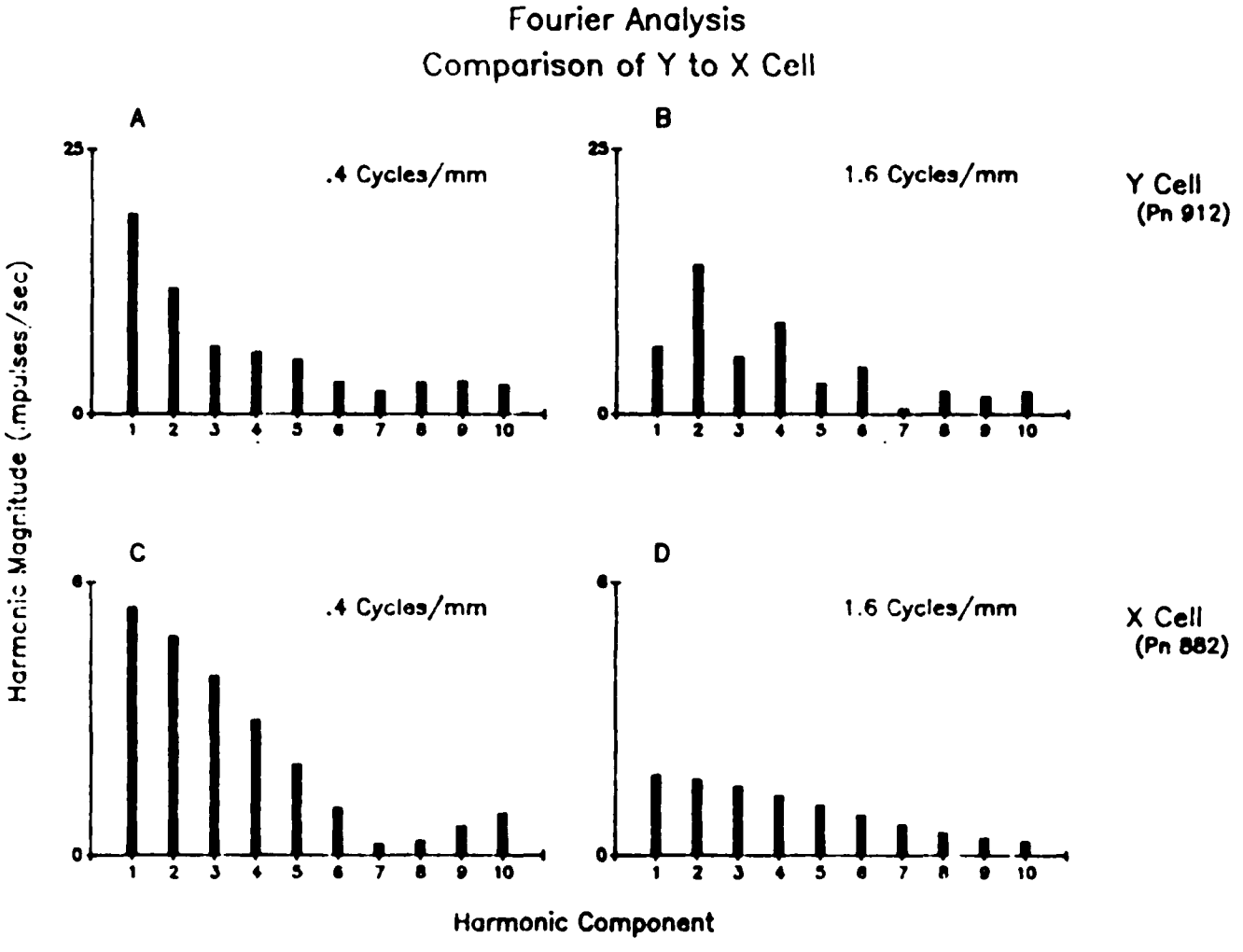
Fourier Analysis
Comparison of Y to X Cell
A
B
C
D
.4 Cycles/mm
1.6 Cycles/mm
.4 Cycles/mm
1.6 Cycles/mm
Y Cell
(Pn 912)
X Cell
(Pn 882)
Harmonic Magnitude (impulses/sec)
Harmonic Component
0
1 2 3 4 5 6 7 8 9 10

Figure 20

Fourier analysis of a transient Y cell's peak responses at low and high spatial frequencies. The stimulus was a contrast reversal grating with a contrast of .5 which was sinusoidally modulated at 1 Hz. The spatial frequency of the grating was .4 cycles/mm in (A) and 2.4 cycles/mm in (B).

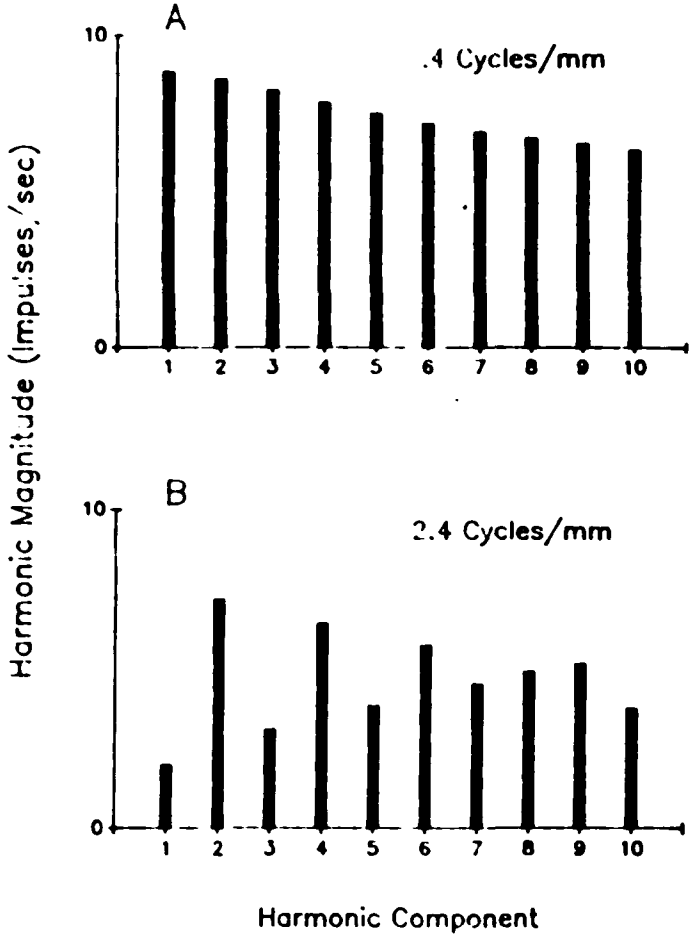

Fourier Analysis

Transient Y Cell (Pn 293)

harmonics with increasing spatial frequency.

Figure 21 presents the second/first harmonic ratios, calculated for four Y cells, as a function of spatial frequency. For the reasons previously noted for X cells, only spatial frequencies eliciting substantial response rates were included in ratio determinations. A comparison among these four cells reveals that the optimum spatial frequency for second harmonic activity varied widely across Y cells. One explanation for this variability might well be related to differences in the retinal locus among Y cells. Since, however, the exact location of a given Y cell was not identified it is impossible to make any statements regarding the relationship between retinal eccentricity and the spatial resolution of Y cells' nonlinear subunits. Not all of the variability, however, appeared to be related to variation in retinal location. Two subgroups of Y cells, distinct according to a number of functional characteristics, tended to differ in terms of the spatial frequency which elicited maximal second harmonic responses. Thus, the preferred spatial frequency of the subunits appears to be, in part, dependent on the type of Y cell examined. Additional differences between these two subgroups will be discussed in detail in subsequent sections.

Figure 21 also reveals that the optimum spatial frequency of many Y cells' nonlinear mechanism was quite

Figure 21

Second/first harmonic ratios as a function of spatial frequency for four Y cells. Ratios were calculated as described for Figure 6. For all cells the stimulus was a contrast reversal grating sinusoidally modulated at 1 Hz. The contrast of all gratings was .5.

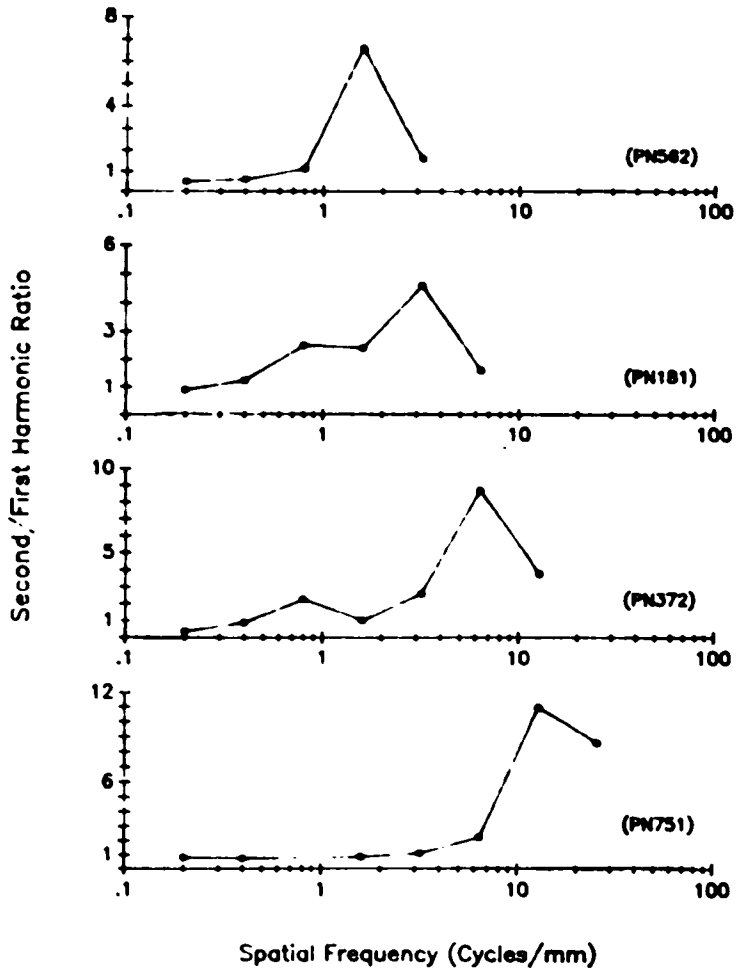

Second/First Harmonic Ratio

Y Cells

high. For the majority of Y cells (62%) second harmonic magnitudes peaked at spatial frequencies between 6.4 and 12.8 cycles/mm which is equivalent to .3 to .6 cycles/degree assuming that 1 degree of visual angle corresponds to 48 microns on the frog's retina (Maturana, Lettvin, McCulloch, and Pitts, 1960). The second harmonic component of a few Y cells (9%) was optimally responsive to spatial frequencies as high as 25 cycles/mm (1.2 cycles/degree). In a direct comparison to cat Y cells, which exhibit maximal frequency doubling to spatial frequencies higher than .5 cycles/degree (Hochstein and Shapley, 1976a), the subunits of many frog Y cells would appear to be somewhat inferior in their resolution capabilities. Consider, however, the spatial resolution of a an individual cell's subunits relative to the resolution of its linear component. The spatial frequencies which were optimal for subunit activity in the majority of frog Y cells were five to seven octaves higher than the optimal frequency for the cells' linear mechanisms. In the cat, the size of an individual subunit is approximately one-third the size of the cell's linear center, indicating only a three octave difference in spatial frequency sensitivity between nonlinear subunits and linear components.

Given the exceptional spatial sensitivity of the subunits of a few frog Y cells, steps were taken to insure

that these measures were not artifactual, i.e., resulting from coincidental nonlinearities in the stimulus display. One possibility considered was that a nonlinear interaction between the display oscilloscope and the V2 stimulator resulted in some minor fluctuations in mean intensity at these high spatial frequencies. Thus, the responses observed in these Y cells would, in fact, be 'on-off' responses to adventitious full field stimulation. Careful examination of the input/output dynamics of the display oscilloscope at these high spatial frequencies, however, did not reveal any fluctuations in intensity unrelated to the intended reversal pattern.

It could still be argued, however, that incidental nonlinearities in the equipment may have occurred occasionally and, therefore, may have not been detected during an examination of the equipment. A number of considerations suggest that, even if this were the case, it cannot adequately explain these cells' responses. Firstly, many of the Y cells showing exceptional sensitivity produced either pure 'on' or 'off' responses to full field stimulation at the temporal modulation used for the null test. Thus, it is unlikely that they would produce on-off' responses to low level fluctuations in mean intensity. Secondly, as noted earlier, robust second harmonic activity at these high spatial frequencies was characteristic of one group of Y cells but not necessarily of the other. The

exceptional spatial frequency sensitivity of many Y cells, therefore, appears to be a genuine property of the nonlinear subunits of a particular subgroup of Y cells.

3.3.2 Receptive Field Profile

Most of the Y cells, in which RF profiles were examined, were clearly divisible into two major groups - labelled Y1 and Y2 - based upon different RF organizations. In addition to RF organization, a number of functional differences served to further distinguish between these two subgroups. One of these differences - spatial preference of the nonlinear mechanism - was briefly mentioned earlier, the rest will be discussed subsequently.

3.3.2.1 Y1 Cells

Many of the Y cells (50%) possessed a RF which was quite large (approximately 5 mm) and Gaussian-like in distribution of sensitivity across the RF. There was no consistent trend among these cells in terms of full field response: four were 'off', two 'on', and two 'on-off'. For 'on-off' cells both 'on' and 'off' regions were spatially coextensive and the relative weights of these two components remained relatively stable throughout the full extent of the RF. Figures 22A and 22B show examples of this RF organization in an 'off' and an 'on-off' Y cell, respectively.

Figure 22

Receptive field profiles of two Y1 cells. (A) and (B) display the functions from an 'off' and an 'on-off' cell, respectively. The response measure is the mean response rate of 'on' responses (open circles) and 'off' responses (filled circles). The receptive field was mapped with a .5mm wide bar which was square wave modulated, at a rate of 1 Hz, above and below the mean intensity of the background. The contrast of the bar, relative to the background, was .5. The X axis indicates the location of the bar, in mm, on the retina.

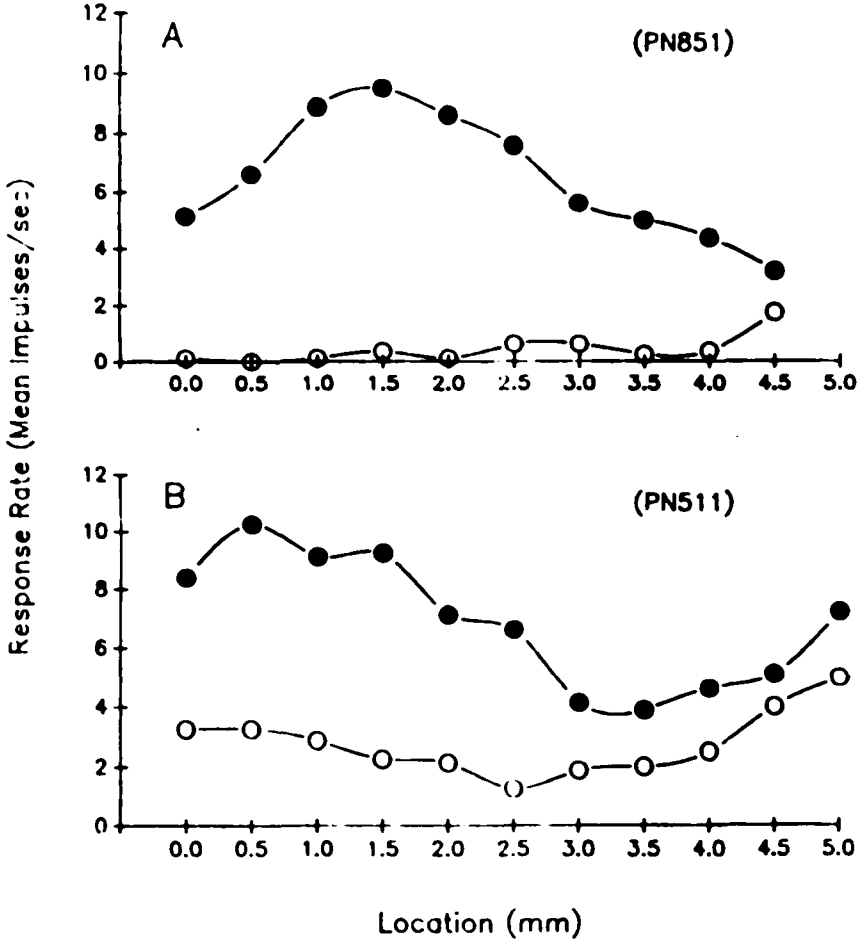

Receptive Field Profile

Y1 Cells

o—o "On" Responses

●—● "Off" Responses

3.3.2.2 Y2 Cells

The second major type of RF organization found in Y cells was generally smaller than the aforementioned group (approximately 3 mm). Examination of the RF revealed a central area (1.5 mm) flanked by smaller regions (1mm) which produced responses opposite in sign to those elicited from the center. Of 16 Y cells in which the RF was explored, (31%) fell into the Y2 category. As in the Y1 group, there was no typical full-field response type among Y2 cells: two were pure 'off', two were 'on-off' and one was 'on' with a very minor 'off' component. Examples of this type of RF organization in an 'on-off' and an 'off' Y cell are shown in Figures 23A and 23B respectively.

While the RF organization, characteristic of the Y1 cells, was also found in X cells the flanking organization of the Y2 RF appeared to be specific to Y cells.

3.3.2.3. Other

Of the three remaining Y cells, in which the RF was explored, only one cell clearly possessed a RF type distinct from that of either Y1 or Y2 cells. This cell produced 'on-off' responses to changes in full field illumination. Its RF (Figure 24) possessed a narrow central 'off' region with some evidence of a very minor

Figure 23

Receptive field profiles of two Y2 cells. (A) and (B) display the functions of an 'on-off' and an 'off' cell, respectively. The response measure is the mean response rate of 'on' responses (open circles) and 'off' responses (filled circles). The bar used to map the receptive field was .5 mm in width, had a contrast of .5 relative to the background, and was square wave modulated above and below the mean intensity of the background. For the 'on-off' cell in (A), the stimulus was temporally modulated at a rate of .125 Hz. For the 'off' cell in (B), a 1 Hz modulation was used.

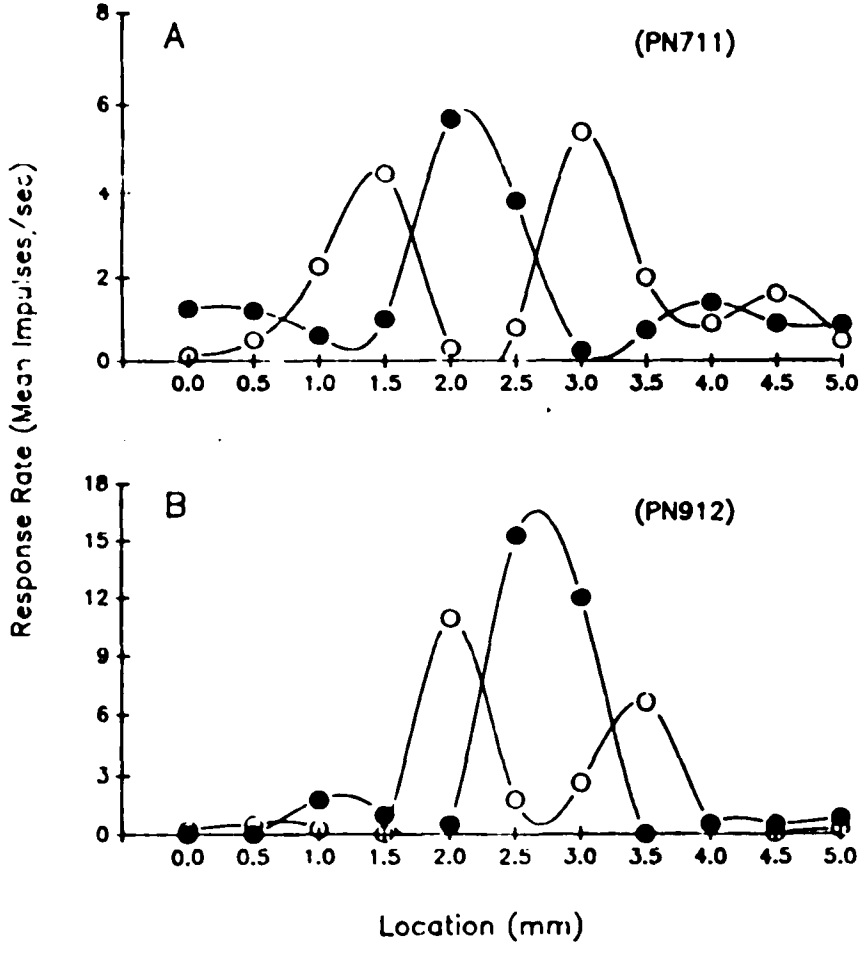

Receptive Field Profile

Y2 Cells

o—o "On" Responses

●—● "Off" Responses

Figure 24

Receptive field profile of a Y cell distinct from the Y1 or Y2 type. The response measure is the mean response rate of 'on' responses (open circles) and 'off' responses (filled circles). The bar used to map the receptive field was .5 mm in width, had a contrast of .5 relative to the background and was square wave modulated above and below the mean intensity of the background at a rate of 1 Hz.

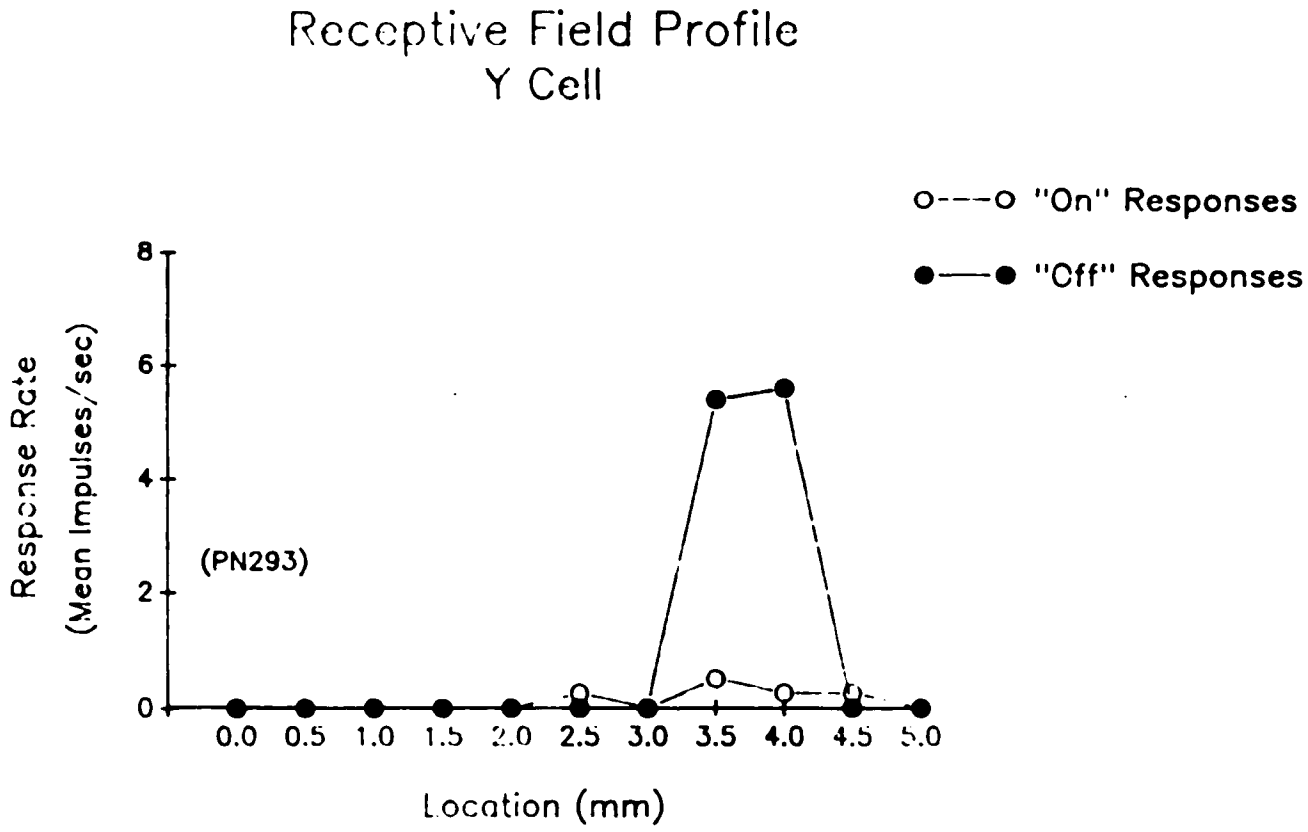
Receptive Field Profile
Y Cell
o---o "On" Responses
●—● "Off" Responses
Response Rate
(Mean Impulses/sec)
8
6
4
2
0
(PN293)
0.0 0.5 1.0 1.5 2.0 2.5 3.0 3.5 4.0 4.5 5.0
Location (mm)

'on' region. For the other two cells the possibility existed that the temporal modulation of the bar used to map the RF was not optimal for exposing flanking regions. Therefore, it is unclear whether or not these two cells may have in fact been Y2 cells. All of these cells had small RFs (1.5 mm in extent) compared with that of the other Y cells .

3.3.3 Y1 vs Y2: Spatial Summation

As previously noted, the high spatial frequency cut-off for the nonlinear mechanism tended to be higher for one group of Y cells than the other; these two groups corresponded, respectively, to Y1 and Y2 cells. The optimum spatial frequency ranged from 6.4 to 12.8 cycles/mm for Y1 cells and from 1.6 to 6.4 cycles/mm in Y2 cells (see Table 1).

These two groups also differed in terms of the effect that increasing spatial frequency had upon responding as spatial summation became progressively more nonlinear. Figure 25 shows both the maximum response rate and second/first harmonic ratio as a function of spatial frequency for a Y1 and Y2 cell. Most Y1 cells (77%) displayed a substantial decrease in responding, prior to maximum second harmonic activity at higher spatial frequencies, when a moderate spatial frequency was presented. The two exceptions included one cell which

Table 1

Optimal Spatial Frequency For Maximal Second Harmonic Magnitudes by Y Cell Subgroup

		Spatial Frequency (cycles/mm)				
		1.6	3.2	6.4	12.8	Total
Y Cell	Y1	0	0	6	3	9
Subgroup	Y2	2	2	1	0	5
	Total	2	2	7	3	

Figure 25

Second/first harmonic ratio and maximum response rate as a function of spatial frequency for a Y1 and a Y2 cell. Filled squares represent the harmonic ratio while open squares represent maximum response rate. The Y1 cell is shown in the top graph, the Y2 cell in the bottom graph. Second/first harmonic ratios were obtained in the same manner as described for Figure 6. The response rate corresponding to the peak position of the grating, for a given spatial frequency, was designated as the maximum response rate. For both Y cells, the stimulus was a contrast reversal grating, with a contrast of .5, which was sinusoidally modulated at a rate of 1 Hz.

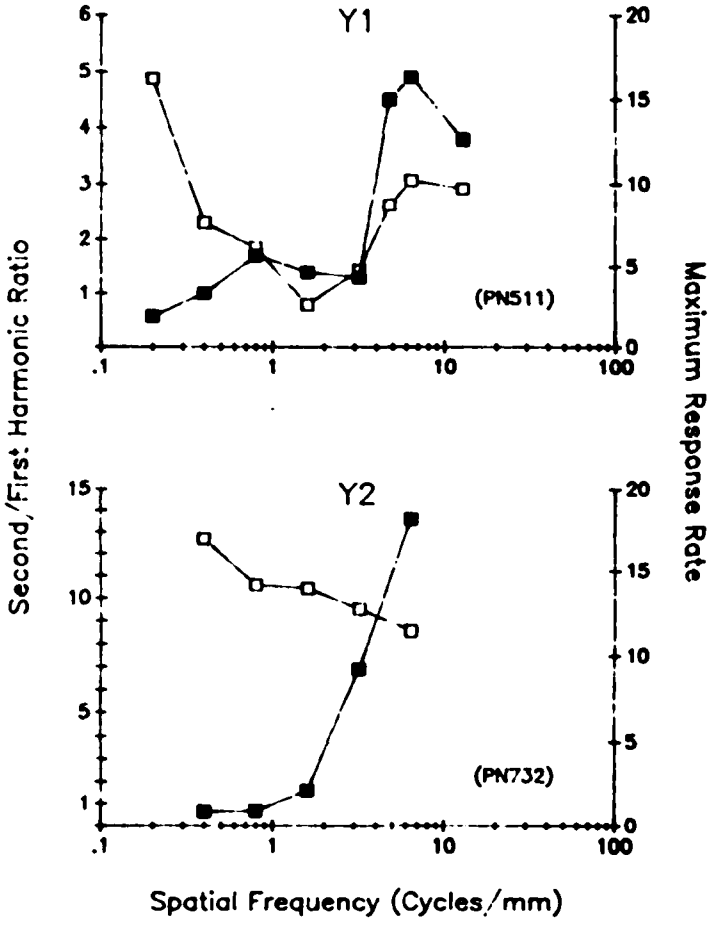

Second/First Harmonic Ratio

Y1 vs Y2 Cell

■—■ Second/First Ratio

□—□ Response Rate

clearly showed no indication of a response decrease and another for which the existence of response depression was moot due to the limited number of spatial frequencies examined during the course of the cell's null test. The shift from linear to nonlinear spatial summation was never marked by similar discontinuities in Y2 cells.

The first and second harmonic magnitudes, obtained from a Y1 cell showing this midway response depression, are plotted as a function of stimulus spatial phase for four spatial frequencies in Figure 26. Although responding, at a moderate spatial frequency (.8 cycles/mm) was completely dominated by second harmonics at all phase angles, the first harmonic continued to provide a significant contribution to responding. At a spatial frequency one octave higher (1.6 cycles/mm), both first and second harmonics decreased substantially reflecting the overall depression in responding. When a slightly higher spatial frequency was presented (3.2 cycles/mm) mean levels of responding, as well as the magnitudes of the first two harmonics, increased. As spatial frequency was increased beyond 3.2 cycles/mm, second harmonic magnitudes continued to rise to their maxima at 6.4 cycles/mm.

Given that both first and second harmonics increased in magnitude at higher spatial frequencies, it is unlikely that the response decrease, at a lower spatial frequency, was the result of a loss of sensitivity in either linear or

Figure 26

Response depression in a Y1 cell. The magnitudes of both first (filled circles) and second (open diamonds) harmonics are plotted as a function of spatial phase for each of four spatial frequencies (A,B,C and D). The spatial frequency of the grating is indicated above each function. By convention, responses with a temporal phase, relative to the stimulus, of less than 180 degrees are assigned positive values while responses possessing a relative temporal phase equal to or greater than 180 degrees are assigned negative values. Only responses obtained during the second half of the grating's temporal cycle are displayed. The solid line in (A) represents half of the best fit sinusoid for the first harmonic component. The stimulus was a contrast reversal grating which was sinusoidally modulated at 1 Hz and had a contrast of .5 .

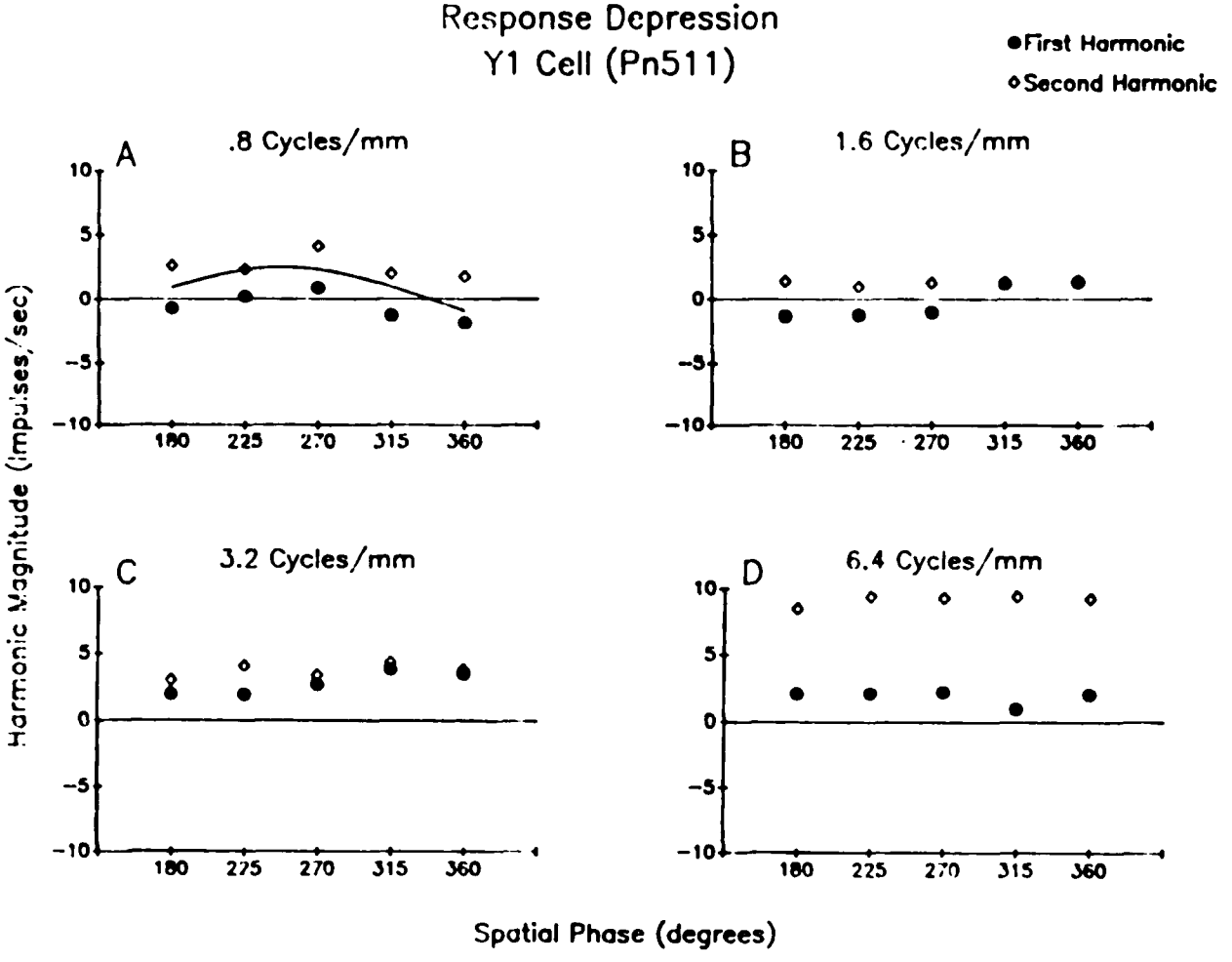
Response Depression
Y1 Cell (Pn511)
●First Harmonic
◇Second Harmonic
A
.8 Cycles/mm
B
1.6 Cycles/mm
C
3.2 Cycles/mm
D
6.4 Cycles/mm
10
5
0
-5
-10
180
225
270
315
360
Harmonic Magnitude (impulses/sec)
Spatial Phase (degrees)

nonlinear mechanisms. The most likely explanation is that the decrease in responding was the result of inhibitory processes. This possibility will be further explored in the Discussion.

The spatial frequency at which this response depression occurred, 1.6 cycles/mm, was remarkably consistent among Y1 cells. Response depression specific to this spatial frequency was also seen, with two exceptions, in a group of Y cells which were identical to Y1 cells in terms of the spatial sensitivity of their nonlinear subunits. These cells were not originally included in the Y1 group because their RF organization was unknown. The exceptions included one cell which showed response depression at both 1.6 and 3.2 cycles/mm and another which showed response depression only at a spatial frequency of 3.2 cycles/mm .

3.3.3.1 Spatial Summation in Y Cells Other Than Y1 and Y2

Even though cells with RFs different from those of Y1 or Y2 cells were few in number and probably cannot be considered as representative of a third, homogeneous subgroup of Y cells, a few points should be made regarding specifics of their performance during null tests. Firstly, none of these cells showed any evidence of the response depression, common to Y1 cells, during null tests. Secondly, the nonlinear components of two of these cells

exhibited moderately low spatial frequency cut-offs similar to those observed for Y2 cells. One of these cells, described earlier, was clearly distinct from Y2 cells (see Figure 24). This suggests, at the very least, that low resolution nonlinear subunits are not unique to a flanking RF profile.

3.3.4 Response to Drifting Gratings

Twenty-three Y cells were examined with drifting gratings. Figure 27 shows the responses of a typical Y cell to drifting gratings of five spatial frequencies ranging from .2 to 3.2 cycles/mm. At low spatial frequencies, Y cells' responses to drifting gratings were modulated according to drift rate and were, therefore, identical to responses recorded from X cells. Increasing the spatial frequency of drifting gratings resulted, however, in a shift from modulated to unmodulated responses in many Y cells (see Figure 27D, for example) not accompanied by the elevation in mean discharge as was reported for Y cells in the cat (Enroth-Cugell and Robson, 1966). In a few Y cells, minor frequency doubling was apparent at a high spatial frequency but, as shown in Figure 27D the bulk of responding was unmodulated. The SFR of the Y cell shown in Figure 27 is presented in Figure 28. A slight discrepancy in the high frequency decline of mean response rate compared to harmonic measures can be seen in the SFR, at

Figure 27

Averaged response histograms from a Y cell to drifting gratings ranging from .2 to 3.2 cycles/mm (A,B,C,D, and E). The spatial frequency, in cycles/mm, is given above each histogram. The drift rate of all gratings was 1 Hz. The duration of each record represents one temporal cycle of the stimulus. The contrast of the gratings was .5.

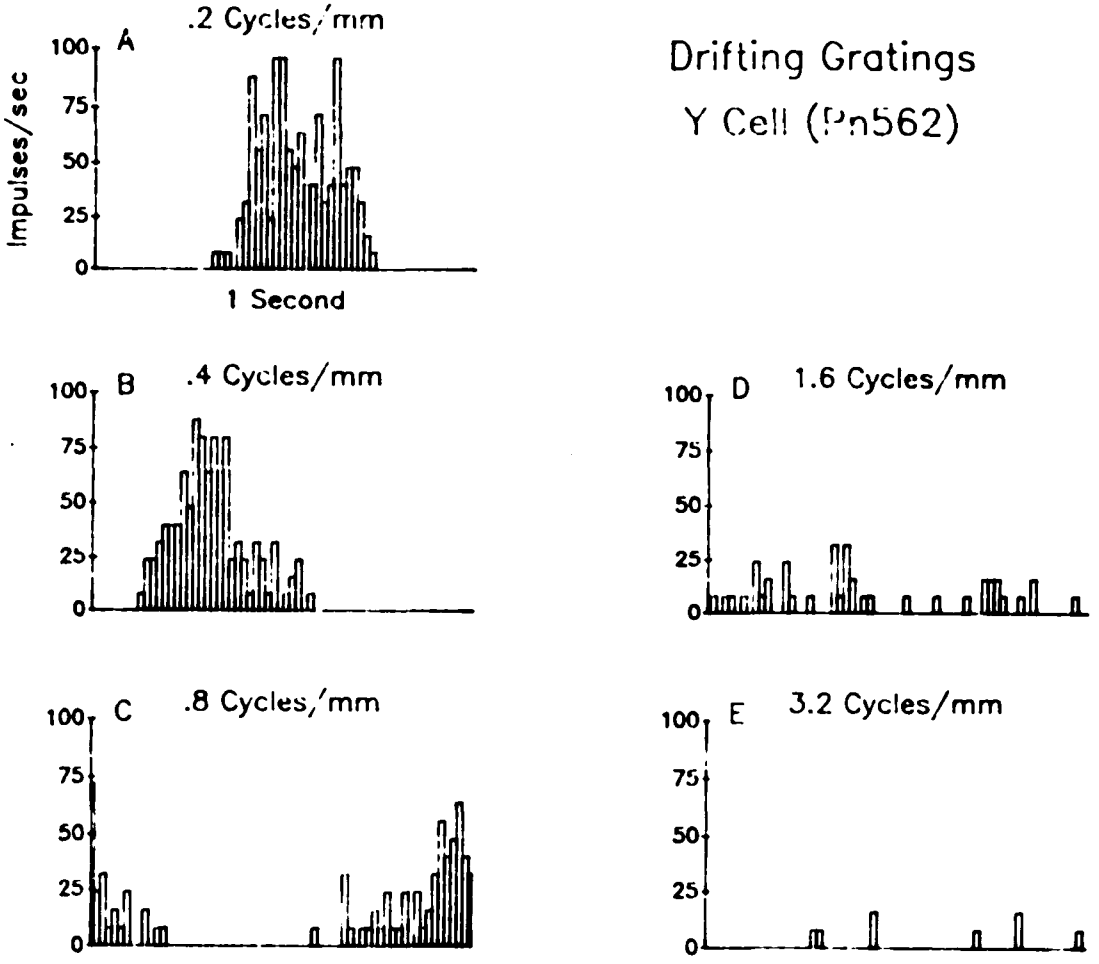
Drifting Gratings
Y Cell (Pn562)
A
.2 Cycles/mm
Impulses/sec
100
75
50
25
0
1 Second
B
.4 Cycles/mm
C
.8 Cycles/mm
D
1.6 Cycles/mm
E
3.2 Cycles/mm

Figure 28

SFR, of the Y cell in Figure 27, illustrating the lack of correspondence between response rate and harmonic measures at a high spatial frequency. Three response measures are plotted as a function of spatial frequency: mean response rate (filled circles), first harmonic magnitude (filled squares), and second harmonic magnitude (open squares). The stimulus was a 1 Hz drifting grating with a contrast of .5.

SFR

Y Cell (Pn562)

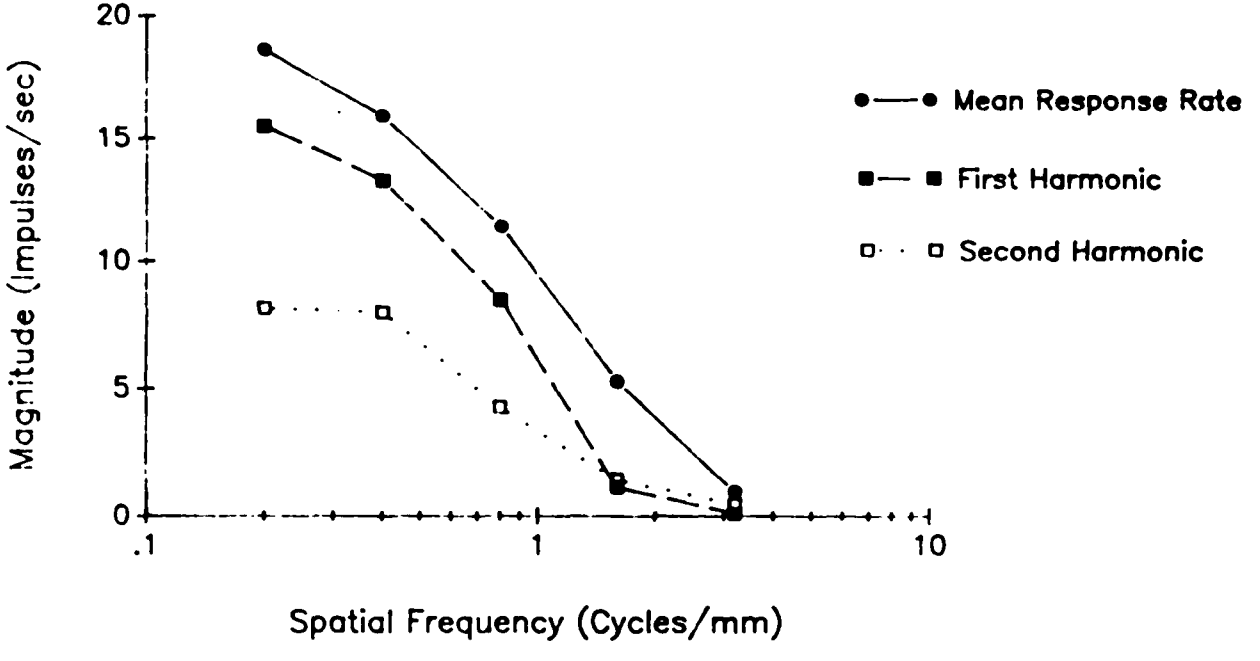

1.6 cycles/mm, as both first and second harmonics approach zero more rapidly than response rate, indicating a loss of response modulation. The minor frequency doubling apparent in the histogram of this cell is reflected in the minor increase in the second harmonic relative to the first harmonic at higher spatial frequencies in the SFR.

The unmodulated responding seen at higher spatial frequencies does not represent spontaneous activity since most frog Y cells did not have a spontaneous discharge. Rather, it stems from activity of the same mechanism responsible for generating second harmonic responses to contrast reversal gratings. In fact, the spatial frequency at which unmodulated responding appeared was the same at which second harmonics had dominated responding during the null test for most Y cells.

It is unclear why frog Y cells do not show the increase in mean discharge to drifting gratings at high spatial frequencies seen in cat Y cells. In fact, the overall response rate of frog Y cells to high spatial frequencies is exceptionally low, compared to that for slightly lower spatial frequencies. Furthermore, a substantial number of Y cells, in the frog, ceased responding entirely to drifting gratings at spatial frequencies which had elicited maximum second harmonic activity during the null test. A preliminary examination of the effect of stimulus rotation upon one of these cells'

responses to drifting gratings (see Figure 29) revealed a finely tuned preference for a given rotation at a high but not a low spatial frequency. Because rotation of the stimulus display encompasses both orientation as well as directional changes in drifting gratings, it is unclear if the rotational preference of the cell in Figure 29 is the result of orientation or directional selectivity. Directional selectivity, however, seems to be the more likely basis for the results presented in Figure 29 given that contrast reversed gratings presented at 0 degrees rotation had elicited high response rates and robust second harmonics while drifting gratings presented at the same rotation elicited negligible responding. Regardless of the mechanism responsible for rotational selectivity demonstrated by this Y cell, the likelihood exists that a non-optimal grating rotation may have accounted for the decrease in responsiveness of many Y cells to drifting gratings with high spatial frequencies.

3.3.5 Spatial Frequency Response Curves

Since many frog Y cells displayed a relatively discrete shift from modulated to unmodulated responding with spatial frequency it is possible to isolate the linear component's contribution to the shape of the SFR by using the first harmonic's magnitude as the response measure when constructing SFR curves. This facilitates accurate

Figure 29

The effect of stimulus rotation upon a Y cell's responses to both low (.4 cycles/mm) and high (3.2 cycles/mm) spatial frequency drifting gratings. The drift rate was 1 Hz and contrast was .5. Gratings were rotated between 0 and 180 degrees about the central point of the stimulus display. Mean response rate as a function of stimulus rotation to both spatial frequencies is shown in (A). (B) and (C) present the magnitudes of the first and second harmonics plotted as a function of stimulus rotation for a spatial frequency of .4 and 3.2 cycles/mm, respectively.

Effect of Stimulus Rotation Upon a Y Cell's Response to Drifting Gratings (Pn93)

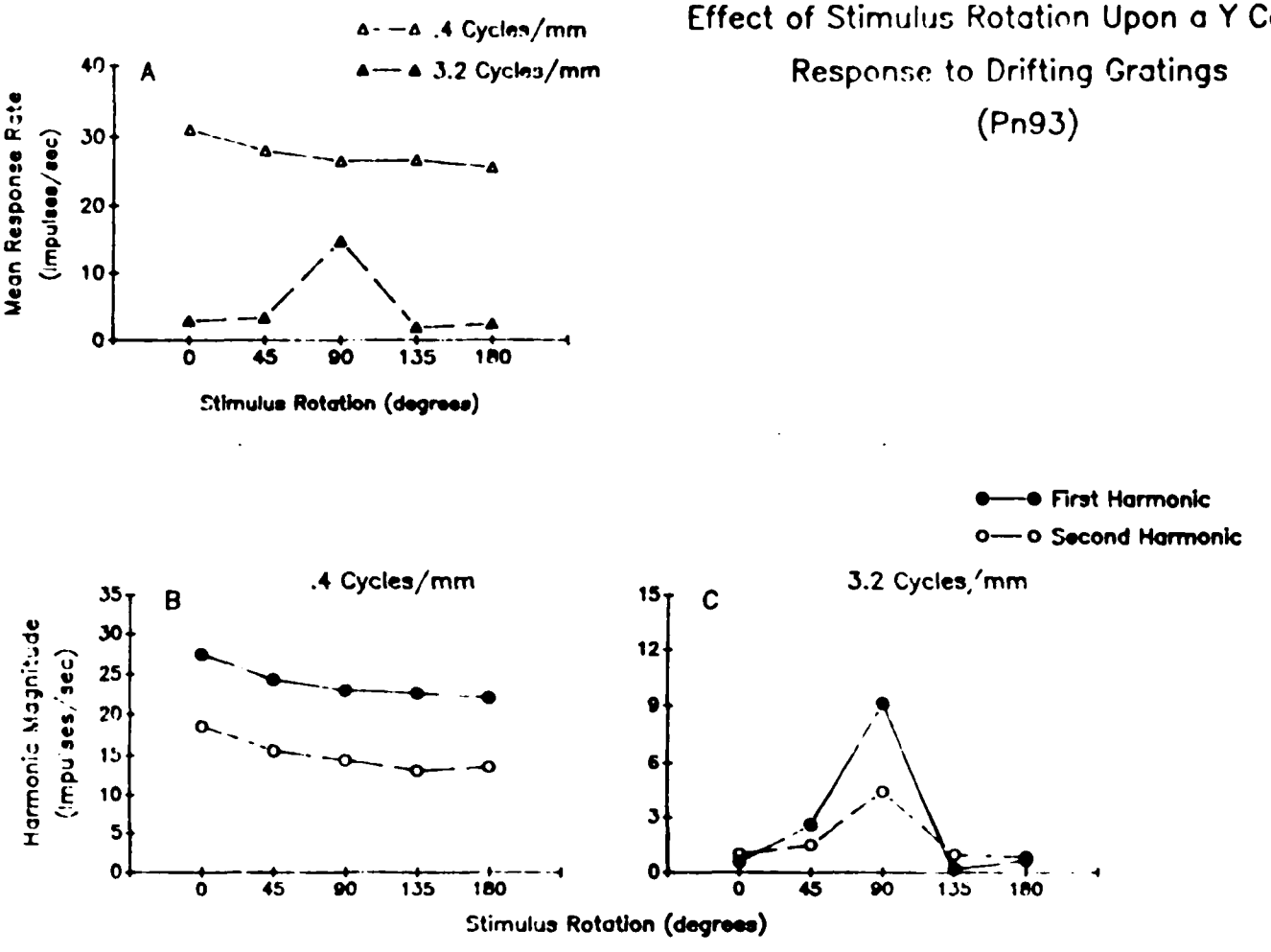

comparisons between the SFR of the linear mechanism of Y and X cells especially at high frequencies where nonlinear mechanisms dominate in the Y cell.

Drift rate had no effect on the optimal spatial frequency for 83% of the Y cells examined. Of these cells the majority displayed optimal responsivity to the lowest spatial frequency used in these tests (.2 cycles/mm). Since, however, the RFs of many of these cells were quite extensive, it was necessary to include responsiveness to changes in full field illumination (i.e., 0 cycles/mm), when such information was available, in order to accurately determine whether or not a low frequency decline, indicative of a suppressive surround, existed. Table 2 indicates that the percentage of 'on', 'off', and 'on-off' cells clearly lacking a low frequency decline was approximately equal.

The rate of decline to high spatial frequencies varied somewhat among cells lacking a low frequency decline. Similar to the trend noted previously for X cells, 'off' Y cells were more likely to display a rapid high frequency cut-off than were either 'on' or 'on-off' cells. Figure 30 presents the SFRs of an 'off' and and 'on' cell for comparison. The drift rate of the grating, 1 Hz, was optimal for both cells. As Figure 30 demonstrates, the differences in high frequency decline among Y cells, with different Hartline response characteristics and lacking

Table 2

Y Cells Showing No Interaction Between Optimal Spatial Frequency and Drift Rate

		Low frequency decline		
		Present	Absent	Total
Hartline	on	1(33%)	2(66%)	3(16%)
Response	off	3(33%)	6(66%)	9(47%)
Type	on-off	3(43%)	4(57%)	7(37%)
	Total	7(37%)	12(63%)	

Figure 30

SFRs of an 'on' and an 'off' Y cell showing no low frequency decline but differing in the rate of high frequency decline. The relative response measure is the magnitude of the first harmonic plotted as a percentage of the maximal response obtained with the optimal spatial frequency. Full field changes in intensity are plotted on the X axis as 0 cycles/mm. The drift rate of the gratings was 1 Hz. Full field intensity was sinusoidally modulated above and below the mean intensity level at a rate of 1 Hz. The contrast of all stimuli was .5.

SFR
On vs Off Y Cells

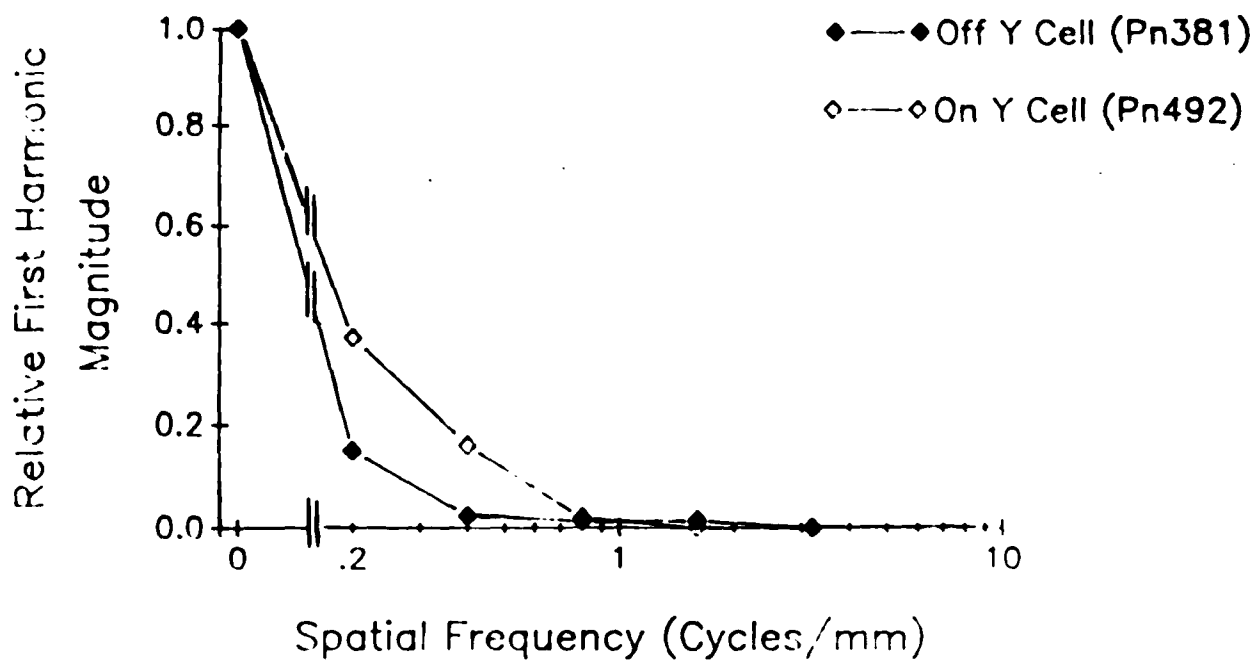

low frequency decline, were rarely as conspicuous as that observed in X cells (see Figure 15 for example).

Low frequency attenuation, independent of drift rate, was evident in the SFRs of seven Y cells (three 'off', one 'on', and three 'on-off'). Figure 31 shows an example of a Y cell with a temporally independent low frequency decline. The gradual decline in responsiveness to high spatial frequencies apparent in Figure 31 was common to all Y cells possessing low frequency declines. One of these Y cells, 'on-off' to full field stimulation, displayed maximum responsivity to an unusually high spatial frequency, approximately two octaves higher than the preferred frequency demonstrated by other Y cells. The SFR of this cell, obtained at the preferred drift rate, is shown in Figure 32. Examination of the high frequency portion of this cell's SFR reveals a marked disparity between overall response rate and harmonic measures, much greater than that observed in the rest of the Y cells. This Y cell was, in fact, the only Y cell which produced high levels of unmodulated responding at higher spatial frequencies.

Of the Y cells examined, 17% revealed interactions between drift rate and optimal spatial frequency. All of these Y cells displayed gradual high frequency declines. The most frequent form of this interaction was one in which low spatial frequency attenuation occurred at slower drift rates but was absent at higher rates. An example of this

Figure 31

SFRs of a Y cell showing no effect of stimulus drift rate upon optimal spatial frequency. The response measure is the magnitude of the first harmonic. The stimuli were gratings drifted at .125 Hz (filled diamonds), 1 Hz (open diamonds), and 4 Hz (filled squares). The contrast of the gratings was .5 .

Optimal Spatial Frequency
Independent of Drift Rate

Y Cell (Pn761)

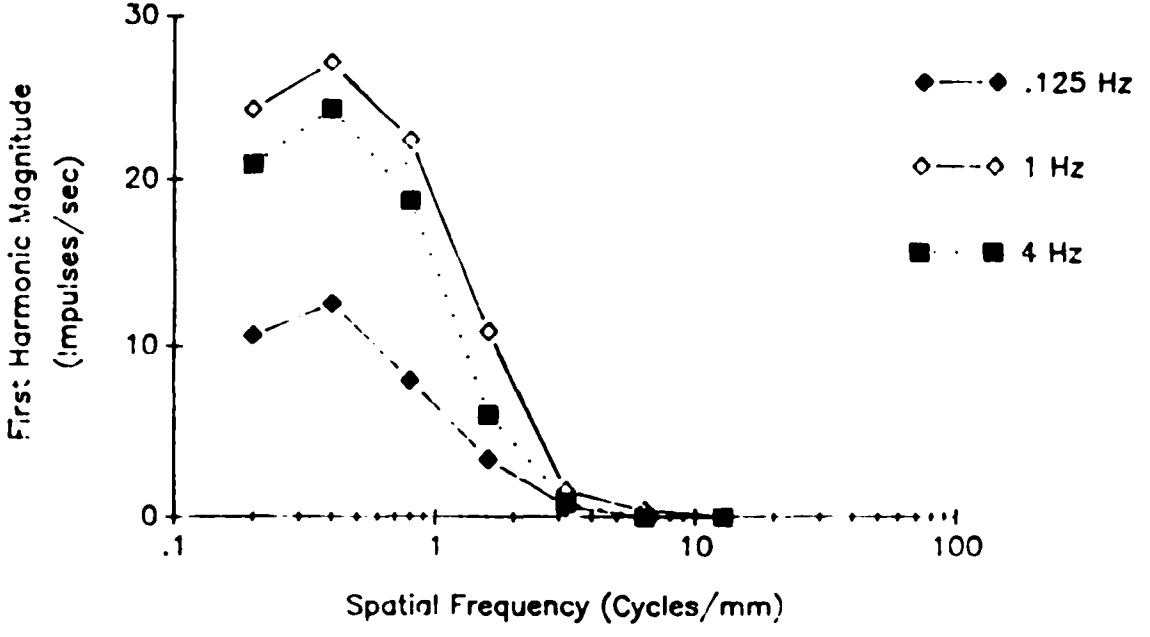

Figure 32

SFR from a Y cell with a high optimal spatial frequency. Three response measures are plotted as a function of spatial frequency: mean response rate (filled circles), first harmonic magnitude (filled squares), and second harmonic magnitude (open squares). The stimulus was a 1 Hz drifting grating with a contrast of .5.

SFR

Y Cell (PN843)

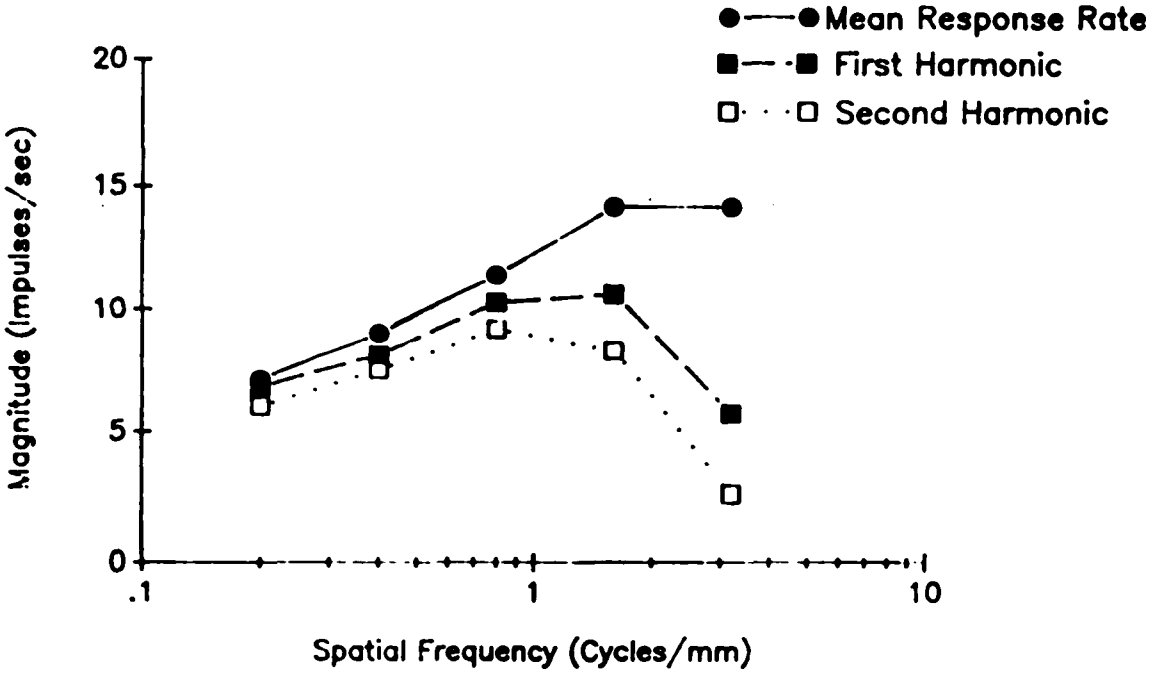

is shown in Figure 33A. This is consistent with the notion that the temporal characteristics of the inhibitory surround are slower than those of the center. Only one cell showed evidence of surround suppression at a moderate but not a slow drift rate. SFRs obtained at two drift rates for this cell are shown in Figure 33B. This is the same cell, described in the preceding section (see Figure 24), that revealed a RF profile distinct from either Y1 or Y2 cells.

3.3.5.1 Y1 VS Y2 CELLS

The SFRs from a Y1 and Y2 cell - both 'on-off' to full field illumination - are presented in Figure 34. The grating's drift rate was optimal for both cells. A comparison between Y1 and Y2 cells reveals two major consistent differences in the shape of their SFRs. Y1 cells were most responsive to full field stimulation and a very low spatial frequency. The SFRs of all Y2 cells, on the other hand, revealed low frequency declines. Four out of the five Y2 cells examined displayed no interaction between optimal spatial frequency and grating drift rate. The fifth Y2 cell exhibited the typical form of interaction shown in Figure 33A. None of the Y1 cells' optimal spatial frequency was affected by drift rate.

Figure 34 reveals that Y1 and Y2 cells also differed in the rate of their high frequency declines. Regardless

Figure 33

Interactions between optimal spatial frequency and stimulus drift rate in Y cells. The response measure is the magnitude of the first harmonic. Gratings were drifted at a rate of .125 Hz (filled diamonds) and 1 Hz (open diamonds). Contrast was .5. The most common effect of changes in drift rate upon the low spatial frequency limb of Y cells' SFRs is demonstrated by the cell in (A). The SFRs from another cell, presented in (B), illustrate an atypical form of interaction between drift rate and low spatial frequency cut-off.

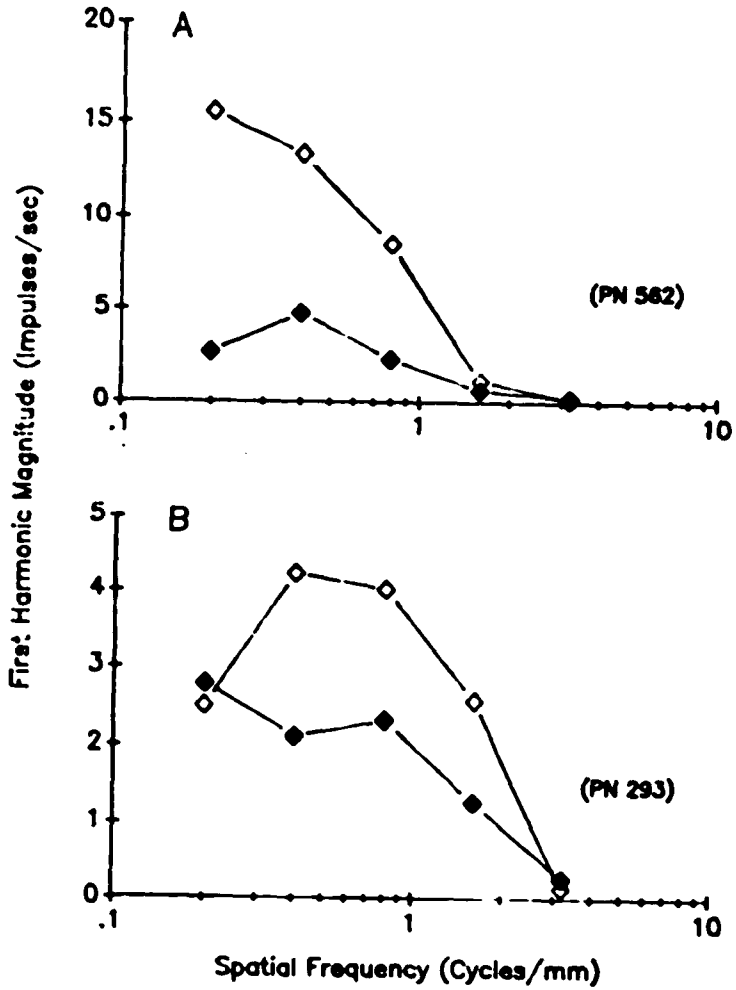

Interactions Between Drift Rate and Optimal Spatial Frequency

Y Cells

◆—◆ .125 Hz

◇---◇ 1 Hz

Figure 34

SFRs from a Y1 and a Y2 cell. The relative response measure is the mean response rate plotted as a percentage of the maximal response obtained at the optimal spatial frequency. Full field stimulation is plotted on the X axis as 0 cycles/mm. With the exception of full field stimulation, stimuli consisted of gratings drifted at a rate of 1 Hz. Full field intensity was square wave modulated at 1 Hz. The contrast of all stimuli was .5.

SFR
Y1 vs Y2 Cell

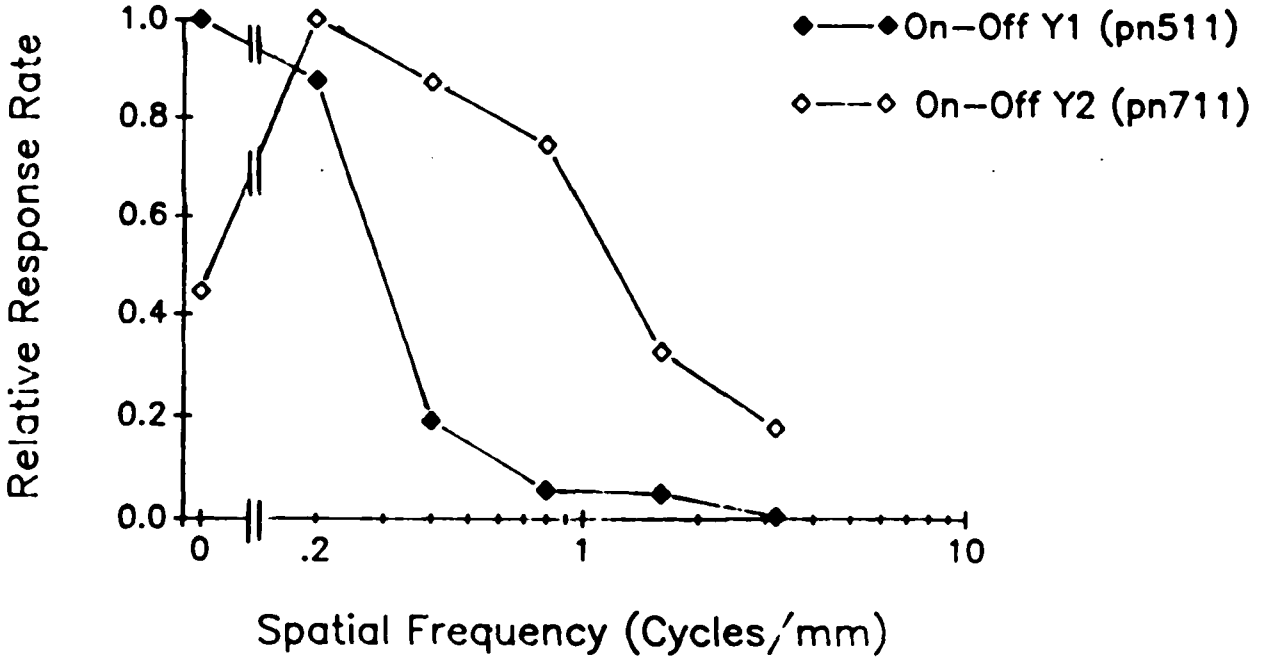

of Hartline response type, Y1 cells always displayed a more rapid decrease in responsiveness to higher spatial frequencies than did Y2 cells.

Given the difference in RF size between Y1 and Y2 cells the difference in the shape of their SFRs is not surprising. The Y1 cells' optimal responsivity to large stimuli as well as their rapid decrease in responsiveness to high spatial frequencies are expected given the wide extent of their RFs. Y2 cells' responsiveness to higher spatial frequencies attests to the smaller size of their RFs relative to Y1 cells. The observation that a low frequency decline, absent in all Y1 cells examined, was characteristic of all Y2 cells suggests that a suppressive surround is a property of the Y2, but not Y1, RF.

Since the center of the Y2 RF is bounded by antagonistic regions a strong possibility exists that these flanking regions are responsible for surround inhibition. Examination of the RF profile of a Y2 cell (see Figure 23B) with the cell's preferred spatial frequency of .4 cycles/mm reveals that one-half cycle, or bar, of the grating (1.25mm) is approximately equal to the width of the center region. This spatial frequency therefore would maximally stimulate the center and flanking regions in an antagonistic fashion. However, a bar which extends across 2.5 mm of the RF, corresponding to the spatial frequency at which response attenuation occurred in this cell (.2

cycles/mm), would mutually stimulate both center and flanking regions. The flanking regions therefore appear to provide a major source of surround inhibition. Additional observations suggest that the center also inhibits flanking responses. Firstly, center elicited responses completely dominated responding to full field stimulation in two out of five Y2 cells. Window/shutter tests, to be discussed in section 3.5.2, in which stimulation was restricted to either center or flanking regions provided a second indication that the center is responsible for inhibiting flanking responses. When the center region was occluded in these tests, a substantial accentuation of flanking responses to uniform changes in intensity was observed.

3.4 $\overline{X}$ Cells

The $\overline{X}$ category, containing a large number (26) of cells, was clearly heterogeneous. The only feature common to these cells was that they were neither clearly X- nor Y-like in their behavior during the null test. All of these cells were similar, however, in that nonlinearities in spatial summation were evident at very low spatial frequencies and did not substantially increase in strength at higher spatial frequencies as was the case in Y cells. Because of the tremendous variability in behavior among these cells, it was impossible to designate a given cell, or even a number of cells, as characteristic of the whole

group. In order, however, to impose some organization upon a discussion of these cells' behavioral properties, the following sections will focus upon only three of the most commonly occurring trends in performance during the null test. It must be emphasized that these trends simply reflect points along a behavioral continuum and are not intended to imply the existence of well-defined subgroups within the $\overline{X}$ class.

3.4.1 Spatial Summation

In order to summarize differences among $\overline{X}$ cells during the null test, mean second/first harmonic ratios as a function of spatial frequency, representing each of three variations, are presented for comparison in Figure 35. The most frequent trend (Figure 35A) was similar, if not identical, to that first described in $\overline{X}$ cells by Gordon and Shapley (1978). These were cells in which second harmonics appeared at low spatial frequencies and were maintained at increasingly higher spatial frequencies without showing a substantial increase in magnitude relative to the first harmonic. Figure 35B illustrates the next most frequent variation in which second harmonic responses were most evident at low spatial frequencies but nearly absent at slightly higher spatial frequencies. Finally, there were a number of cells which did not respond to sinusoidal temporal modulation but for which a square wave modulation

Figure 35

Second/first harmonic ratios as a function of spatial frequency demonstrating three variations in response among $\bar{X}$ cells during the null test. Harmonic ratios were obtained in the same manner as that described for Figure 6. Stimuli were contrast reversal gratings with a contrast of .5. Contrast reversal was sinusoidally modulated at a rate of .125 Hz for the cell in (A) and at 1 Hz for the cell in (B). Contrast was square wave reversed above and below mean background intensity, at a rate of .125 Hz, for the cell in (C).

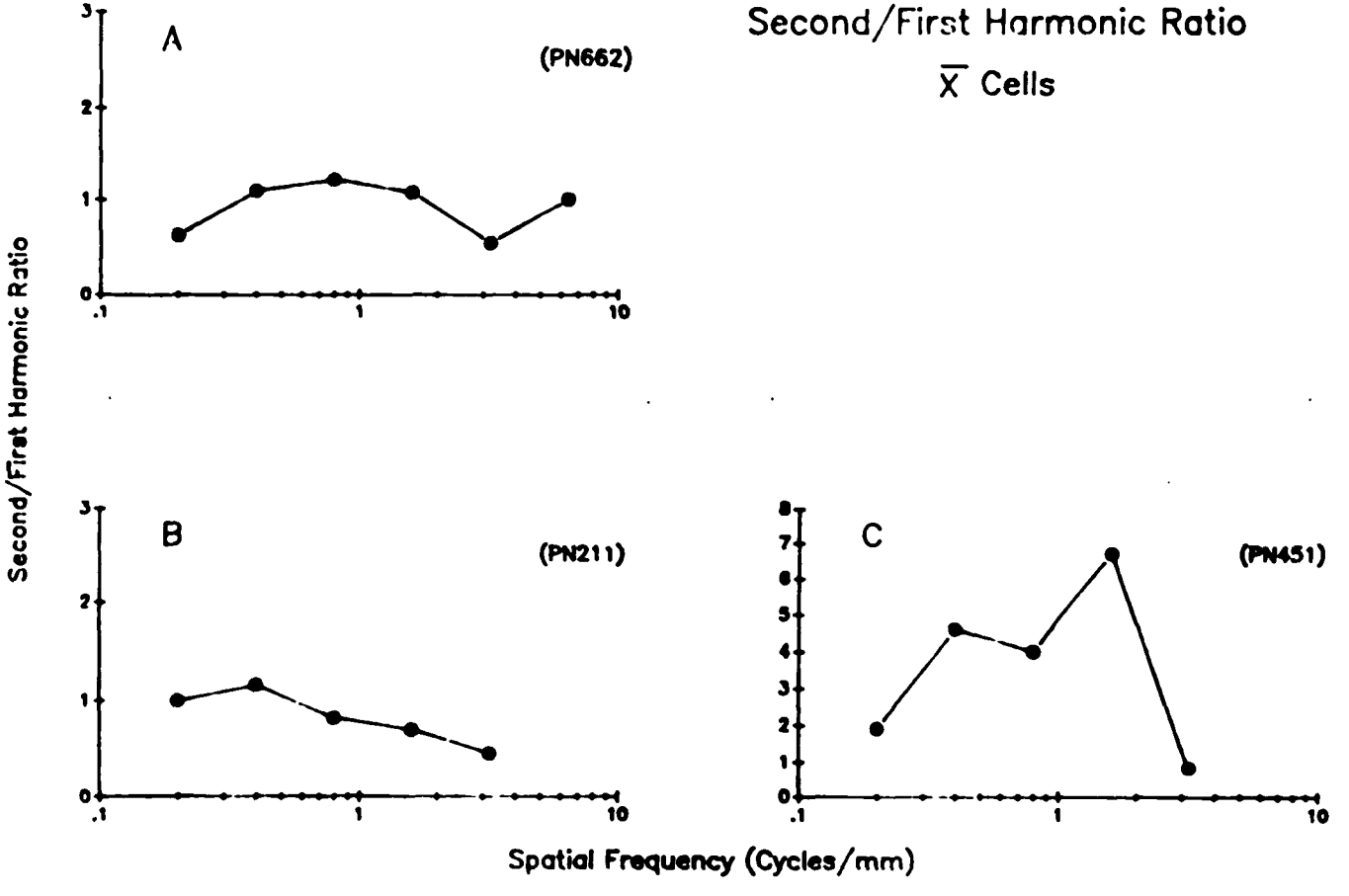
Second/First Harmonic Ratio
$\overline{X}$ Cells
A
(PN662)
B
(PN211)
C
(PN451)
Second/First Harmonic Ratio
Spatial Frequency (Cycles/mm)
.1
1
10

of a contrast reversal grating was required. Figure 35C reveals that the second/first harmonic ratio for these cells was considerably higher than that of other $\overline{X}$ cells especially for moderate to high spatial frequencies.

Figure 36 shows the relationship between harmonic magnitudes and stimulus spatial phase during the null test for an $\overline{X}$ cell representative of the first trend shown in Figure 35A. At the lowest spatial frequency (.2 cycles/mm) the first harmonic approximates a sinusoidal dependence upon the grating's spatial phase and dominate the response at every phase angle. At a slightly higher spatial frequency (Figure 36B) a tremendous reduction in magnitude of the first harmonic is evident and second harmonics dominate the response at spatial phases corresponding to the null position for the first harmonic. Note that the sign of the second harmonic is variable across stimulus spatial phase thereby indicating that the second harmonic did not consistently occur at the same point of the stimulus' temporal cycle as seen previously in X and Y cells (see for example Figures 7 and 17). These changes in the temporal occurrence of the cell's second harmonics were observed at all spatial frequencies during the null test (Figures 36B and 36D). Further increases in spatial frequency resulted in minor increases in second harmonic magnitude. The increase in second/first harmonic ratio with increasing spatial frequencies in this and other cells

Figure 36

Magnitudes of first and second harmonics as a function of spatial phase of a contrast reversal grating for an $\overline{X}$ cell characteristic of the variation illustrated in Figure 35 (A). The results from four spatial frequencies are shown in (A,B,C, and D). The spatial frequency of the grating is indicated above each function. Filled circles represent the first harmonic component, open diamonds represent the second harmonic component. Responses produced during the first and second halves of the grating's temporal cycle are plotted as positive and negative values, respectively. The solid lines in all four graphs represent the best fit sinusoid determined for the first harmonic component. (A) shows responses over a full spatial cycle of the grating while the remaining three graphs display responses for the first half of the spatial cycle. The reversal rate of the grating was .125 Hz and the contrast was .5

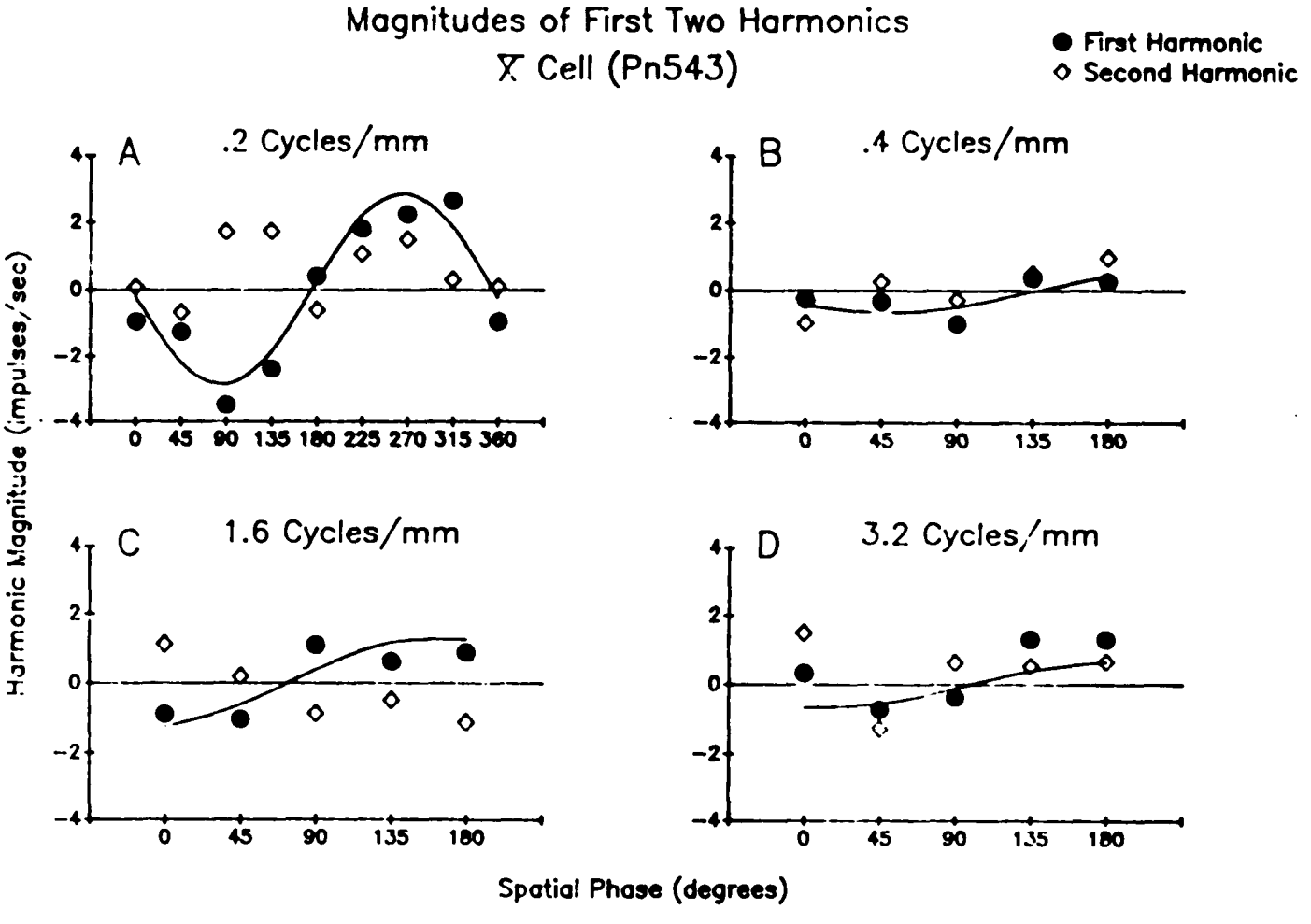
Magnitudes of First Two Harmonics
X Cell (Pn543)
First Harmonic
Second Harmonic
A
.2 Cycles/mm
B
.4 Cycles/mm
C
1.6 Cycles/mm
D
3.2 Cycles/mm
Harmonic Magnitude (impulses/sec)
Spatial Phase (degrees)
0 45 90 135 180 225 270 315 360
0 45 90 135 180

showing this trend was never as impressive as that seen in Y cells. (Compare Figure 35A with any of the ratios displayed in Figure 21, for example). While the first harmonic displayed a sinusoidal dependence upon spatial phase at a low spatial frequency in this and a number of other similar cells, this phase dependence was absent in a few cells. The majority of cells in this group were 'on-off' to full-field stimulation. The remaining cells either produced pure 'on' or 'off' responses.

A different relationship between the second harmonic and spatial frequency was seen in another 'group' of $\overline{X}$ cells (Figure 37) all of which produced 'on-off' responses to uniform changes in illumination. Unlike the $\overline{X}$ cell previously described, second harmonics were typically evident only at a low spatial frequency. As Figure 37 indicates first and second harmonics appeared to alternate, but imperfectly, across spatial phase at low spatial frequencies with neither clearly displaying a sinusoidal dependence upon spatial phase. Similar alternations between the first two harmonics across spatial phase were observed in other cells producing second harmonics only at low spatial frequencies; the specific form of the alternation being somewhat different for each cell. What is especially unusual regarding the cell presented in Figure 37 is the relationship of the first harmonic to stimulus spatial phase at a spatial frequency of .4

Figure 37

Magnitudes of first and second harmonics as a function of spatial phase of a contrast reversal grating for an $\overline{X}$ cell characteristic of the trend illustrated in Figure 35 (B). The results from three spatial frequencies are shown in (A,B,and C). The spatial frequency of the grating is indicated above each function. The first harmonic component is represented by filled circles, the second harmonic by open diamonds. Responses produced during the first and second halves of the grating's temporal cycle are plotted as positive and negative values, respectively. The solid line in (A) represents the best fit sinusoid determined for the first harmonic component while the dashed line in B simply connects the data points of the first harmonic measures. (A and B) show responses over a full spatial cycle of the grating while (C) displays responses for one half of the spatial cycle. The reversal rate of the grating was 1 Hz and the contrast was .5.

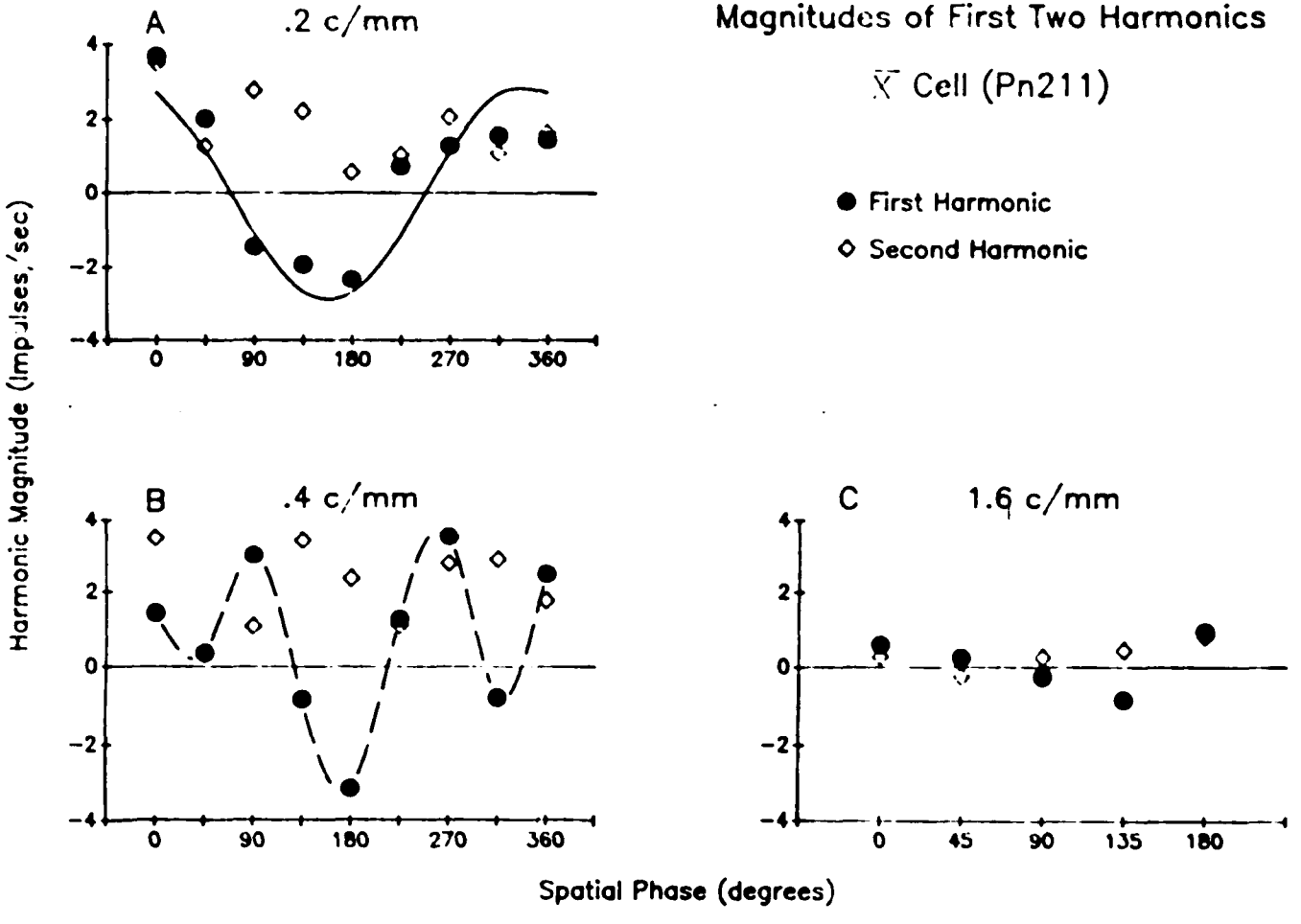
Magnitudes of First Two Harmonics
X Cell (Pn211)
First Harmonic
Second Harmonic
A
.2 c/mm
B
.4 c/mm
C
1.6 c/mm
Harmonic Magnitude (Impulses/sec)
Spatial Phase (degrees)
0
90
180
270
360
45
135
4
2
0
-2
-4

cycles/mm, the optimal spatial frequency for this cell according to its SFR. Across most of the spatial cycle of the grating the first harmonic displays a 90 degree peak-to-peak separation. Thus the first harmonic's magnitude appeared to cycle twice to one spatial cycle of the stimulus.

The third most common trend among $\overline{X}$ cells was seen in a group of 'on-off' cells which responded only to square wave modulated contrast reversals during the null test. The magnitudes of the first two harmonics of one of these cells are plotted as a function of spatial phase in Figure 38 for a square wave reversed grating. At a low spatial frequency the first harmonic displayed a sinusoidal dependence upon stimulus phase. The magnitude of the second harmonic, however, was far greater than that of the first harmonic at most stimulus phase angles for all low to moderate spatial frequencies. Note also that the magnitude of the second harmonic varied with spatial phase at low spatial frequencies (.2 to .8 cycles/mm). With increasing spatial frequency the second harmonic became progressively more insensitive to the phase angle of the grating but, unlike Y cells, did not concomitantly increase in magnitude.

It could be argued that the appearance of robust second harmonics in these $\overline{X}$ cells was more a result of square wave modulation than a function of these cells'

Figure 38

Magnitudes of first and second harmonics as a function of spatial phase of a contrast reversal grating for an $\bar{X}$ cell characteristic of the trend illustrated in Figure 35 (C). Filled circles represent the first harmonic component, open diamonds represent the second harmonic component. Responses produced during the first and second halves of the grating's temporal cycle are plotted as positive and negative values, respectively. The solid line in (A) represents the best fit sinusoid determined for the first harmonic component. (A and B) show responses over a full spatial cycle of the grating while (C and D) display responses for one half of the spatial cycle. Contrast was square wave reversed at a rate of .125 Hz.. The contrast of all gratings was .5. The results from four spatial frequencies are shown in (A,B,C and D). The spatial frequency of the grating is indicated above each function.

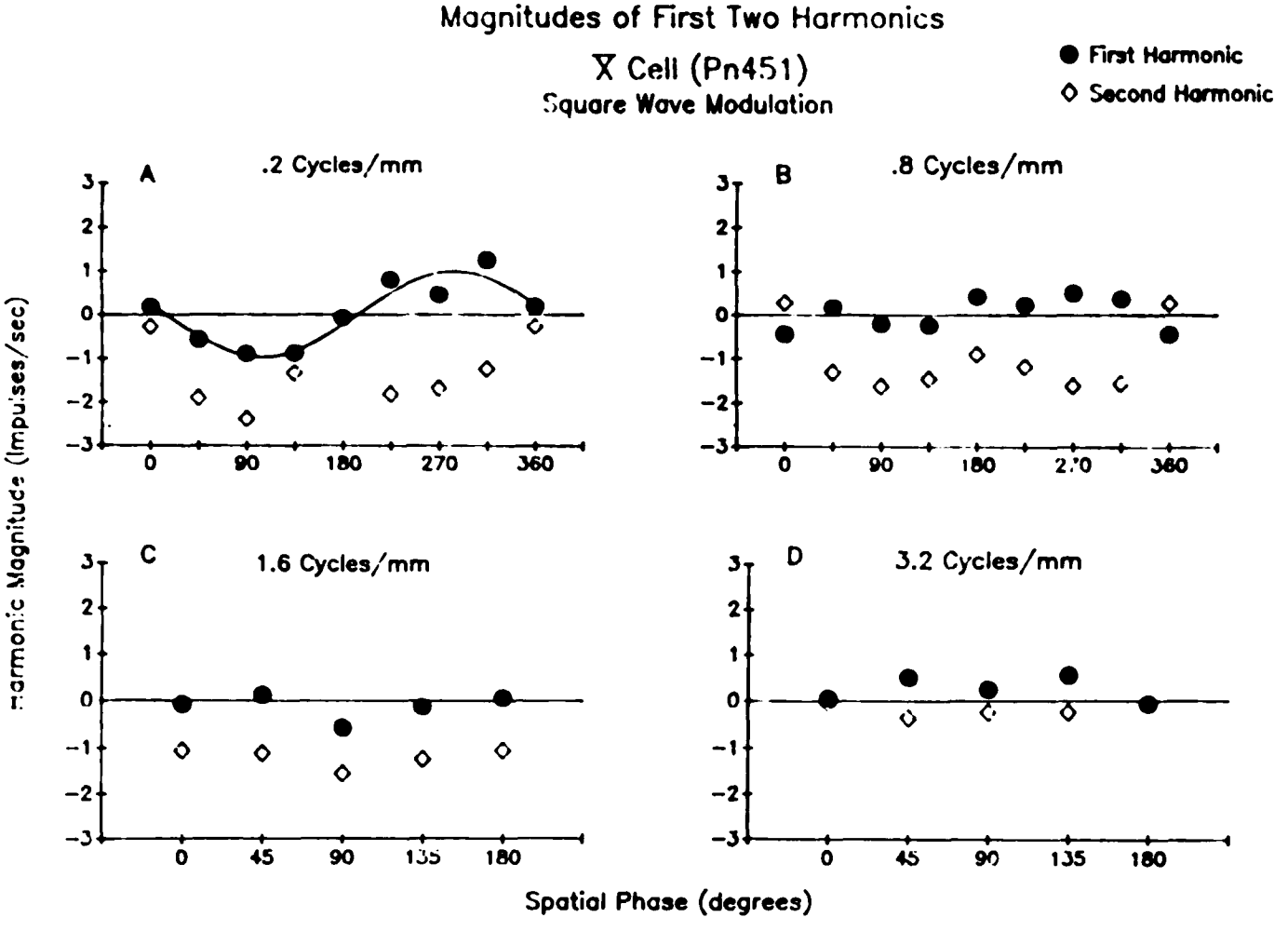
Magnitudes of First Two Harmonics
X Cell (Pn451)
Square Wave Modulation
First Harmonic
Second Harmonic
A
.2 Cycles/mm
B
.8 Cycles/mm
C
1.6 Cycles/mm
D
3.2 Cycles/mm
Harmonic Magnitude (Impulses/sec)
Spatial Phase (degrees)

summation processes. One way to resolve this issue is to compare the effects of square vs sinusoidal modulation upon responding and its harmonic components. This was done in one $\overline{X}$ cell which responded optimally to square wave modulation but had also responded, at an extremely low rate, to initial presentations of sinusoidally modulated gratings. First and second harmonic magnitudes, as a function of stimulus phase, are presented in Figure 39 for both a sinusoidally and a square wave reversed grating. Only one spatial frequency is shown since this cell's response rate dropped to zero for slightly higher spatial frequencies when sinusoidal modulation was employed. While harmonic magnitudes were relatively lower when sinusoidal modulation was employed, Figure 39 indicates that they, nevertheless, reflected the same trends observed when an abrupt reversal was used.

It appears, therefore, that the form of nonlinear summation observed in these $\overline{X}$ cells, specifically responsive to abrupt stimulus changes, is, indeed a property of the cells' integration processes. In fact, an X cell, similarly responsive only to square wave contrast reversals, did not demonstrate any deviations from linear spatial summation.

$\overline{X}$ cells also varied tremendously in terms of the relationship between response temporal phase and stimulus spatial phase. A general feel for this variability can be

Figure 39

Comparison between an $\overline{X}$ cell's responses to sinusoidal and to square wave reversals during the null test. The response measures are the magnitudes of the first (filled circles) and second (open diamonds) harmonic components. Only those responses recorded during the first half of the spatial cycle of the grating are displayed. The stimulus was a contrast reversal grating which was square wave modulated in (A) and sinusoidally modulated in (B). The spatial frequency of the grating was .2 cycles/mm. Stimulus contrast was .5 and reversal rate, for both forms of modulation, was 1 Hz.. The solid and dashed lines represent the best fit sinusoids for the first and second harmonics, respectively.

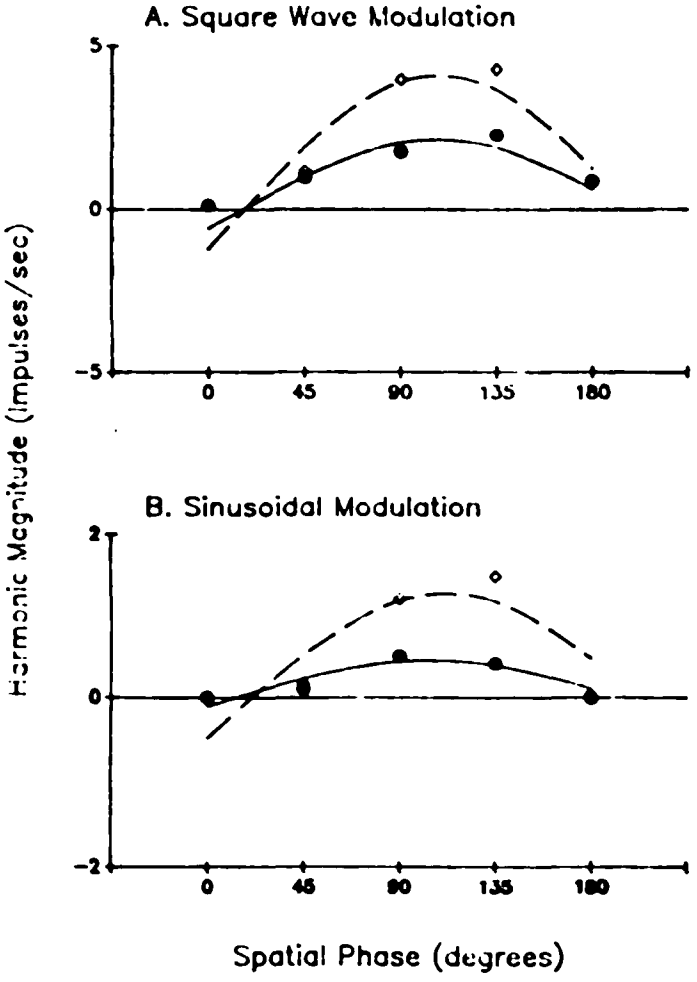

Null Test

Comparison Between Square Wave And Sinusoidal Modulation

$\bar{X}$ Cell (Pn532)

● First Harmonic

◇ Second Harmonic

obtained by examining the changes in the signs of first and second harmonic responses with stimulus spatial phase in Figures 36 to 38. One of the more interesting relationships between the temporal phase of the response and the spatial phase of the stimulus was exhibited by the cell, shown in Figure 37, in which the first harmonic appeared to cycle twice in magnitude to one spatial cycle of a .4 cycle/mm grating. The function relating temporal phase of the response to spatial phase of the stimulus for this cell (Figure 40) similarly indicates that the first harmonic component shifted temporally by approximately 270 degrees four times during one spatial cycle of the stimulus. This represents a substantial departure from X and Y cells (see Figures 8 and 18) in which the temporal phase of the first harmonic shifted, by 180 degrees, once throughout 360 degrees of spatial phase angles of the grating.

3.4.2 Response to Drifting Gratings and Spatial Frequency Response Curves

As expected given the substantial variability among $\overline{X}$ cells' responses to contrast reversal gratings during the null test, these cells' responses to drifting gratings could not be characterized by any particular feature. The SFRs of the majority of $\overline{X}$ cells were generally more complex than those described for either X or Y cells. Diverse

Figure 40

Temporal phase of first (filled circles) and second (open diamonds) harmonics of an $\overline{X}$ cell's response as a function of spatial phase of a low (A) and moderate (B) spatial frequency contrast reversed grating. Temporal phases less than 180 degrees reflect responding during the first half of the stimulus' temporal cycle while phases equal to or greater than 180 degrees indicate responding during the second half of the stimulus cycle. The spatial frequency of the grating is given, in cycles/mm, above each graph. One complete spatial cycle of the grating is represented in each graph. The contrast of the grating was .5 and reversal rate was sinusoidally modulated at 1 Hz.

Response Temporal Phase as a
Function of Stimulus Spatial Phase
$\overline{X}$ Cell (Pn211)

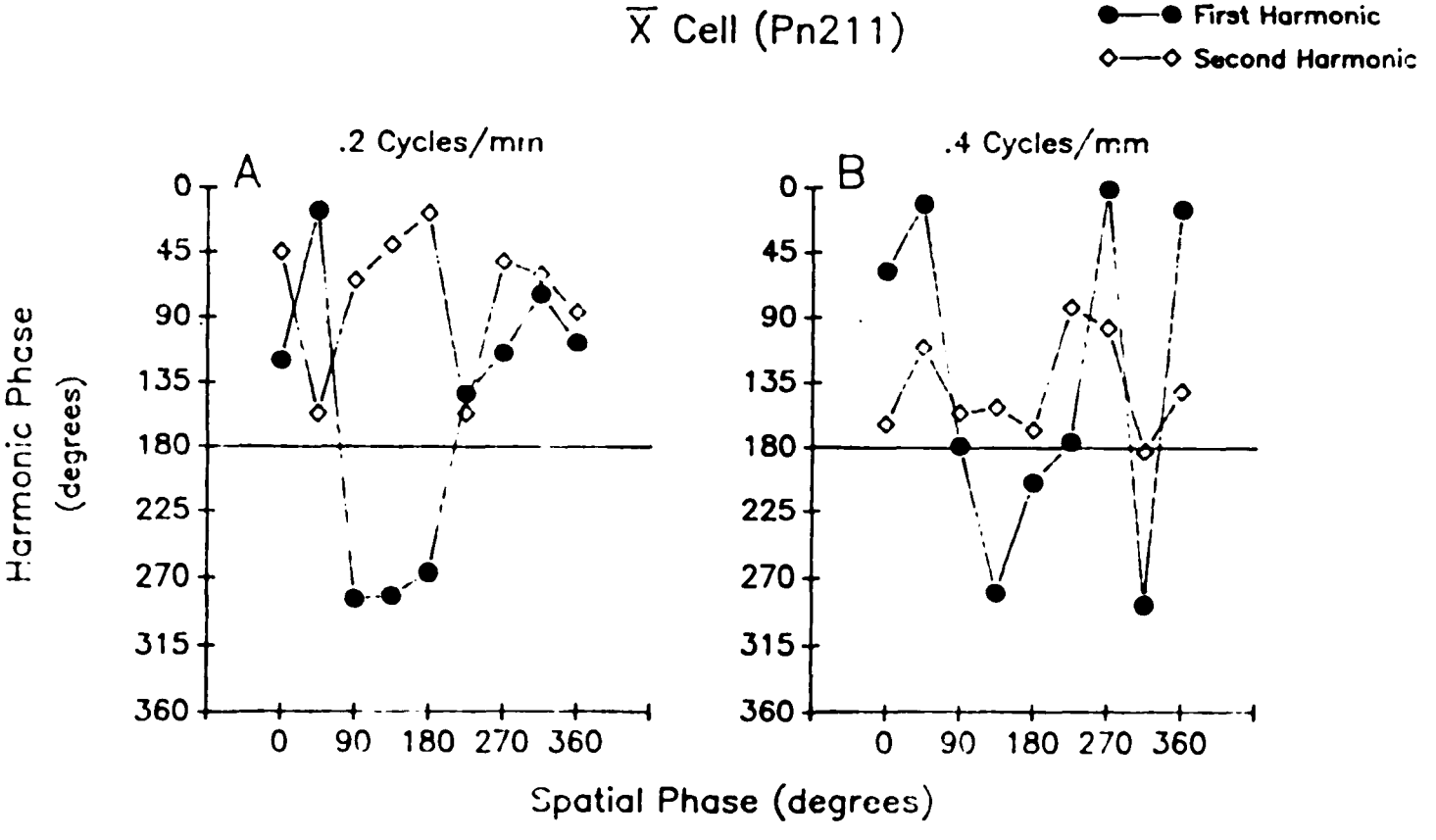

multiple interactions among spatial frequency, drift rate, and harmonic response components were often observed. Many $\overline{X}$ cells responded in such an unusual manner to drifting gratings that the resulting SFRs were ill defined. Furthermore, SFRs could not be determined for $\overline{X}$ cells which were responsive only to abrupt temporal modulations since drifting gratings typically elicited no responses.

A low frequency decline was absent in most of the $\overline{X}$ cells which had produced second harmonics over a wide range of spatial frequencies during the null test. Other features of the SFR varied widely among these cells. Both abrupt and gradual declines in responsiveness to higher spatial frequencies were observed with equal probability. No relationship between the form of the high frequency roll-off and other functional properties of the cells - i.e. full field response type or temporal preference - was observed. The SFRs of two cells in this group showed an elevation in responsiveness at a spatial frequency approximately three octaves higher than their optimal spatial frequency. No change in responsiveness to this higher spatial frequency was apparent, however, during the null test. Figure 41 presents the SFRs of one of these cells at two drift rates. The magnitudes of the first two harmonics are plotted as the response measures. In these two cells, the preferred drift rate caused an increase in the first harmonic component at a higher than optimal

Figure 41

SFRs of an $\overline{X}$ cell obtained at two drift rates: .125 Hz (A) and 1 Hz (B). Two response measures are plotted as a function of spatial frequency: first harmonic magnitude (filled squares) and second harmonic magnitude (open squares). Stimulus contrast was .5.

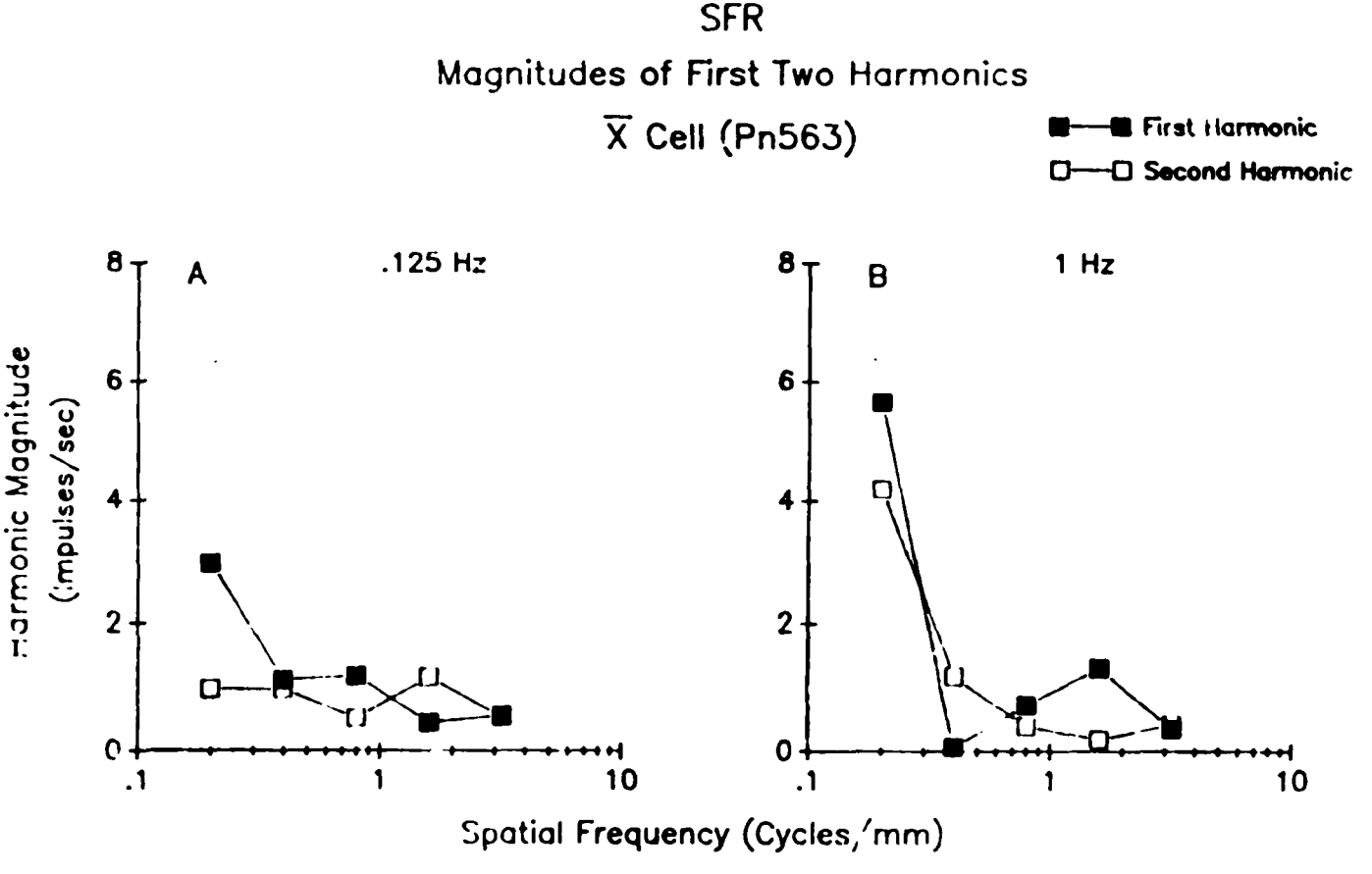
SFR
Magnitudes of First Two Harmonics
X̄ Cell (Pn563)
First Harmonic
Second Harmonic
A
.125 Hz
B
1 Hz
Harmonic Magnitude (Impulses/sec)
8
6
4
2
0
.1
1
10
Spatial Frequency (Cycles/mm)

spatial frequency. Nonoptimal temporal modulation resulted in a minor increase in second harmonics at the same spatial frequency. Figure 41 also demonstrates a differential effect of drift rate upon the relative magnitudes of the first two harmonics at a lower spatial frequency: the second harmonic clearly dominates at .4cycles/mm but only at a moderate drift rate.

The appearance of second harmonics during SFR determinations was common among $\overline{X}$ cells which had produced second harmonics only at low spatial frequencies during the null test. The SFRs, obtained at two drift rates, of one of these $\overline{X}$ cells is shown in Figure 42 with both mean response rate and the magnitudes of the first two harmonics plotted on the Y axis. Responding was maximal at .4cycles/mm for both slow and moderate drift rates. The dominant harmonic component of this maximal response was, however, dependent upon drift rate. The differential effect of drift rate upon the dominant harmonic was different from that seen in the group of $\overline{X}$ cells discussed in the preceding paragraph. In these cells the preferred drift rate (1 Hz) resulted in an increase in the second harmonic at the optimum spatial frequency while at a slow drift rate, the first harmonic dominated. This interaction between dominant harmonic and drift rate was a common observation in this 'group' of $\overline{X}$ cells, with second harmonics appearing only when a given cell's preferred

Figure 42

SFRs of another $\overline{X}$ cell obtained at two drift rates: .125 Hz (A) and 1 Hz (B). Three response measures are plotted as a function of spatial frequency: mean response rate (filled circles), first harmonic magnitude (filled squares), and second harmonic magnitude (open squares). Stimulus contrast was .5.

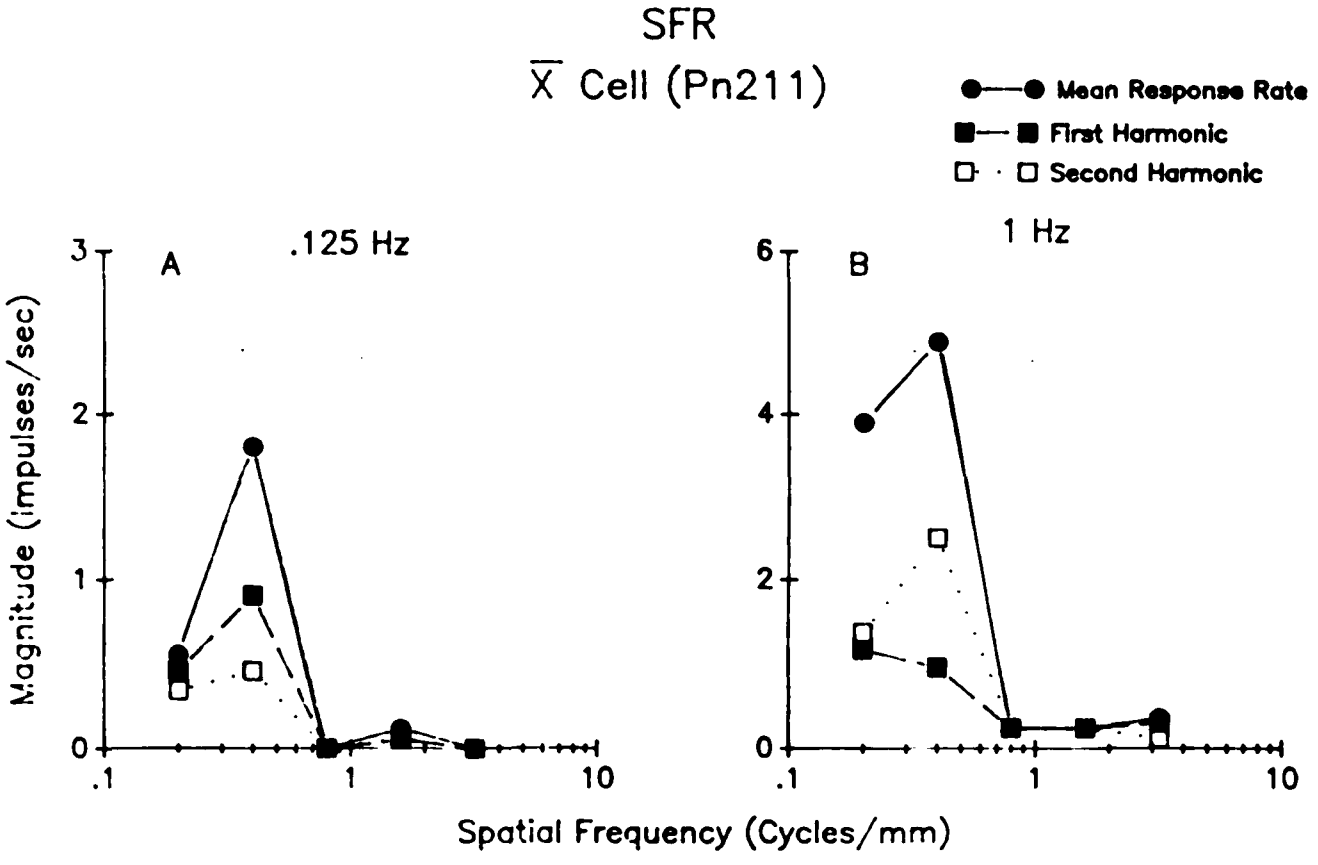
SFR
X̄ Cell (Pn211)
Mean Response Rate
First Harmonic
Second Harmonic
A
.125 Hz
B
1 Hz
Magnitude (impulses/sec)
Spatial Frequency (Cycles/mm)
0
1
2
3
4
6
.1
1
10

drift rate was used. In terms of other features of the SFR, such as optimum spatial frequency and the shape of high frequency roll-off, no consistent trends were observed among these cells.

3.4.3 Receptive Field Profile

RF profiles varied markedly among $\overline{X}$ cells. Exploration of the RF was complicated by the fact that many $\overline{X}$ cells responded only when large regions of their RF were stimulated. An additional complication was the fact that the RF was mapped with stimuli modulated at a temporal frequency deemed optimal for the cell based on its responses to uniform changes in illumination. Yet, as suggested by the complex interaction between temporal modulation and dominant harmonic response component in many $\overline{X}$ cells' SFRs, the possibility exists that different components of an $\overline{X}$ cell's RF may have different temporal properties. Thus, the use of one temporal modulation in mapping the RF may not have fully exposed all RF components.

Figure 43 presents three of the more common RF profiles observed among $\overline{X}$ cells. Many $\overline{X}$ cells appeared to possess large, diffuse RFs in which 'on' and 'off' regions appeared to alternate (Figure 43A). This RF organization was typical of many cells which had produced second harmonics over a wide range of spatial frequencies during

Figure 43

Receptive field profiles of three $\overline{X}$ cells. The response measure is the mean response rate of 'on' responses (open circles) and 'off' responses (filled circles). Receptive fields were mapped with a narrow bar, the intensity of which was square wave modulated above and below the mean level of the background. The contrast of the bar was .5. The width of the bar was 1mm for the cell in (A) and .5 mm for the cells in (B) and (C). The modulation rate of the bar was .125 Hz for all three cells.

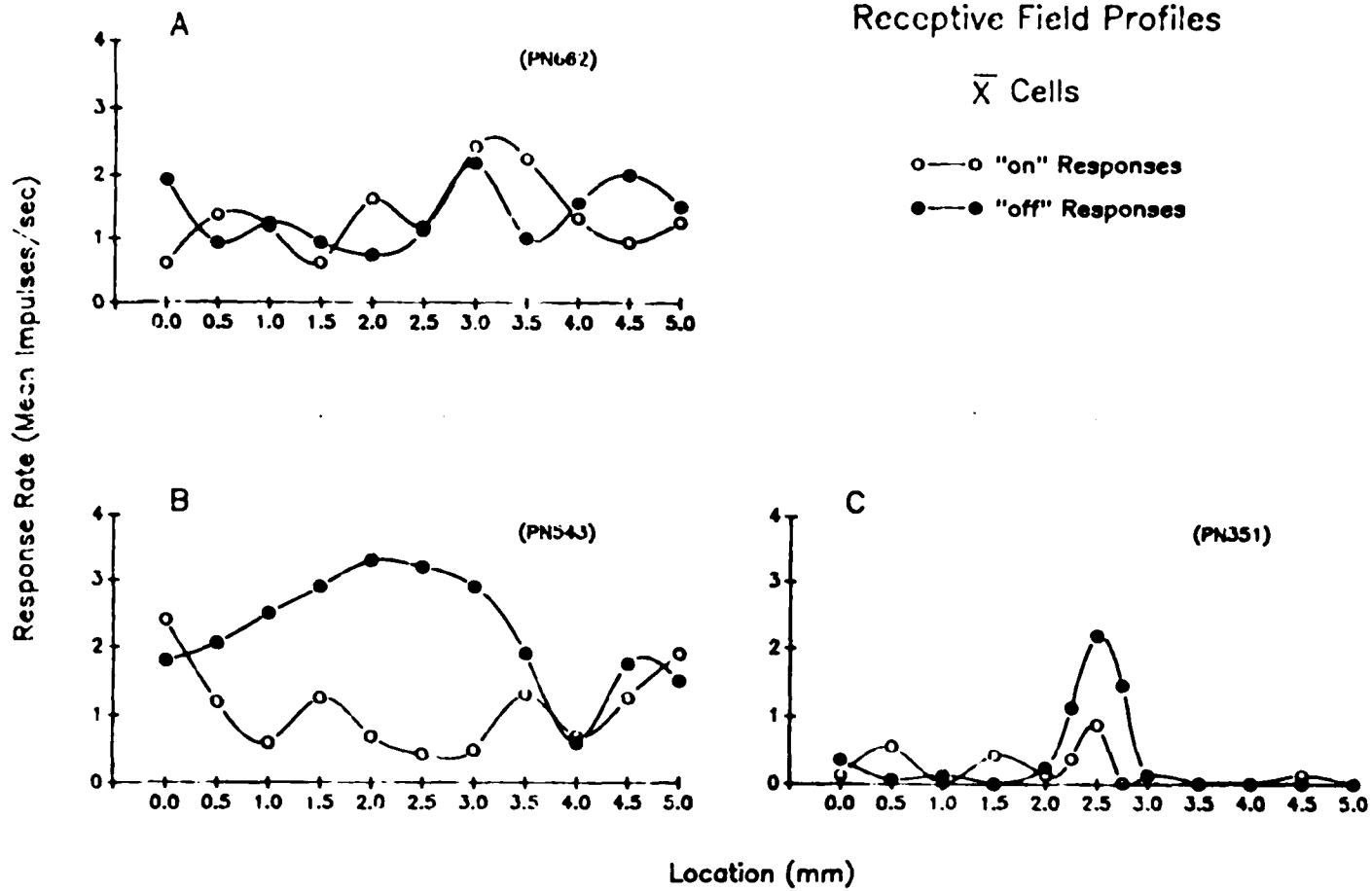
Receptive Field Profiles
$\bar{X}$ Cells
o—o "on" Responses
●—● "off" Responses
A
(PN662)
B
(PN543)
C
(PN351)
Response Rate (Mean Impulses/sec)
Location (mm)
0.0 0.5 1.0 1.5 2.0 2.5 3.0 3.5 4.0 4.5 5.0
0 1 2 3 4

the null test. Given, however, the fact that the wide stimuli required to map these cells' RFs undoubtedly obscured boundaries between individual components, the precise spatial relationship between 'on' and 'off' regions, as well as the total RF extent, illustrated in Figure 43A may not be entirely accurate.

Another RF profile observed with some regularity in $\overline{X}$ cells is presented in Figure 43B. There is a large center region throughout which are distributed smaller and less responsive regions producing responses opposite in sign to those of the center. This RF organization was more common in those cells producing frequency doubled responses to low spatial frequencies but was also observed, to a lesser degree, in other $\overline{X}$ cells.

Finally, a few $\overline{X}$ cells possessed a very small RF, seen in Figure 43C, in which both 'on' and 'off' regions appeared to be superimposed. This RF organization was seen in $\overline{X}$ cells demonstrating a preference for square wave modulation and in those producing second harmonic responses over a wide range of spatial frequencies.

3.5 Window vs. Shutter Tests in Y Cells

In order to determine the relative RF locations of linear and nonlinear summating mechanisms within Y cells, comparative responsiveness of the two mechanisms within central (window condition) and peripheral (shutter

condition) regions of the RF was examined. Optimal spatial frequencies for the linear and nonlinear processes, based on results from the null test, were chosen as the low and high spatial frequencies, respectively, for the window/shutter tests. The width of the window was often much narrower than one cycle of a low spatial frequency grating. Therefore the change in intensity within the RF did not vary greatly with spatial phase. The responses of all Y cells, however, continued to display a marked dependence upon spatial phase for low spatial frequencies even though response amplitude was considerably lower than when the entire grating was presented.

The extent of the nonlinear subunits was found to differ considerably between the Y1 and Y2 subgroups. Detailed descriptions of the results from each of these two groups are individually presented in the following section.

3.5.1 Y1 Cells

Window/shutter analyses were conducted in six Y1 cells. The effect of window vs shutter conditions upon mean response rate of one of these cells to both low and high spatial frequencies is demonstrated in Figure 44. There was an attenuation in responsiveness to a low spatial frequency in the shutter condition relative to the window condition. Conversely, a high spatial frequency grating presented to the RF periphery elicited a substantially

Figure 44

The effect of window vs shutter conditions on the responsiveness of a Y1 cell to a low and a high spatial frequency grating. Mean response rate is plotted as a function of spatial phase for a low spatial frequency, .4 cycles/mm (filled squares), and for a high spatial frequency, 6.4 cycles/mm (open squares). For both conditions, results obtained for only half of the stimulus spatial cycle are displayed. Responses produced during the first and second halves of the grating's temporal cycle are plotted as positive and negative values, respectively. The stimulus was a contrast reversal grating presented at a reversal rate of 1 Hz. Contrast was .5. In the window condition, the grating was restricted to a narrow portion (1 mm wide) of the receptive field center. In the shutter condition, the grating was presented to the receptive field regions surrounding the 'window' area. The solid line represents the best fit sinusoid determined for mean response rate to the low spatial frequency grating.

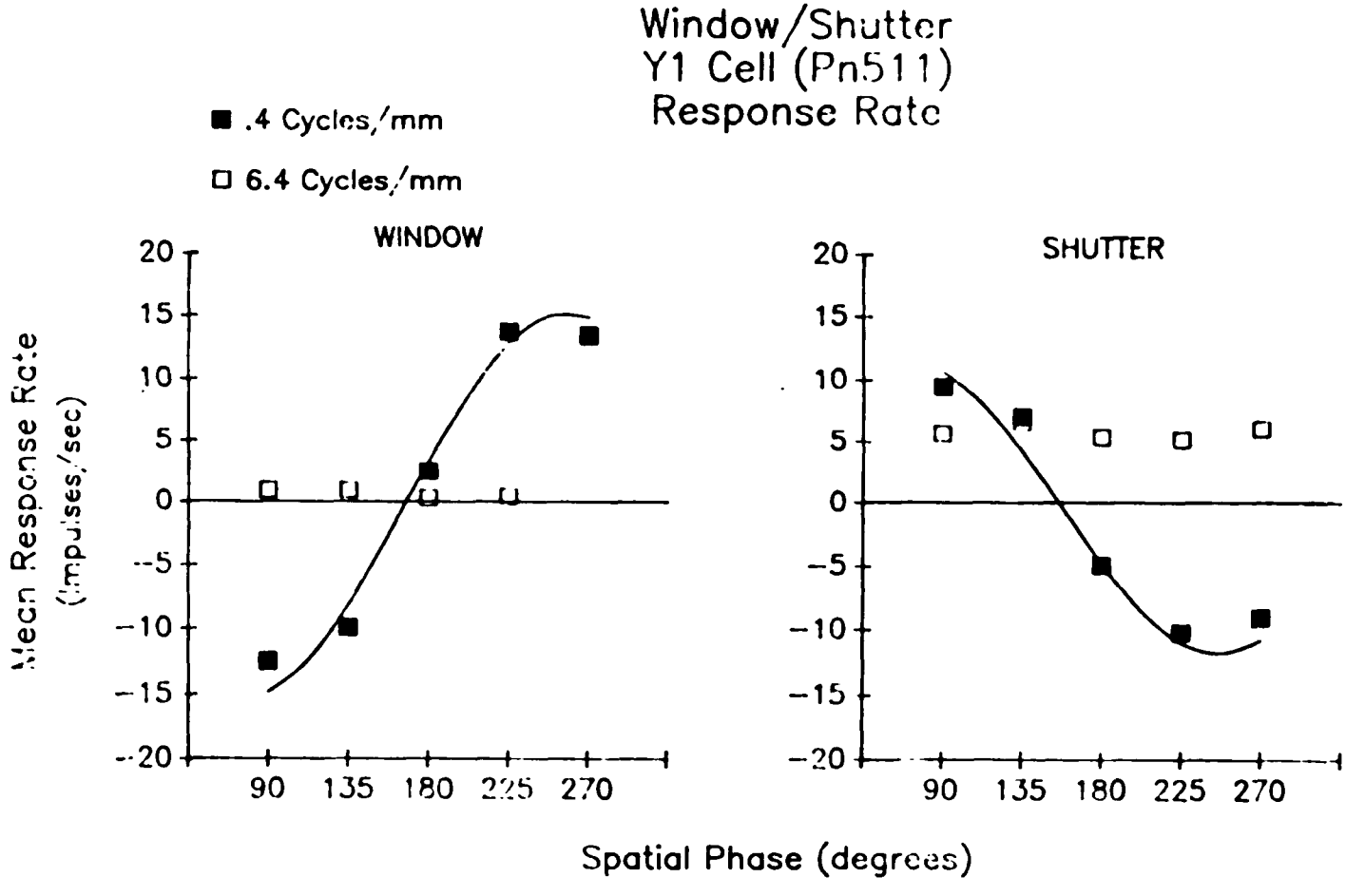
Window/Shutter
Y1 Cell (Pn511)
Response Rate
.4 Cycles/mm
6.4 Cycles/mm
WINDOW
SHUTTER
Mean Response Rate
(Impulses/sec)
20
15
10
5
0
-5
-10
-15
-20
90
135
180
225
270
Spatial Phase (degrees)

higher response rate than when it had been restricted to the center of the RF. The effect of differential RF occlusion upon the first two harmonic components of responding to the two spatial frequencies is shown in Figure 45. The relative weight of the first two harmonics remained unchanged between the two conditions for a low spatial frequency: the first harmonic was dominant at all spatial phases in both window and shutter presentations. When a high spatial frequency was presented, window and shutter presentations had dramatically different effects upon harmonic response components. The magnitudes of both first and second harmonics were very low and neither clearly dominated responding when a high spatial frequency was restricted to the central portion of the RF. During the shutter condition, responding was dominated by the second harmonic comparable in magnitude to that observed during the null test for this spatial frequency.

Results identical to those described above were obtained in two other Y1 cells. The remaining Y1 cells differed in the relative effect of the two conditions upon responding to high, but not low, spatial frequencies. Window/shutter test results obtained from one of these cells are shown in Figure 46, which displays mean response rate, and Figure 47 which presents the corresponding harmonic magnitudes. A comparison of overall response rate to a high spatial frequency between window and shutter

Figure 45

The effect of window vs shutter conditions upon the first (filled circles) and second (open diamonds) harmonics of a Y1 cell's responses to low and high spatial frequencies. This is the same cell as in Figure 44. All stimulus parameters are the same as those described for Figure 44. The results obtained with a spatial frequency of .4 cycles/mm are shown in (A) and (B); corresponding data for 6.4 cycles/mm are presented in (C) and (D). All four graphs present results obtained for only half of the stimulus spatial cycle. Responses produced during the first and second halves of the grating's temporal cycle are plotted as positive and negative values, respectively. The solid lines in (A and B) represent the best fit sinusoids determined for the first harmonic response components.

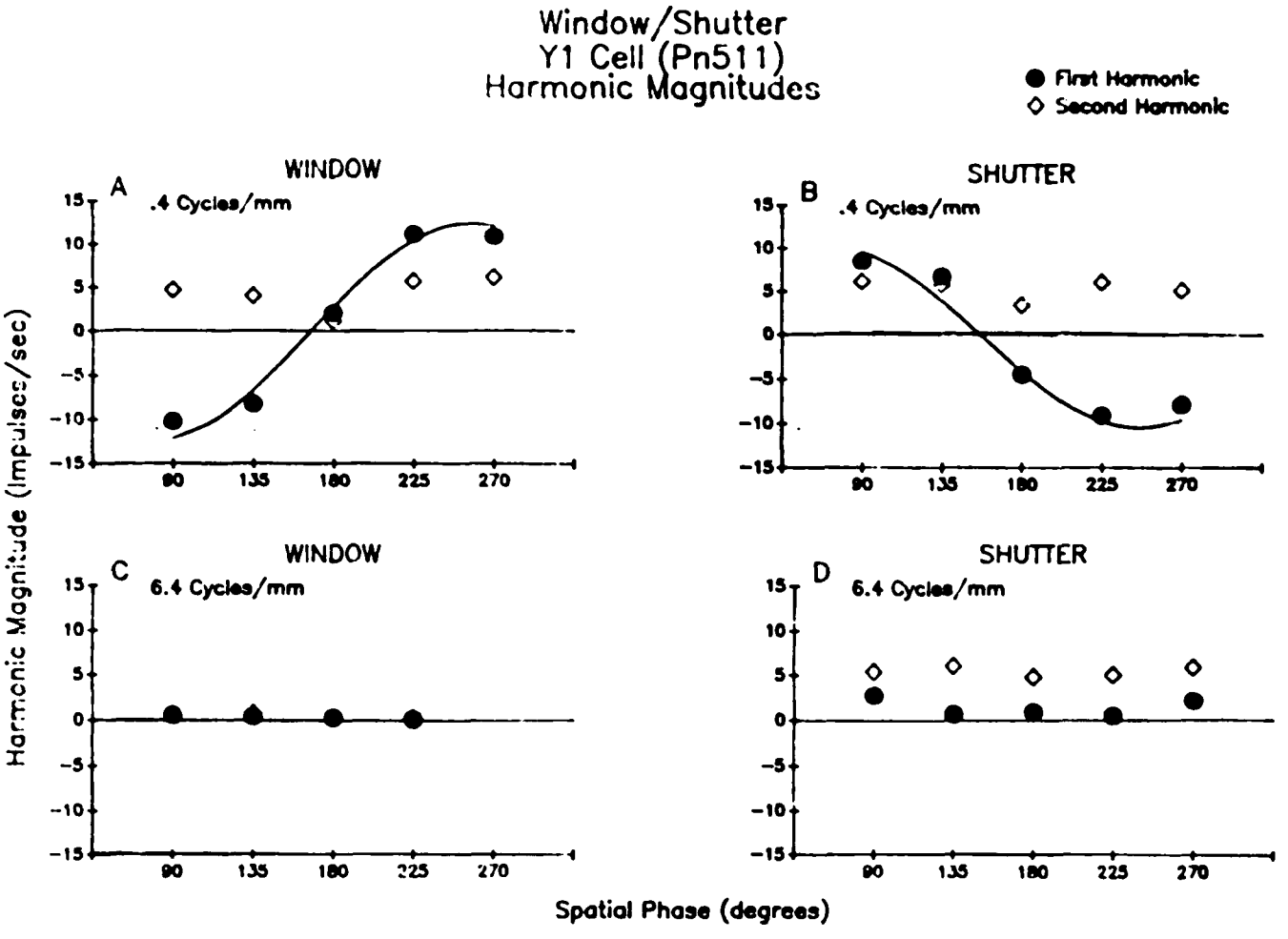
Window/Shutter
Y1 Cell (Pn511)
Harmonic Magnitudes
First Harmonic
Second Harmonic
WINDOW
A
.4 Cycles/mm
SHUTTER
B
.4 Cycles/mm
WINDOW
C
6.4 Cycles/mm
SHUTTER
D
6.4 Cycles/mm
Harmonic Magnitude (Impulses/sec)
15
10
5
0
-5
-10
-15
90
135
180
225
270
Spatial Phase (degrees)

Figure 46

The effect of window vs shutter conditions on the responsiveness of another Y1 cell to a low and a high spatial frequency grating. Mean response rate is plotted as a function of spatial phase for a low spatial frequency, .2 cycles/mm (filled squares), and for a high spatial frequency, 12.8 cycles/mm (open squares). For both conditions, results obtained for only half of the stimulus spatial cycle are displayed. Responses produced during the first and second halves of the grating's temporal cycle are plotted as positive and negative values, respectively. The stimulus was a contrast reversal grating presented at a reversal rate of 1 Hz. Contrast was .5. In the window condition, the grating was restricted to a narrow portion (1 mm wide) of the receptive field center. In the shutter condition, the grating was presented to the receptive field regions surrounding the 'window' area. The solid line represents the best fit sinusoid determined for mean response rate to the low spatial frequency grating.

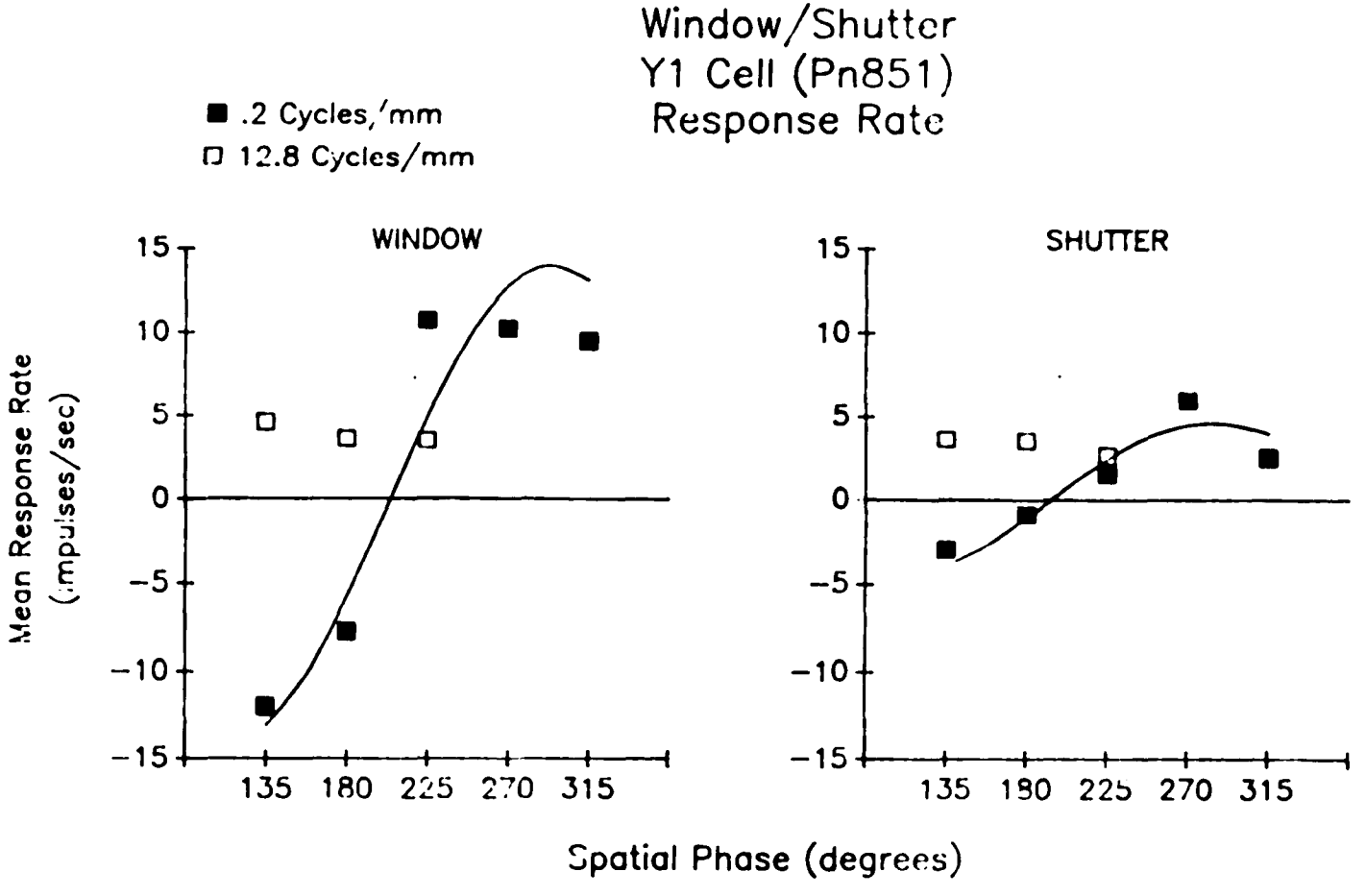
Window/Shutter
Y1 Cell (Pn851)
Response Rate
.2 Cycles/mm
12.8 Cycles/mm
WINDOW
SHUTTER
Mean Response Rate
(impulses/sec)
15
10
5
0
−5
−10
−15
135
180
225
270
315
Spatial Phase (degrees)

Figure 47

The effect of window vs shutter conditions upon the first (filled circles) and second (open diamonds) harmonics of a Y1 cell's responses to low and high spatial frequencies. This is the same cell as in Figure 46. All stimulus parameters are the same as those described for Figure 46. The results obtained with a spatial frequency of .2 cycles/mm are shown in (A) and (B); corresponding data for 12.8 cycles/mm are presented in (C) and (D). All four graphs present results obtained for only half of the stimulus spatial cycle. Responses produced during the first and second halves of the grating's temporal cycle are plotted as positive and negative values, respectively. The solid lines in (A and B) represent the best fit sinusoids determined for the first harmonic response components.

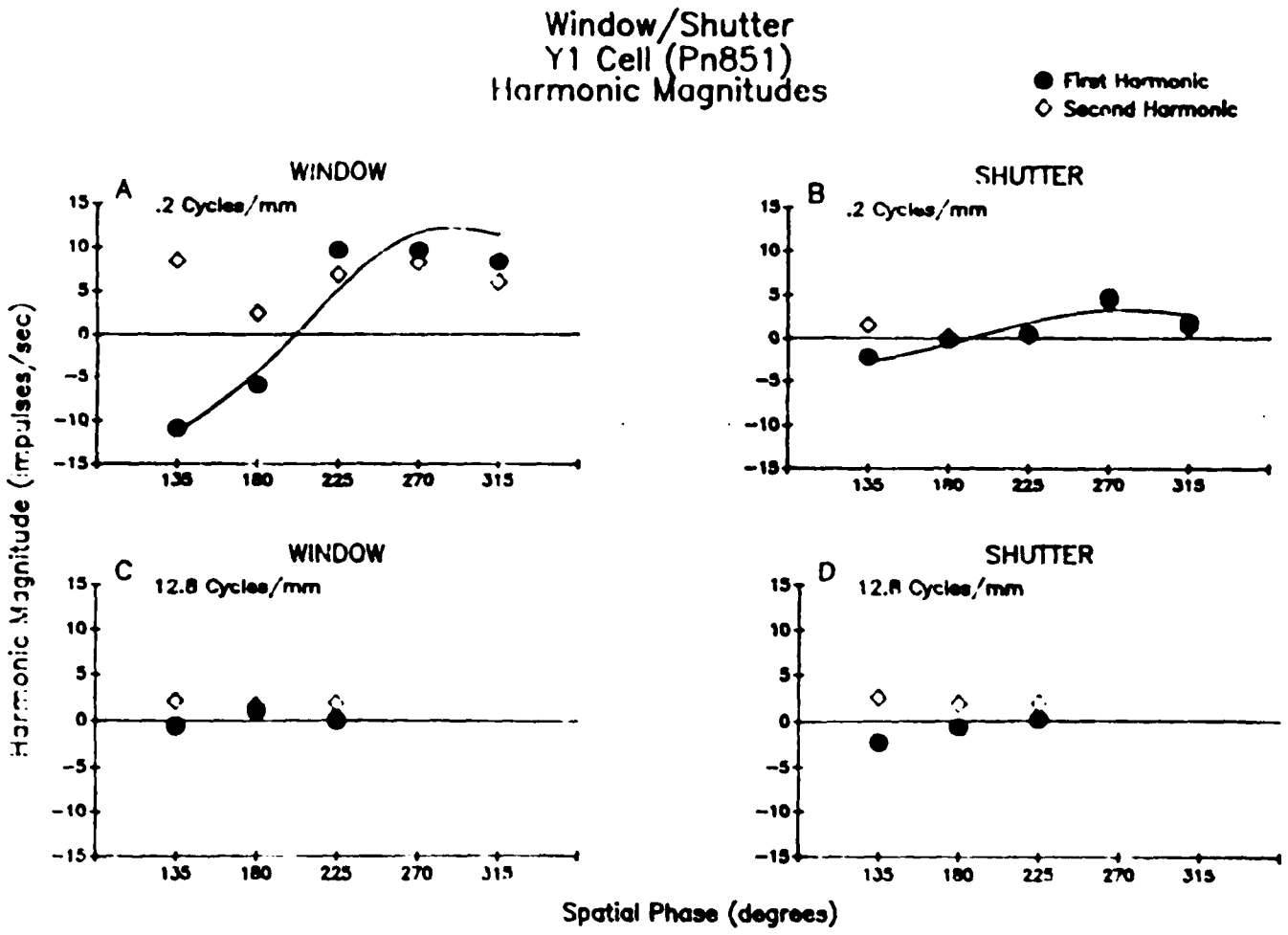
Window/Shutter
Y1 Cell (Pn851)
Harmonic Magnitudes
First Harmonic
Second Harmonic
WINDOW
A
.2 Cycles/mm
SHUTTER
B
.2 Cycles/mm
WINDOW
C
12.8 Cycles/mm
SHUTTER
D
12.8 Cycles/mm
Harmonic Magnitude (impulses/sec)
15
10
5
0
-5
-10
-15
135
180
225
270
315
Spatial Phase (degrees)

conditions (Figure 46) reveals no difference. Similarly, Figures 47C and 47D indicate that second harmonics, of approximately equal magnitude, dominated responding to a high spatial frequency during both conditions.

For all Y1 cells examined, the nonlinear component displayed a wider spatial extent than that of the linear component. The results obtained in the Y1 cells, therefore, suggest that the RF model proposed by Hochstein and Shapley (1976b) for Y cells in the cat is also applicable to Y1 cells in the frog: nonlinearly integrating subunits are widely distributed across a central linear summating region. One apparent difference between cat Y cells and frog Y1 cells deserves brief mention. In cats, the Y cell's fundamental response to low spatial frequencies was substantially diminished during shutter presentation. The decrease produced by shutter presentation was comparatively less impressive in the frog, undoubtedly because of the sizable extent of Y1 cells' RFs.

3.5.2 Y2 Cells

The differential effect of window vs shutter presentations upon linear and nonlinear response components seen in Y1 cells was not observed in the three Y2 cells similarly examined. Results obtained from a representative Y2 cell are shown in Figures 48 and 49.

Figure 48

The effect of window vs shutter conditions on the responsiveness of a Y2 cell to a low and a high spatial frequency grating. Mean response rate is plotted as a function of spatial phase for a low spatial frequency, .4 cycles/mm (filled squares), and for a high spatial frequency, 1.6 cycles/mm (open squares). For both conditions, results obtained for only half of the stimulus spatial cycle are displayed. Responses produced during the first and second halves of the grating's temporal cycle are plotted as positive and negative values, respectively. The stimulus was a contrast reversal grating presented at a reversal rate of 1 Hz. Contrast was .5. In the window condition, the grating was restricted to a narrow portion (1 mm wide) of the receptive field center. In the shutter condition, the grating was presented to the receptive field regions surrounding the 'window' area. The solid line represents the best fit sinusoid determined for mean response rate to the low spatial frequency grating.

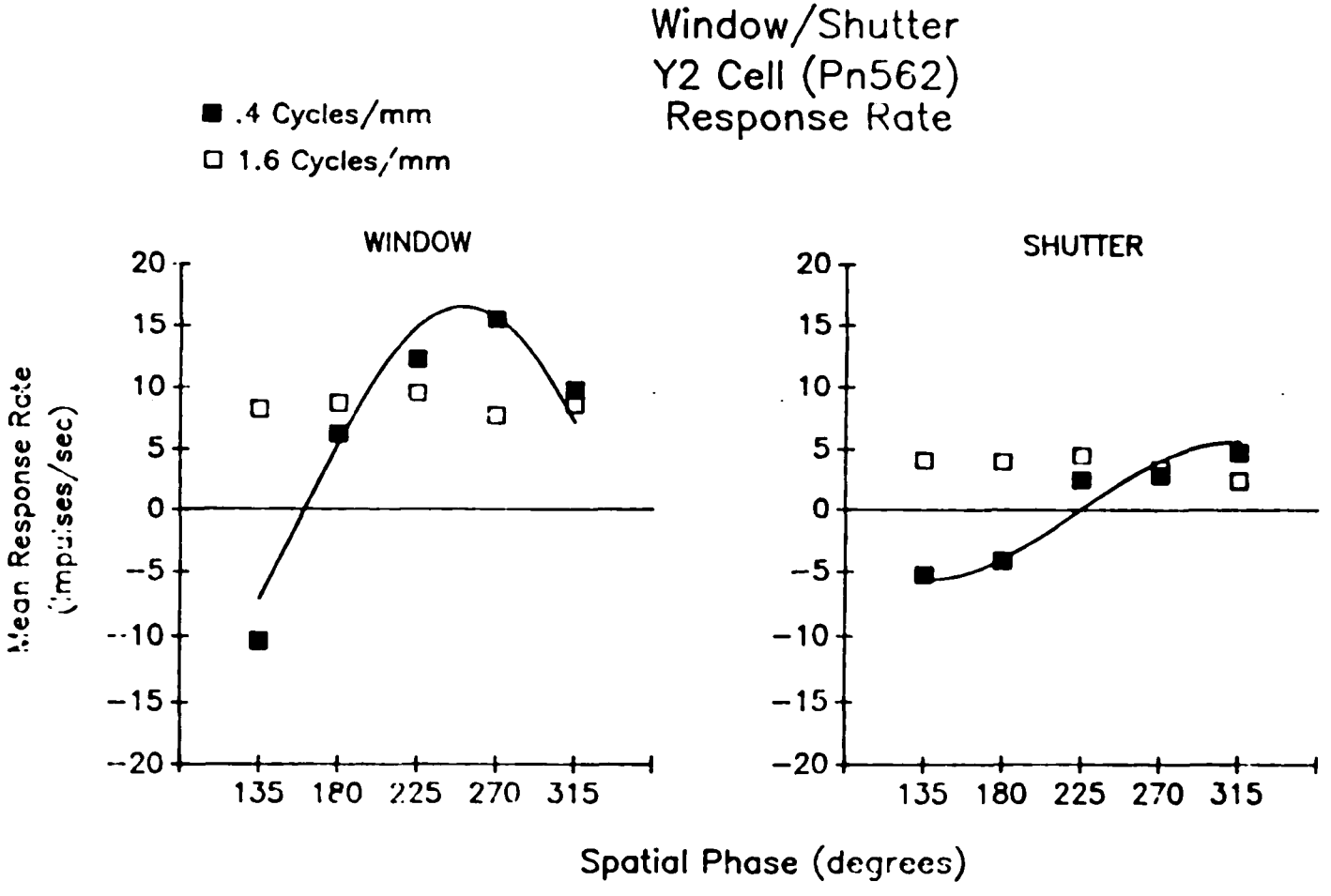
Window/Shutter
Y2 Cell (Pn562)
Response Rate
.4 Cycles/mm
1.6 Cycles/mm
WINDOW
SHUTTER
Mean Response Rate
(impulses/sec)
20
15
10
5
0
-5
-10
-15
-20
135
180
225
270
315
Spatial Phase (degrees)

Figure 49

The effect of window vs shutter conditions upon the first (filled circles) and second (open diamonds) harmonics of a Y2 cell's responses to a low and a high spatial frequency grating. This is the same cell as in Figure 48. All stimulus parameters are the same as those described for Figure 48. The results obtained with a spatial frequency of .4 cycles/mm are shown in (A) and (B); corresponding data for 1.6 cycles/mm are presented in (C) and (D). All four graphs present results obtained for only half of the stimulus spatial cycle. Responses produced during the first and second halves of the grating's temporal cycle are plotted as positive and negative values, respectively. The solid lines in (A and B) represent the best fit sinusoids determined for the first harmonic response components.

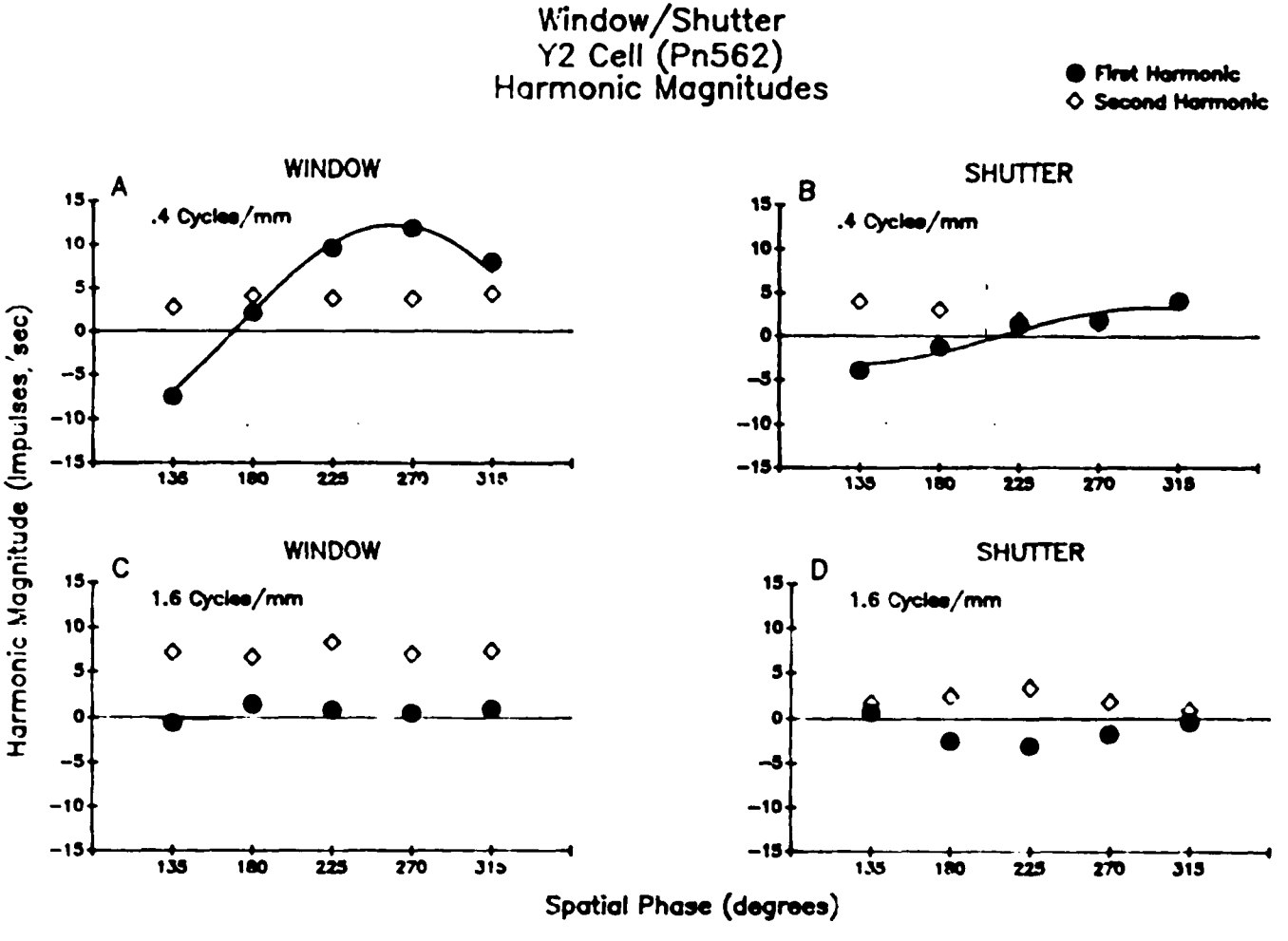
Window/Shutter
Y2 Cell (Pn562)
Harmonic Magnitudes
First Harmonic
Second Harmonic
WINDOW
A
.4 Cycles/mm
SHUTTER
B
.4 Cycles/mm
WINDOW
C
1.6 Cycles/mm
SHUTTER
D
1.6 Cycles/mm
Harmonic Magnitude (Impulses/sec)
Spatial Phase (degrees)

During the shutter condition responding to both low and high spatial frequencies was considerably decreased relative to window presentation (Figure 48). Figure 49 shows that responding to the low spatial frequency, during the window condition, was dominated by the first harmonic at most spatial phases except at the null position. Window presentation of a high spatial frequency elicited dominant second harmonic responses which were phase independent. When the low spatial frequency was restricted to the RF periphery both first and second harmonic magnitudes were equally diminished. A corresponding decrease in second harmonic responses was observed during shutter presentation of the high spatial frequency. The remaining Y2 cells yielded identical results.

Because responding to both high and low spatial frequencies was similarly affected in each condition, it is unlikely that linear and nonlinear components are differentially distributed within the Y2 RF as they are in Y1 cells. Additional tests were performed to determine whether or not the nonlinear subunits extended into the regions flanking the Y2 RF center. Uniform changes in intensity were restricted to regions corresponding to the window and shutter conditions used during grating presentation. In order to distinguish between central and flanking responses, intensity was temporally modulated according to a square wave function which had proven to be

most effective at isolating these two components during prior exploration of the RF. Figures 50C and 50D present the results of this test along with the corresponding results obtained with low (Figures 50A and 50D) and high (Figures 50B and 50E) spatial frequency gratings. Figure 50 reveals that maximum responsiveness to both a low and a high spatial frequency was associated with center elicited 'off' responses. Conversely, under conditions in which the flanking 'on' response prevailed, responding to low and high spatial frequencies was substantially reduced. More importantly, however, was the fact that dominant second harmonic responses to the high spatial frequency were only associated with a dominant center response.

Both linear and nonlinear components, thus, appear to be equally restricted to the RF center of Y2 cells indicating a significant departure from the RF organization of frog Y1 cells and cat Y cells.

An alternative explanation for the observed differences between Y1 and Y2 cells was considered; that the apparent difference in the spatial extent of the nonlinear mechanism was related to the relative difference in overall RF extent. Therefore, it could be possible that the subunits of both Y1 and Y2 cells are spatially restricted to the center component of the RF but, because the center of Y1 cells is so large, the subunits fortuitously appear to spread beyond the traditional

Figure 50

Relative strength of receptive field components of a Y2 cell during window and shutter conditions with comparison to responding to low and high spatial frequencies. The width of the window was .5 mm. Uniform changes in intensity used to elicit center and flanking responses (C and F) were square wave reversed at a rate of 1 Hz. For (A, B, D, E) contrast reversal gratings - .4 cycles/mm and 1.6 cycles/mm - were sinusoidally modulated at a rate of 1 Hz. The contrast of all stimuli was .5. Responses obtained during the window condition are indicated in the left column (A, B,C), those obtained during the shutter condition are shown in the right column (D,E,F). The upper two graphs of each column present the magnitudes of the first two harmonics plotted as a function of spatial phase for a low and a high spatial frequency grating. The spatial frequency of the grating is given above each graph. The percent of the response to uniform intensity changes attributable to center or flanking regions during a given condition is presented in the bottom graph in each column (C and F). The solid lines represent the best fit sinusoids for the first harmonic response components.

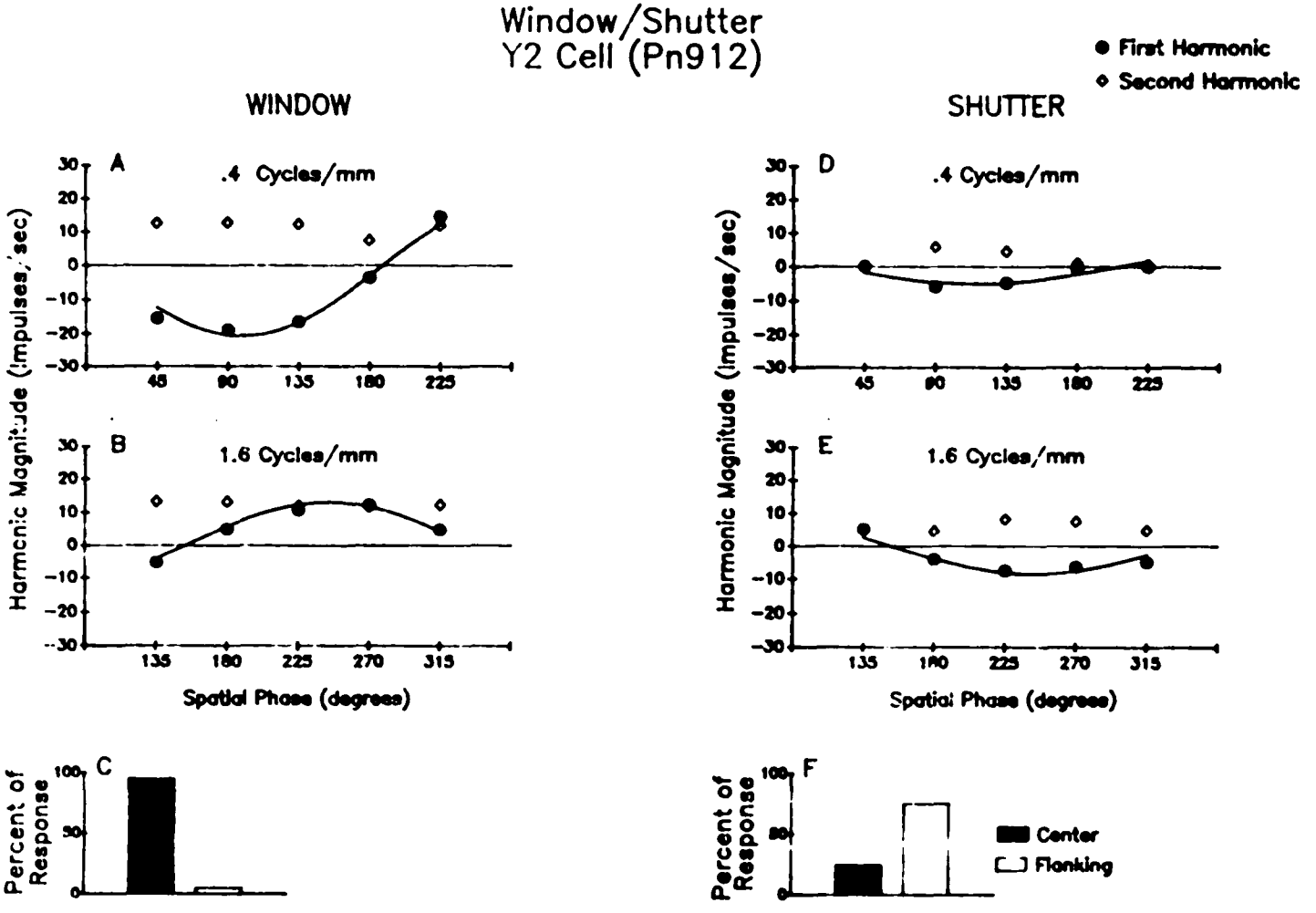
Window/Shutter
Y2 Cell (Pn912)
● First Harmonic
◇ Second Harmonic
WINDOW
SHUTTER
A
.4 Cycles/mm
B
1.6 Cycles/mm
D
.4 Cycles/mm
E
1.6 Cycles/mm
Harmonic Magnitude (impulses/sec)
Spatial Phase (degrees)
C
F
Percent of Response
Center
Flanking

center. This possibility is highly unlikely, however, given the differential effect peripheral stimulus presentation had upon the the responsiveness of linear vs nonlinear components in Y1 cells.

3.6 Contrast Gain Control

The effect of contrast upon the magnitude and temporal phase of responding to a range of temporal frequencies was examined in six X cells and nine Y cells. Responding to four contrast reversal rates (.25, 1, 4, and 16 Hz.) was examined at each of four contrasts (.34, .5, .63, and .76). None of the cells showed any response to 16 Hz; thus, this temporal frequency will be eliminated from further discussions. For a given cell, the stimulus grating was positioned at the peak phase angle as determined during the null test. The spatial frequency of the grating was that which had proven to be optimal for the cell's linear component. For many Y cells a high spatial frequency, which had elicited maximal second harmonic activity during the null test, was used in addition to the low spatial frequency. Both low and high spatial frequency gratings were employed for one X cell, described earlier (see section 3.2.1), which had shown very minor frequency doubling only at a very high spatial frequency.

It was not the purpose of these tests to provide a complete contrast/response curve; they were designed,

rather, to determine the effect of high contrasts upon two measures of responsiveness, most notably to fast stimulus rates, and to provide, therefore, some indication of whether or not contrast gain effects observed in cat retinal ganglion cells were present in the frog. Thus, a moderate contrast was used as the lowest of the four contrasts in these tests. Another reason for limiting the range of contrasts was based on practical considerations. The determination of contrast effects, even with this limited range, required a substantial amount of time. Since, contrast effects were examined only after many other analyses had been completed, there was a high risk in losing the cell. In fact, about three times as many contrast effect determinations than are reported herein were started but shortly abandoned because the cell was lost. A compromise was adopted, therefore, which would provide some indication, albeit preliminary, of the existence of a contrast gain mechanism and its relationship to X and Y cells in the frog.

The effect of contrast upon responding showed enough variability within a given cell class to warrant a certain amount of caution in drawing any specific conclusions about interclass differences. In general, however, increases in contrast resulted in more dramatic changes in Y cells' responsiveness to fast stimulus rates as compared to X cells.

3.6.1 Y Cells

For the majority of Y cells (six out of nine) the most obvious effect of increasing contrast was manifested as an enhancement of responsiveness - an increase in amplitude, an advance in response temporal phase, or both - to fast stimulus rates.

Figure 51A shows the relative temporal phase of the dominant harmonic component of the response - the first harmonic - at three reversal rates as a function of contrast for a representative Y cell. Because a low spatial frequency was used, second harmonic contribution to responding was negligible and therefore not presented in the graph. At a low spatial frequency, responding to a fast reversal rate (4 Hz) displayed a substantial phase advance with increasing contrast. A noticeable phase lag, at slower rates, was also observed as contrast was increased. As seen in Figures 51B and 51C, no substantial interaction between contrast and temporal modulation was observed, however, when either first harmonic magnitudes or average impulse rates were compared among the three reversal rates. This finding, that a differential increase in response magnitude need not accompany contrast dependent phase advances at low spatial frequencies, was observed in five of the six Y cells demonstrating some form of

Figure 51

The effect of contrast upon three aspects of a Y cell's response. The stimulus consisted of a contrast reversal grating, with a spatial frequency of .4 cycles/mm, at the phase angle representing the peak position for this particular Y cell. Three reversal rates were employed: .25 Hz (filled circles), 1 Hz (open circles), and 4 Hz (open triangles). The relative temporal phase of the first harmonic response component is plotted as a function of contrast in (A). The relative phase measure was determined in the following manner. The temporal phase of the response at the lowest contrast (.34) was arbitrarily designated 0 degrees. Subsequent changes in temporal phase, with increasing contrast, are thus plotted as either positive or negative deviations from this 'starting phase'. Positive phase values indicate a temporal advance of the response with contrast. Conversely, negative phase values identify contrast dependent phase lags in the response. Mean response rate as a function of contrast is displayed in (B). The magnitude of the first harmonic component is plotted as a function of contrast in (C).

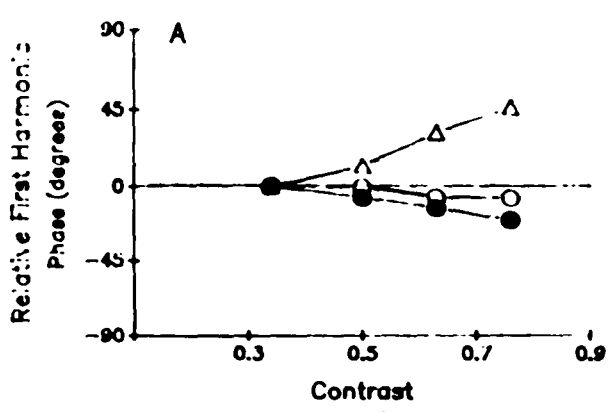

Contrast Gain
Y Cell (Pn562)
Phase and Magnitude

●—● .25 Hz
○—○ 1 Hz
Δ—Δ 4 Hz

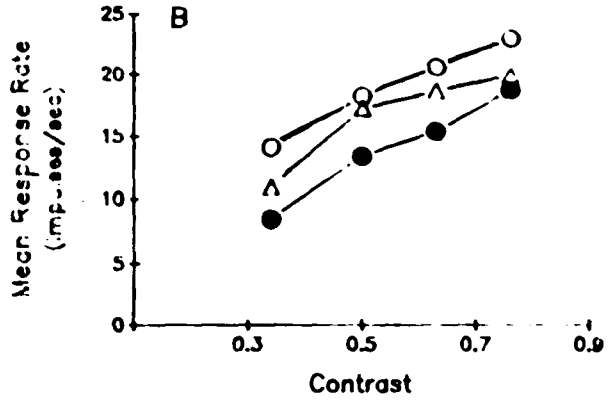

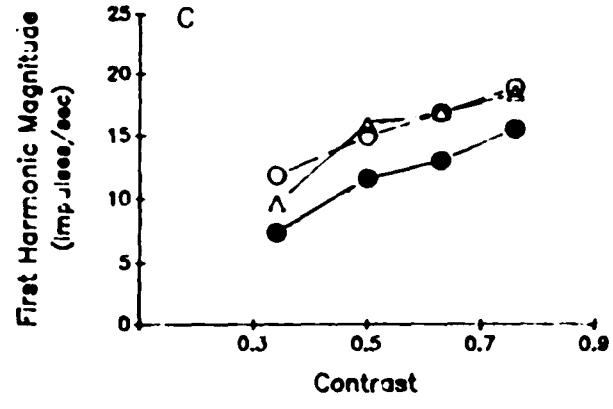

contrast/temporal frequency interaction. Only one cell exhibited a temporal frequency specific effect of contrast on both response magnitude and phase measures for a fast reversal rate.

Four of the six Y cells, exhibiting some form of a contrast dependent enhancement of responding to fast stimulus rates at a low spatial frequency, were also tested with a high spatial frequency. In two of these cells, the effect of contrast at high spatial frequencies on response magnitude was profoundly different from that observed at low spatial frequencies.

Figure 52A presents the magnitude of the dominant harmonic response component at three temporal frequencies as a function of contrast at both a low and high spatial frequency. At a low spatial frequency, the greatest increase in first harmonic magnitude as a function of contrast occurred when a moderate reversal rate (1Hz) was employed. Increasing the grating's contrast had little affect upon response magnitude when contrast was reversed at a faster rate (4Hz). At a high spatial frequency, however, responding to the fast reversal rate was noticeably augmented relative to slow and moderate rates as contrast was increased.

While the effect of contrast upon response magnitude to different temporal frequencies was contingent upon spatial frequency for these two cells, contrast dependent

Figure 52

The effect of contrast upon the magnitude of the dominant harmonic component of a Y cell's response. The stimulus consisted of a contrast reversal grating, positioned to obtain the peak response from this specific cell, modulated at each of three rates: .25 Hz (filled circles), 1 Hz (open circles) and 4 Hz (open triangles). (A) shows the effect of increasing contrast upon the magnitude of the first harmonic when a low spatial frequency grating, .4 cycles/mm, was employed. (B) shows the effect of increasing contrast upon the magnitude of the second harmonic for a high spatial frequency - 6.4 cycles/mm.

Contrast Gain
Y Cell (Pn732)
Harmonic Magnitudes

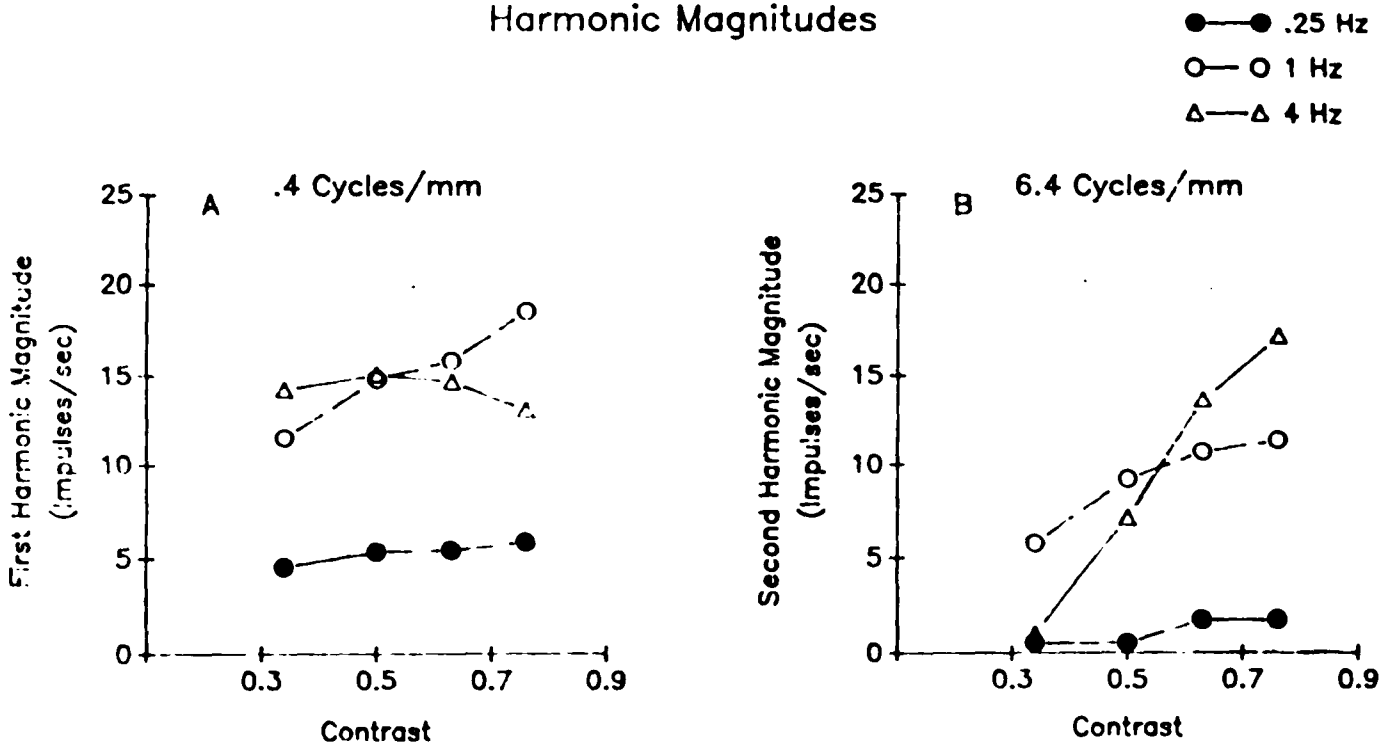

phase advances specific to the fast reversal rate were less differentially affected by spatial frequency. Figure 53 indicates that the most substantial phase advance with increasing contrast, regardless of spatial frequency, occurred to the fastest stimulus modulation. The temporal frequency specific phase advance, however, was more robust when a high spatial frequency was employed. There is also some evidence of a slight phase lag in responding to the slowest reversal rate, as a function of contrast, at the higher spatial frequency.

The two remaining Y cells, examined with both a low and a high spatial frequency, exhibited no accentuation of the contrast/temporal frequency interaction observed at a low spatial frequency when a high spatial frequency was employed. In fact, fast temporal modulation of a high spatial frequency elicited negligible levels of responding from these two cells.

In Y cells, therefore, the effect of increasing contrast upon responding to fast stimulus changes can be independently manifested as either an amplification or an acceleration of the response. For most Y cells, only an acceleration of the response is observed when responding is dominated by the first harmonic at a low spatial frequency. Both acceleration and amplification are evident, at least in a few Y cells, when spatial summation is nonlinear at a high spatial frequency. The Y cells not showing this

Figure 53

The effect of contrast upon the temporal phase of the dominant harmonic component of a Y cell's responses. This is the same Y cell as in Figure 52. All stimulus parameters are identical to those detailed for Figure 52. (A) presents the relative temporal phase of the first harmonic component at a spatial frequency of .4 cycles/mm. (B) presents the relative temporal phase of the second harmonic component at a spatial frequency of 6.4 cycles/mm. Normalization of response temporal phase was done in the same manner as described for Figure 51. Advances in temporal phase are indicated by positive values, phase lags are indicated by negative values.

Contrast Gain
Y Cell (Pn732)
Harmonic Phase

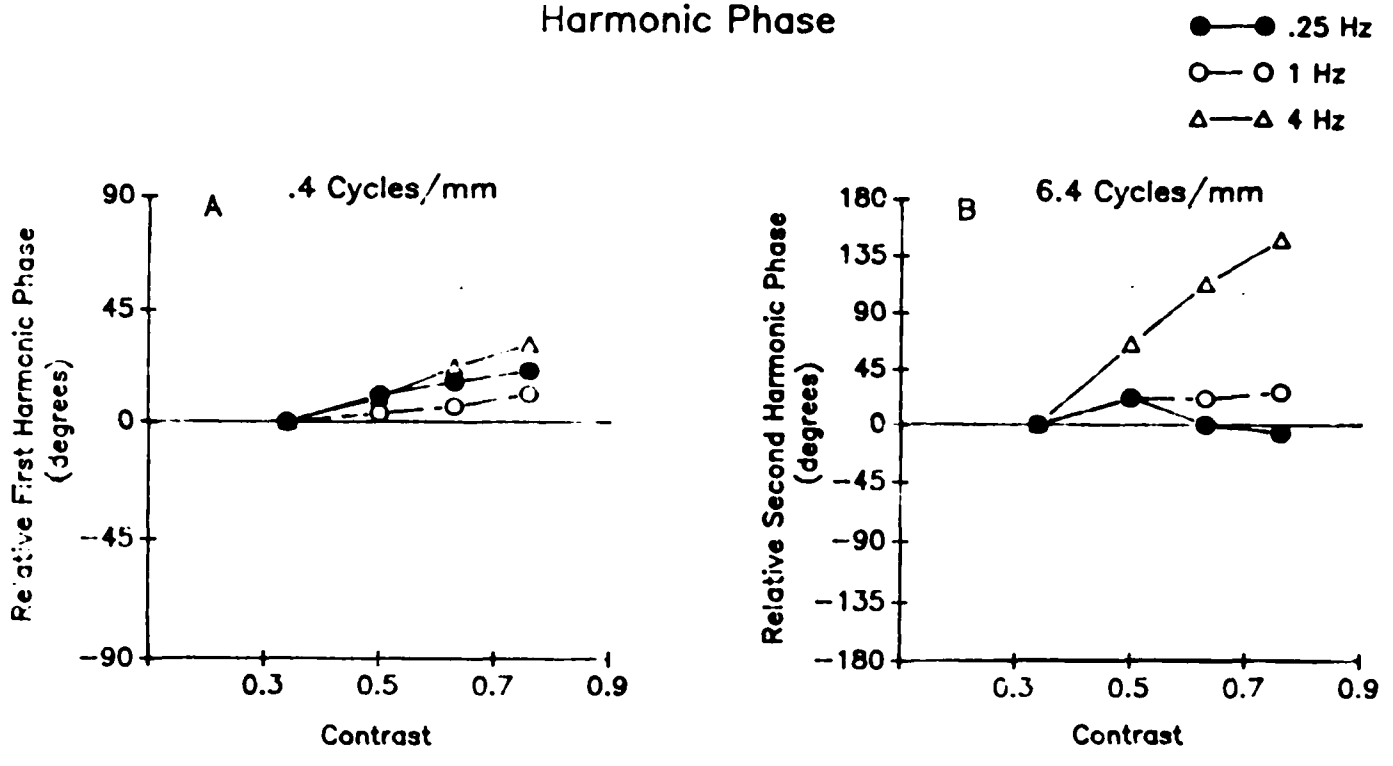

differential effect of spatial frequency were not clearly unique in any other respect from those which had done so.

The three Y cells which had not displayed any enhancement of responding to fast reversal rates as a function of contrast showed considerable variation in terms of their specific contrast/response functions. For one cell the greatest rate of response increase as a function of contrast occurred to a moderate reversal rate for both low and high spatial frequencies. Another cell showed very little response increase with increasing contrast at any reversal rate. In fact, there was a minor depression of response rate at a relatively high contrast, which was especially noticeable at the fastest temporal modulation. This cell was not examined with a high spatial frequency grating. The third cell presented yet another variation; the fastest growing response magnitude as a function of contrast occurred at the slowest temporal modulation regardless of spatial frequency.

3.6.1.1 Comparison Between Y1 and Y2 Cells

Of the nine Y cells examined for contrast effects, five were Y2 cells and three were clearly Y1 cells. The RF organization of the remaining cell was unknown, but because this cell was functionally identical to Y1 cells it was tentatively considered a Y1 cell. An advance in response phase during fast stimulus modulations, at low spatial

frequencies, was observed in two of the Y1 cells and four of the Y2 cells. The two cells which had displayed a clear effect of spatial frequency upon response magnitudes to fast modulations were both Y2 cells. Two of the three Y cells, not exhibiting any differential effect of contrast upon responding, were Y1 cells. Y2 cells, therefore, were more likely than Y1 cells to display contrast dependent response enhancement to fast stimulus changes. There was enough overlap between Y1 and Y2 cells, regarding specific contrast effects, to warrant restraint in rendering any conclusive statements about the two subgroups.

3.6.2 X Cells

Relatively fewer X than Y cells were examined for contrast effects owing, for the most part, to the short time period during which X cells could be "held" successfully. Therefore, the results presented herein for X cells should be regarded as somewhat preliminary. Some general observations, however, were made. Firstly, most X cells did not respond to the fast reversal rate (4 Hz) which had, in the majority of Y cells, displayed the greatest interaction with contrast in either advancing phase and/or increasing the magnitude of responding. Secondly, the effect of contrast upon response magnitude, regardless of the stimulus' temporal frequency, varied widely among the six X cells. The overall response rate of

two X cells, for example, did not increase substantially as contrast was increased. Thirdly, only one X cell showed evidence of a preferential phase shift in responding to a faster reversal rate; this, however, was observed only when a high spatial frequency was used. This was the same X cell which had produced minor frequency doubled responses to a very high spatial frequency during the null test (see section 3.2.1). Finally, two X cells displayed a minor differential increase in response magnitude with contrast to a moderate but not a slow reversal rate.

Figure 54 displays the results of contrast gain tests at a low spatial frequency in the one X cell responsive to the fast (4 Hz) reversal rate. Figure 54A reveals that the magnitude of the first harmonic increased with contrast at approximately the same rate for all temporal frequencies. This, as noted previously, was also observed in most of the Y cells for low spatial frequency gratings. Unlike the majority of Y cells, however, this X cell displayed no substantial phase shifts in responding to any temporal modulation (Figure 54B).

There was a minor augmentation of responding in two X cells, specific for a moderate reversal rate, as contrast was increased. Higher contrasts, however, resulted in phase advances in responses to both temporal frequencies. Figure 55A presents first harmonic magnitude as a function of contrast at two reversal rates for one of these cells.

Figure 54

The effect of contrast upon the magnitude and temporal phase of the first harmonic component of an X cell's responses. The stimulus was a contrast reversal grating positioned at a phase angle corresponding to this particular cell's peak position. The spatial frequency of the grating was .2 cycles/mm. Three reversal rates were used: .25 Hz (filled circles), 1 Hz (open circles), and 4 Hz (open triangles). Harmonic magnitude as a function of contrast is presented in (A) while the corresponding function for relative harmonic phase is shown in (B). Normalization of response temporal phase was done in the same manner as described for Figure 51. Advances in temporal phase are indicated by positive values, phase lags are indicated by negative values.

Contrast Gain
X Cell (Pn422)
Harmonic Magnitude and Phase

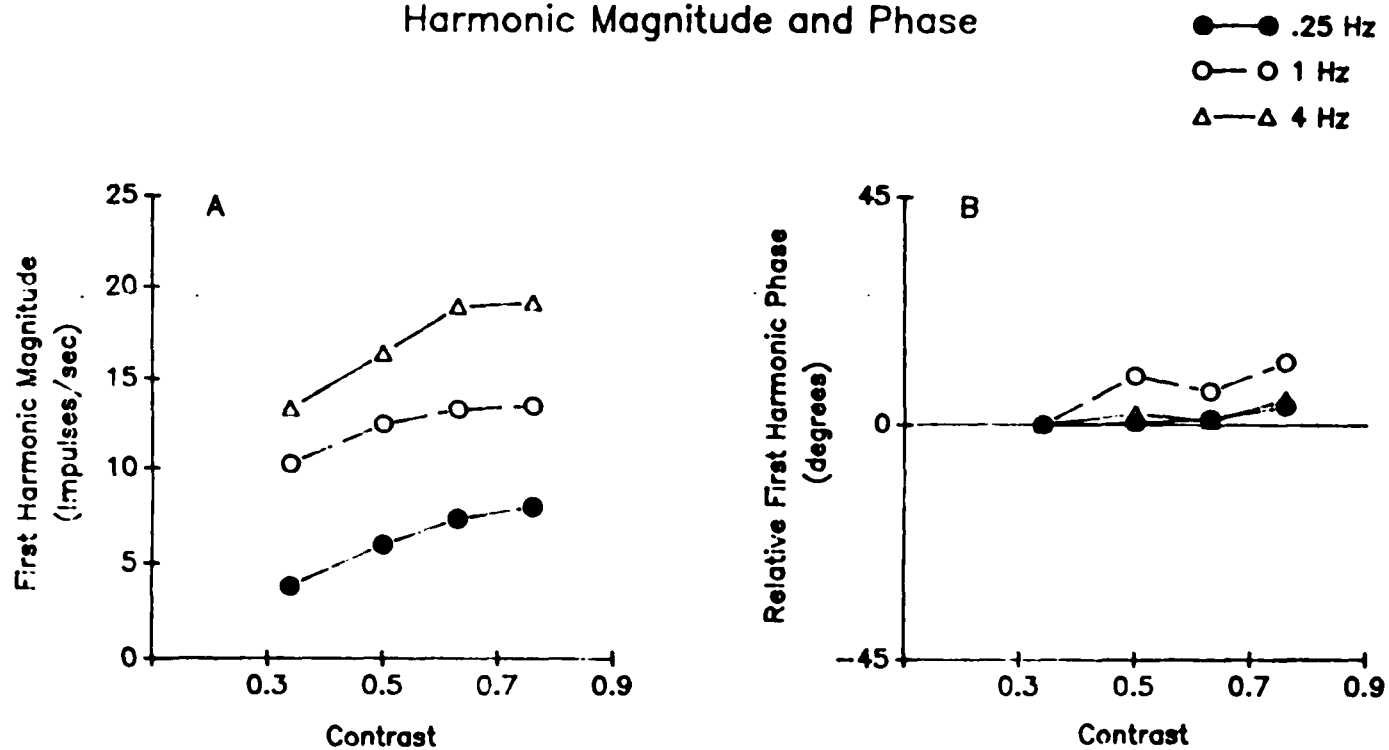

Figure 55

The effect of contrast upon the magnitude and temporal phase of the first harmonic component of another X cell's responses. The results obtained from only two reversal rates - .25 Hz (filled circles) and 1 Hz (open circles) - are displayed since this cell was unresponsive to faster rates. The stimulus was a contrast reversal grating positioned at a phase angle corresponding to this particular cell's peak position. The spatial frequency of the grating was .2 cycles/mm. Harmonic magnitude as a function of contrast is presented in (A) while the corresponding function for relative harmonic phase is shown in (B). Normalization of response temporal phase was done in the same manner as described for Figure 51. Advances in temporal phase are indicated by positive values, phase lags are indicated by negative values.

Contrast Gain
X Cell (Pn873)
Harmonic Magnitude and Phase

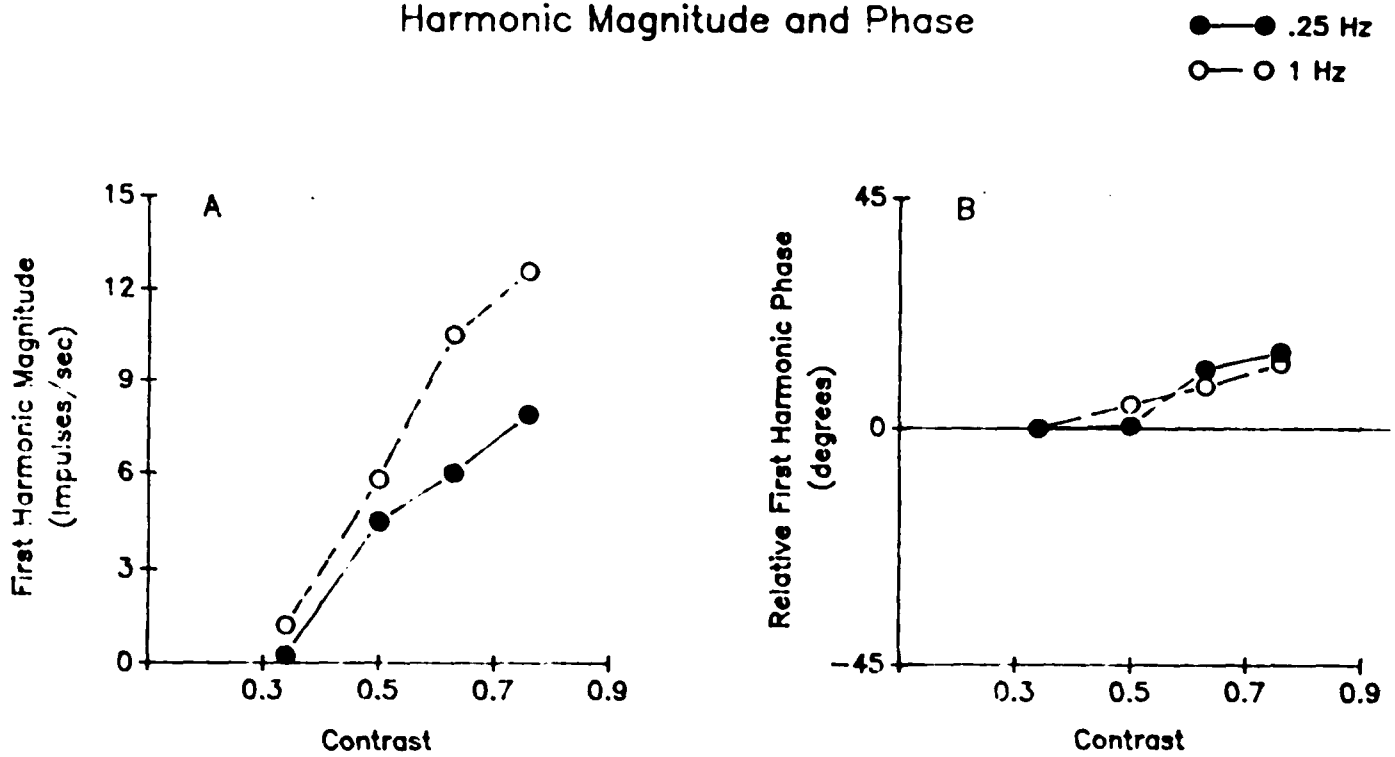

Corresponding phase measures are shown in Figure 55B.

As noted earlier, the one X cell which had shown contrast effects similar to those observed in Y cells was an 'on-off' X cell producing frequency doubled responses when an exceptionally high spatial frequency was examined during the null test. Figure 56A indicates that responding to a moderate reversal rate increased more rapidly with contrast than did responding to a slow rate when a low spatial frequency was used. Figure 56C reveals, however, a clear phase lag in responses to both slow and moderate reversal rates. When a high spatial frequency grating was used, the effect of contrast upon response magnitude to the two reversal rates was similar to that seen for a low spatial frequency (Figure 56B). The effect of contrast upon response phase, however, was noticeably different at a high spatial frequency (Figure 56D). A consistent phase advance was seen for responses to a moderate rate while the phase shifts to a slow rate were irregular. Although this X cell, at a high spatial frequency, was in some ways similar to many Y cells in terms of contrast/temporal frequency interactions, several features of its contrast dependent behavior serve to distinguish it from most of the Y cells. Primarily, one of the more consistent findings in Y cells, when a low spatial frequency was used, was an acceleration of responding to fast temporal frequencies as contrast was increased. In this X cell, however, increases

Figure 56

The effect of contrast upon the magnitude and temporal phase of the dominant harmonic component of an X cell's responses to a low and a high spatial frequency. The function relating harmonic magnitude to contrast is shown in (A) for the first harmonic at a low spatial frequency (.2 cycles/mm) and in (B) for the second harmonic at a high spatial frequency (25 cycles/mm). The relative temporal phase of the first harmonic at .2 cycles/mm is presented as a function of contrast in (C). The corresponding function for the second harmonic at 25 cycles/mm is shown in (D). The stimulus was a contrast reversal grating, positioned at the peak phase angle for this cell, and modulated according to .25 Hz (filled circles) and 1 Hz (open circles). Normalization of response temporal phase was done in the same manner as described for Figure 51. Advances in temporal phase are indicated by positive values, phase lags are indicated by negative values.

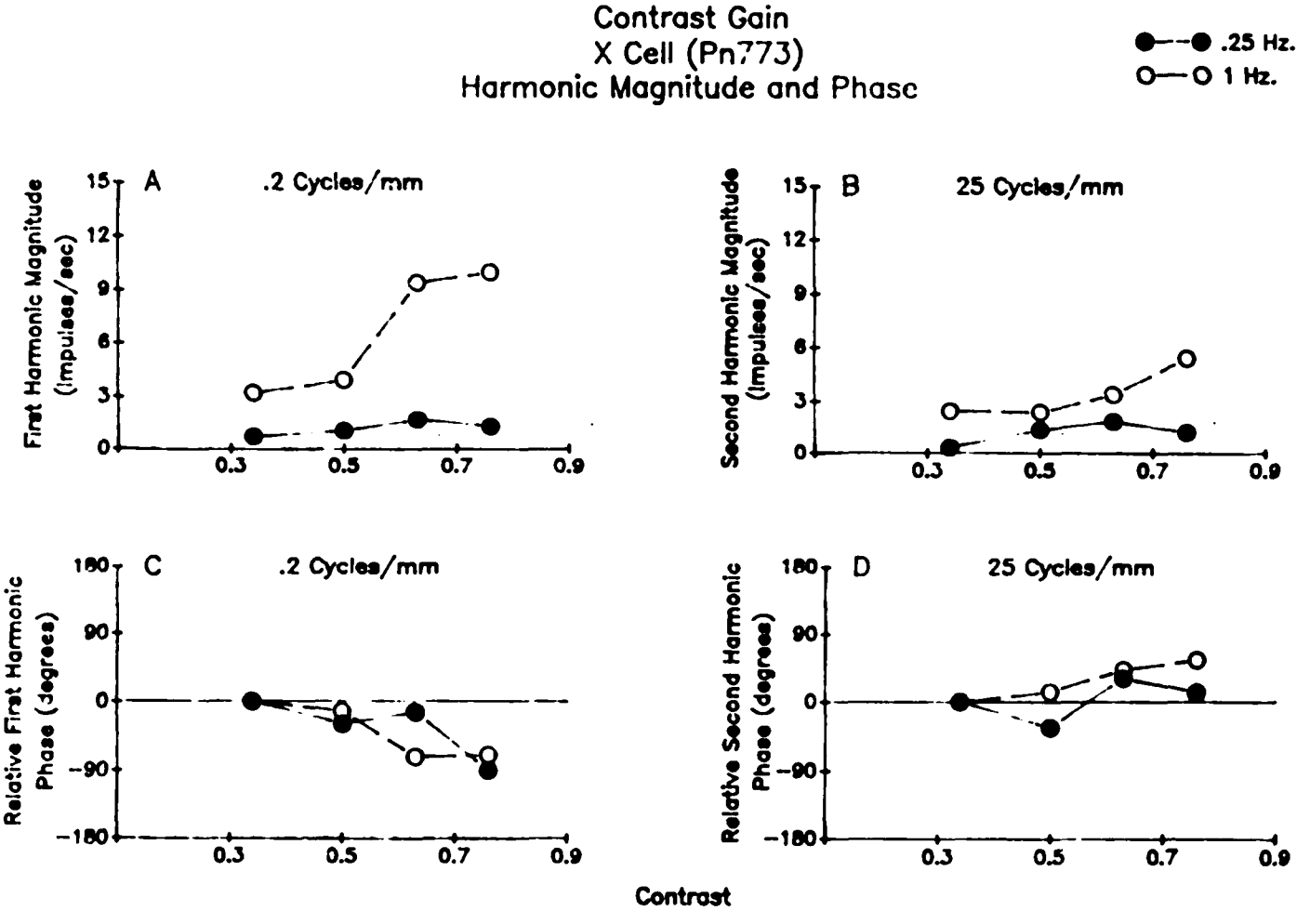
Contrast Gain
X Cell (Pn773)
Harmonic Magnitude and Phase
.25 Hz.
1 Hz.
A
.2 Cycles/mm
First Harmonic Magnitude (Impulses/sec)
B
25 Cycles/mm
Second Harmonic Magnitude (Impulses/sec)
C
.2 Cycles/mm
Relative First Harmonic Phase (degrees)
D
25 Cycles/mm
Relative Second Harmonic Phase (degrees)
Contrast

in the contrast of a low spatial frequency resulted in greater response delays to a comparatively fast rate. Furthermore, the phase advance observed in this X cell's responses, at a high spatial frequency, was less marked than that exhibited by Y cells (compare Figure 56D to Figure 53B, for example).

In conclusion, most of the X cells' responses to different stimulus rates were less frequently affected in a differential manner by contrast. When contrast/temporal frequency interactions were observed, they were never as impressive as those seen in Y cells. It is possible, however, that X cells might have exhibited more profound contrast/temporal frequency interactions if a wider range of contrasts had been employed. As noted earlier, for example, two X cells showed no increase in responding with contrast, thereby possibly indicating saturation of the response at the lowest contrast used.

IV DISCUSSION

The major findings of this research are summarized below; specific issues related to each finding will be discussed in subsequent sections. (1) Frog ganglion cells are divisible into three major classes - X, Y, $\overline{X}$ (W-like) - on the basis of essential differences in spatial summation processes. This confirms the findings reported by Gordon and Shapley (1978) from their examination of frog ganglion cells. (2) As noted by Gordon and Shapley, the general integration processes of each class in the frog were identical to the corresponding class in the cat. A number of specific response features, however, were observed in the present study which served to distinguish many of the frog cells from those in the cat. (3) At least two major subgroups could be identified within the Y class on the basis of differences in RF organization and other functional properties. (4) The existence of a contrast dependent mechanism, bearing a number of critical similarities to the contrast gain control mechanism described in the cat, was established in the frog retina.

4.1 Classification of Frog Ganglion Cells Based upon Spatial Summation Characteristics.

4.1.2 X Cells

Linearity of spatial summation was established in frog X cells according to the same criteria used to identify X cells in the cat: the identification of two null positions, separated by 180 degrees, of a contrast reversal grating, a dominant fundamental harmonic component of the response, and a sinusoidal dependence of response amplitude upon the relative spatial phase of the stimulus. All of these criteria were met over a wide range of spatial frequencies falling within the resolution limits of the cells. The few X cells, producing frequency doubled responses, did so only at a very high spatial frequency (approximately 25 cycles/mm) and the magnitudes of the second harmonic components of these responses were considerably lower relative to those of Y cells.

There is a strong possibility that the occurrence of frequency doubling to high spatial frequencies may have, in fact, been much higher than that actually observed in the X class. The null test was typically terminated, for the majority of X cells, at spatial frequencies which elicited no responses from the cell. The few instances in which frequency doubling was observed in X cells occurred at spatial frequencies approximately two to three octaves

higher than this cut-off spatial frequency. Similar effects of high spatial frequencies upon X cell responses in the cat have not been reported. It is likely, however, that such high spatial frequencies have not been examined in cat X cells for the same reasons they were not assessed in the majority of frog X cells.

The frequency doubled responses of frog X cells might possibly reflect the activity of subunits located within the RFs of neighboring Y cells. That Y cell subunits are capable of influencing X cell responses in the cat, albeit, in a less direct manner than that observed in the frog, has been demonstrated by Shapley and Victor (1979). Shapley and Victor found that peripheral stimulation with a fine spatial frequency grating, which activated nonlinear subunits, simultaneously suppressed the amplitude and advanced the phase of an X cell's response to a centrally located stimulus. The effects of peripheral stimulation were not related to the classical surround mechanism of the X cell, prompting the authors to suggest that this effect originated outside of the X RF and possibly in Y cells' subunits. This peripheral influence upon X cells' responses, however, was indirectly expressed as an alteration in the responsiveness of the linear component. Thus, peripheral stimulation alone did not elicit any responses from the X cells.

The mechanism by which the influence of peripherally

located subunits might be capable of producing second harmonic responses in frog X cells is unknown. Shapley and Victor (1979) have identified the amacrine network as the most likely candidate for the transmission of these peripheral effects. As noted in the introduction, amacrine synapses onto ganglion cells as well as serial synapses among amacrine cells are more common in the anuran retina than in most other vertebrates. It is likely that frog X cells, therefore, receive a considerable amount of their input via intervening amacrine cells as compared to cat X cells which are, according to Kolb (1979), predominantly driven directly by bipolar cells. It should be noted, however, that there is some disagreement regarding the dominant synaptic input onto cat X cells. Watanabe, Fukada, Hsiao and Ito (1985) have reported that amacrine synapses onto cat X cells are more numerous than are bipolar synapses. The discrepancy between the two studies may be related, in part, to the fact that Kolb's observations were limited to proximal dendrites of X cells while Watanabe et al. examined synaptic input onto distal as well as proximal dendrites. Watanabe et al. have also suggested that the discrepancy between their study and that of Kolb might reflect variation in synaptic input among cat X cells. Thus, the possibility cannot be excluded that different groups of X cells, in the cat, are characterized by distinct patterns of synaptic input.

If, indeed, X cells in the frog receive much of their input through amacrine cells, then they may be more subject to peripheral influences, and in a more direct manner, than are many cat X cells. As indicated in the Introduction (section 1.7), numerous types of amacrine cells, differentiated according to various criteria, may serve different functional roles. It is possible, therefore, that the subunits' influence upon frog X cells is conveyed by a different class of amacrine cells than those which directly contribute rectified responses in the subunit.

Frog X cells' responses to drifting gratings were identical to those reported for X cells in the cat: responding modulated according to the drift frequency up to spatial frequencies which approached the resolution limits of a given cell. The rapid high frequency decline seen in the SFRs of the majority of X cells in the frog is also characteristic of cat X cells. As in the cat, this high frequency decline is attributable to the fact that, with increases in spatial frequency, the width of one spatial cycle approaches that of the RF center. As the grating drifts across the RF, therefore, overall intensity across the linear center remains unchanged since an increase in intensity of one half of the cycle is compensated by a decrease in the other.

It is unclear why 'on' and 'on-off' X cells in the frog should generally display more gradual high frequency

declines than do 'off' cells. The fact that a similar trend was observed in Y cells suggests that this represents a specific property of these cells unrelated to spatial summation characteristics. One possible explanation is that sensitivity is not symmetrically distributed across the RFs of 'on' and 'on-off' cells while 'off' cells may be characterized by a Gaussian-like RF profile. In order to determine whether or not this assumption is correct, a direct test of the adequacy of a Gaussian model as descriptive of these cells' RFs is needed. This would, however, require analyses of a wider range of response parameters than was performed in the present study.

Unlike the cat, the SFRs of most X cells in the frog did not reveal a low frequency decline. Gordon and Shapley (1978) have similarly reported that many 'off' X cells in the frog do not display a decrease in sensitivity to low spatial frequencies. Considering that many 'off' cells in the frog lack a suppressive surround (Grusser- Cornehls, Grusser and Bullock, 1963), it is not surprising that 'off' cells' responses to full-field stimulation were typically undiminished relative to the lowest spatial frequency used. There is no adequate explanation, however, for the absence of a low frequency decline in one 'on-off' X cell given that 'on-off' cells in frogs are characterized by an inhibitory surround (Grusser and Grusser-Cornehls, 1976). A few 'on-off' cells have been shown to be directionally

selective (Lettvin, Maturana, McCulloch, and Pitts, 1959) suggesting the possibility that inhibition might be particularly weak if the grating is drifted in the optimal direction. This selectivity cannot, however, account for the 'on-off' X cell's optimal responsivity to full-field stimulation which would not excite a directionally selective mechanism.

No difference was observed in optimum spatial frequency, and thus by implication RF size, between X and Y cells in the frog. This contrasts sharply with findings reported for the cat in which X cells' RFs were always smaller than those of Y cells at a given retinal eccentricity (Enroth-Cugell and Robson, 1966). It should be emphasized, however, that a number of factors may be responsible for obscuring genuine interclass size differences in the frog. Firstly, there is the well established "sampling bias" introduced by recording electrodes whereby larger cells have a greater probability of being isolated. Thus, the most frequently encountered X cells will be those which possess larger cell bodies than the average X cell. Furthermore, as more central regions of the retina are sampled, where the size of all cells are smaller as compared to peripheral regions, a Y cell is more likely to be isolated since it is still larger than neighboring X cells. This latter fact may account for the greater variety of RF sizes among Y cells, compared to X

cells, in this study.

One X cell (see Figures 12 and 13) which had displayed a number of features atypical of the X class in either frog or cat, raises a few questions regarding the processes underlying linear summation. This was the cell which had produced second harmonic responses when a low spatial frequency grating was drifted at 8 Hz but not when contrast reversed at the same rate. Two other features unique to this cell was the exceptionally narrow temporal tuning displayed by the cell for contrast reversed, but not drifted, gratings and a low frequency decline in its SFR only when a moderate (1 Hz) drift rate was employed. The second harmonics must stem from a mechanism other than Y-like subunits given their appearance at a low spatial frequency as well their specific occurrence during drifting but not contrast reversed gratings. Thus, frequency doubling must result from the activity of larger RF components, possibly from a nonlinear interaction between center and surround mechanisms. Also, phase lags between surround and center responses, resulting from spatiotemporal interactions (Dawis, Shapley, Kaplan and Tranchina, 1984), might possibly explain the present findings. Why this nonlinearity was evident only during drifting grating experiments and not during the null test is unclear and requires further investigation.

4.1.2 Y Cells

Like cat Y cells, frog Y cells are characterized by a linearly summating mechanism which is dominant at low spatial frequencies and a nonlinearly summating mechanism which is most responsive at higher spatial frequencies. Y cells in the frog, however, were unique from those in the cat, in terms of their behavior at low spatial frequencies during the null test. Cat Y cells produce frequency doubled responses, at very low spatial frequencies, to positions of a contrast reversal grating which would elicit a null response from an X cell. Y cells in the frog, however, displayed null and peak responses identical to those obtained for X cells when low spatial frequency gratings were used; frequency doubling at null positions was not evident until higher spatial frequencies were employed.

The absence of frequency doubled responses at low spatial frequencies has also been reported for goldfish Y cells (Bilotta and Abramov, 1989) and was attributed to the influence of an inhibitory surround at the level of the individual, nonlinear subunit. Thus, low spatial frequencies would mutually stimulate center and surround thereby 'nulling' the subunit's response. A center/surround organization may also characterize Y cell subunits in the cat (Victor and Shapley, 1979). That

frequency doubling is only diminished but not absent at low spatial frequencies in cat Y cells is probably related to the the fact that the presumptive subunit, the bipolar cell, in the cat has a weaker inhibitory surround than does the bipolar cell in the goldfish (Bilotta and Abramov, 1989). While no comparable estimates of the relative strength of bipolars' surround exists for frogs, the functional similarity between frog and goldfish at low spatial frequencies suggests that a strong center/surround organization may also be characteristic of Y cell subunits in the frog.

Another apparent difference between frog and cat Y cells is in their responses to drifting gratings. Cat Y cells display an overall increase in mean response rate when high spatial frequency gratings are drifted across their RF. This elevation in mean discharge is presumed to arise as a result of the sequential activation of numerous subunits (Hochstein and Shapley, 1976a). While a shift from modulated to unmodulated responses was observed in many frog Y cells, the mean rate of unmodulated responding was less than that of modulated responding. In fact, a substantial number of frog Y cells did not respond at all to high spatial frequencies drifting across their RF. This lack of responsiveness to drifting high spatial frequency gratings is incongruous with the robust frequency doubled responses exhibited by these cells to the same spatial

frequencies when gratings were contrast reversed during the null test. While rotational selectivity, as demonstrated by one Y cell (see Figure 29), may explain the diminished responsivity of a few Y cells, it cannot fully account for the majority of Y cells. It is highly unlikely that a nonpreferred rotation was employed for all cells or that all Y cells even possess this selectivity. Regardless of the mechanisms responsible for the observed differences between frog and cat Y cells, it should be noted that this difference is one of degree and does not represent a qualitative departure from the dual mode of responding to drifting gratings exhibited by cat Y cells. Thus, in both cat and frog, a modulation of responding at low spatial frequencies, the result of the activity of a linearly integrating mechanism, is replaced by unmodulated responses at higher spatial frequencies which result from sequential subunit activation.

Considerable variability among the SFRs of Y cells, regarding the presence or absence of low frequency declines, was observed in the frog. Within a particular subgroup (Y1 vs Y2), however, the low frequency portion of the SFR was consistent among the cells. The absence of a low frequency decline was relatively independent of whether the cell was 'off', 'on', or 'on-off'. For 'off' and 'on' cells, this finding is consistent with earlier reports (Grusser and Grusser-Cornehls, 1976) that inhibitory

surrounds were characteristic of many, but not all cells within each of these two Hartline groups. As noted for 'on-off' X cells, the absence of a low frequency decline in a substantial number of 'on-off' Y cells is surprising, but it does suggest a genuine possibility that an inhibitory surround is not necessarily characteristic of all 'on-off' cells in the frog.

4.1.2.1 Y Cell Subgroups

One of the more interesting and, in fact, surprising, findings resulting from the present research was the existence of at least two, distinct RF types in the Y cell class. There was no relationship between a given RF profile and a particular Hartline response. Following from this, it is unlikely that a given RF type corresponds to any one of the Lettvin groups. Rather, the Y1 and Y2 RF organizations were associated with specific variations in functional properties characteristic of Y cells in general. Similarly distinct subgroups within the Y class have not been described in either the cat or any other species examined to-date.

One of the functional features specific to the Y1 subgroup, the response depression occurring at a specific spatial frequency, has not been reported for Y cells in the cat. For reasons discussed in the Results (see section 3.3.3), this depression is most likely the result of

inhibitory processes. Based on a number of considerations, however, it is unlikely that the mechanism responsible for "nulling" subunit responses at a low spatial frequency in frog Y cells is similarly involved in producing response depression in Y1 cells. Firstly, response depression was never observed in Y2 cells even though subunit activity was suppressed at low spatial frequencies. Secondly, the midway response depression in Y1 cells occurred at a spatial frequency higher than that to which second harmonics had dominated the response at most or all positions of the stimulus grating. This suggests, therefore, that the spatial frequency was too fine to elicit inhibitory activity from the subunits' surrounds. Finally, in the few Y1 cells in which the linear mechanism continued to contribute to responding at this higher spatial frequency, both first and second harmonic magnitudes were similarly depressed.

Based on the above considerations it appears that two inhibitory mechanisms are operable in frog Y cells. One is characteristic of all Y cells and probably stems from a subunit surround as suggested by Bilotta and Abramov for goldfish Y cells. The second is observed in only one subgroup of Y cells: the Y1 cells.

What retinal elements might be involved in these two different inhibitory processes? The center/surround structure of the subunits is presumably organized at the

level of the OPL (Victor and Shapley, 1979). Direct receptor input to bipolar cells gives rise to the center of the subunit and indirect input from horizontal cells provides the surround inhibition. The fact that response depression occurred in Y1 cells, regardless of whether a slow or a fast reversal rate was used during the null test, further suggests that the horizontal cell - with its slow, graded responses (Werblin, 1972; Werblin and Copenhagen, 1974; Werblin and Dowling, 1972) - does not provide the inhibition responsible for this depression. Rather, the most likely candidate is the amacrine cell which has been shown to be highly responsive to stimulus change (Werblin and Copenhagen, 1974). Werblin and Copenhagen have also demonstrated that amacrine cells, when stimulated with moving or flashing stimuli, inhibit the general responsiveness of adjacent 'on-off' ganglion cells. The fact that linear and nonlinear response components were inhibited in many Y1 cells in the present study suggests that these amacrine cells may act to similarly suppress overall responding in Y1 cells. Because of the purely inhibitory effect seen at a midrange spatial frequency, these amacrine cells must represent a class of cells distinct from those involved in generating the characteristic frequency doubled response of the subunits. Why this inhibition is highly specific to a particular spatial frequency for the majority of Y1 cells remains to

be determined.

While the mid-spatial frequency response depression serves to distinguish between Y1 cells and cat Y cells, the distribution of subunits throughout the Y1 RF is identical to that reported for cat Y cells (Hochstein and Shapley, 1976b). The centrally restricted nature of Y2 subunits, however, represents a significant departure from the general Y cell RF model. Other features of the Y2 RF, most notably the existence of a responsive surround, have only recently been reported in frogs (Donner and Gronholm, 1984).

A connection between a flanking RF organization, similar to that of Y2 cells, and nonlinear summating cells in the frog was previously established by Stirling and Merrill (1987) in class IV cells (the dimming detectors or Hartline's 'off' cells). Stirling and Merrill found that the flanking components did not completely surround the center but were, rather, confined to two small regions on opposite sides of the center. As observed in Y2 cells, Stirling and Merrill found that the center exerted a suppressive influence upon the flanking regions. There is some disagreement, however, between the present study and that of Stirling and Merrill regarding surround suppression in linear and nonlinear summating cells. Surround suppression, most likely originating from the flanking regions, was evident in all of the Y2 cells examined.

Stirling and Merrill, however, observed surround suppression in only a small portion of the nonlinear class IV cells and therefore concluded that the flanking components did not exert an inhibitory influence upon the center. Conversely, a suppressive surround was found to be characteristic of the nonflanking, linearly summating class IV cells in Stirling and Merrill's study. In the present study, a suppressive surround was absent in the majority of 'off' - presumably class IV - X cells.

4.1.3 $\overline{X}$ Cells

Because W cells in the cat were originally distinguished from X and Y cells on the basis of functional properties other than spatial summation processes, the association between $\overline{X}$ cells and retinal W cells is necessarily an indirect one, dependent upon similarities in full field responses. Thus, the majority of $\overline{X}$ cells, producing 'on-off' responses, are considered analogous to the phasic 'on-off' W cells in the cat. A minority of $\overline{X}$ cells produced either pure 'on' or 'off' responses to full field stimulation suggesting that they might be equivalent to tonic W cells in the cat which are either 'on-center' or 'off-center'. As noted in the Introduction (section 1.5), however, W cells, at the level of the LGN in the cat, have been divided into linear and nonlinear summating subgroups (Sur and Sherman, 1982). Most of the $\overline{X}$ cells examined in

this study show a strong similarity to the nonlinear W cells which produce second harmonic responses that are relatively insensitive to spatial frequency.

Some mention should be made of the linear W cells reported in the cat LGN. Because these cells differ from cat X cells only to the extent that they do not exhibit a low frequency decline in their SFS, it was impossible to determine whether or nor any frog X cells were in fact linear W-like cells since the inhibitory surround characteristic of cat X cells was not a distinguishing feature of many frog X cells.

A number of other functional features of $\overline{X}$ cells suggest a correspondence with W cells in the cat. Firstly, most $\overline{X}$ cells responded poorly to narrow bars used to map their RFs and to any spatial frequency other than the lowest one used in these experiments. Secondly, many $\overline{X}$ cells were optimally responsive only to the slowest temporal modulations used in this study; note however that a minor but substantial number of cells classified as $\overline{X}$ preferred moderate temporal frequencies. Finally, the $\overline{X}$ class - like the W class in the cat - was functionally heterogeneous.

For the most part, many of the $\overline{X}$ cells encountered in this study were similar to those first described by Gordon and Shapley (1978). The fact that second harmonic responses did not increase substantially in magnitude as spatial

frequency was increased suggests that nonlinear summation in $\overline{X}$ cells is the result of a mechanism much wider in spatial extent than the Y cell's subunit. The absence of a clear sinusoidal dependence upon stimulus spatial phase of the first as well as the second harmonic indicates that the organization of linear and nonlinear components in many $\overline{X}$ cells is unique from that established for Y cells. The functional characteristics displayed by the majority of $\overline{X}$ cells can be explained if one assumes that the $\overline{X}$ RF consists of two components - an 'on' and an 'off' region - which are not concentric but do overlap to some degree, as suggested by Gordon and Shapley (1978). Within each region summation is linear. Assuming that the output of each region is half-wave rectified, a combination of outputs, when both regions are simultaneously stimulated, would produce a frequency doubled response. Because the two regions are not concentrically organized the relative phase angles of the stimulus corresponding to a null position will be different for each region. Thus, there would be no unique null position for the RF as a whole.

The $\overline{X}$ cells, which responded optimally to square wave stimulation, have not been previously described. These cells were unique from other $\overline{X}$ cells in two important ways. First, the second harmonic response component was much greater in magnitude than the first harmonic over a wide range of spatial frequencies used during the null test.

Second, the magnitudes of the second harmonic varied systematically with the spatial phase of the grating although not sinusoidally as did the first harmonic. Because of this dependence upon phase, it is highly probable that 'on' and 'off' regions are aligned within the RF. In fact, many of these cells' RF profiles appeared similar to that shown in Figure 43C. The frequency doubled output of these cells indicates that the responses of each region are half-wave rectified prior to summation as proposed by the Gordon and Shapley model for other $\overline{X}$ cells.

The preference displayed by these cells for abrupt changes in stimulus contrast might suggest that these cells would respond to sinusoidally modulated stimuli if presented at a fast rate. This, however, was not the case; for these cells a 'fast' stimulus change was not equivalent to an 'abrupt' stimulus change. Reid and Shapley (1988), in an attempt to explain similar observations made in cat striate cortical neurons, found that contrast reversal gratings, sinusoidally modulated simultaneously by a wide range of temporal frequencies (sum of sinusoids method), increased responsiveness to faster temporal frequencies. These results can be explained, in part, by the fact that a square wave consists of an infinite series of temporal sinusoids. Sinusoidal modulation of a stimulus according to the sum of sinusoids method used by Reid and Shapley, therefore represents a closer approximation to a square

wave than does a single sinusoidal input. Since the sum of sinusoids method was effective in boosting the responses of these cells to rapid sinusoidal modulation, it appears that these cells' responsiveness is dependent upon the total power contributed by all harmonic components of the stimulus. Thus a cell's preferential responsiveness to square wave modulated stimuli is a result of power at all temporal frequencies within the square wave and not of the abrupt nature of the change, per se.

One issue which needs to be clarified concerns the existence of discrete subgroupings within the $\overline{X}$ class. Different trends among $\overline{X}$ cells were considered as "subgroups" in the Results in order to simplify the presentation of diverse findings. With the exception of the $\overline{X}$ cells responsive only to square wave modulation, the vast majority of $\overline{X}$ cells' behavior during the null test fell along a continuum. Highly variable behavior was also reported for W-like cells in the goldfish (Bilotta and Abramov, 1989). The RF model of the $\overline{X}$ cell, however, does not need to be substantially changed in order to account for each variation. Minor alterations in one or more parameters of 'on' and 'off' regions in the $\overline{X}$ cell RF - their relative spatial and/or temporal frequency sensitivities or perhaps the degree to which these regions overlap - could account for almost all of the behavioral variations observed among $\overline{X}$ cells.

4.2 The Effect of High Contrasts upon Temporal Transfer Properties of Different Cell Classes.

The effects of contrast observed in frog ganglion cells bear a number of general similarities to the contrast gain control mechanism described in the cat. Higher contrasts tended to enhance responsiveness for fast temporal frequencies by selectively amplifying and/or accelerating responses. As in cats, this effect was more pronounced in Y cells than in X cells. The strongest contrast effects in the cat were observed with temporal frequencies ranging from 4 to 15 Hz (Shapley and Victor, 1978). Unfortunately, the range of temporal frequencies, used to determine contrast effects in the frog, did not include frequencies between 4 and 16 Hz. However, the observation that 4 Hz was most effective in revealing contrast effects in frog Y cells suggests that the contrast dependent mechanism has similar temporal dynamics to that in the cat. Given that temperature has a marked effect on temporal responsiveness of ganglion cells (Tranchina, 1981), the effective frequency range may differ somewhat between frog and cat given that experiments are conducted at higher temperatures in the cat than in the cold-blooded frog.

There were a number of marked differences between frog and cat, however, regarding the specific way in which

higher contrasts enhanced responsiveness to fast stimulus rates. Shapley and Victor (1981) noted that, at higher contrasts, a preferential amp'itude increase invariably accompanied a phase advance in responses to high temporal frequencies. Furthermore, these contrast effects were relatively independent of spatial frequency (Shapley and Victor, 1978). The specific manifestation of contrast effects in a number of frog Y cells, however, was clearly dependent upon spatial frequency. When a low spatial frequency grating was used, higher contrasts served to advance response phase but did not always selectively cause an increase in response amplitude at high temporal frequencies. When high spatial frequencies were used, however, the effect of contrast on both amplitude and temporal phase of Y cells' responses was typically comparable to that seen in the cat.

As noted above, contrast effects are typically more robust in Y cells than in X cells in the cat. This was similarly observed in the frog; the gap between X and Y cells, however, was much wider than in the cat. Relatively few X cells showed any evidence of a selective boosting in responses to faster temporal frequencies as contrast was increased. In addition, the effective temporal frequency at which contrast effects were observed in a few X cells was much lower than the frequency effective for frog Y cells.

The differential effect of contrast on X and Y cells in frogs is not simply one of degree as it is in cats. X and Y cells differed in terms of the response component most susceptible to contrast dependent effects, even at low spatial frequencies when Y cells' responses were predominantly linear. In Y cells, the effect of higher contrasts was typically manifested as advances in the temporal phase of responses to fast stimulus rates. When contrast dependent effects were observed in X cells, higher contrasts were more typically associated with an increase in response magnitude to comparatively fast stimulus rates not necessarily accompanied by an acceleration of the response.

The essential features of contrast effects are similar in both frog and cat, i.e., a 'boosting' of responsiveness for rapidly changing stimuli. Thus, the likelihood exists that the mechanism responsible for this enhancement is fundamentally, the same. Based upon a number of similarities between the contrast gain control mechanism and Y cell nonlinear summation, Shapley and Victor (1978, 1979, 1981) have suggested that the subunits of Y cells are the critical elements which 'sense' the contrast. This explains the fact that stronger contrast effects are seen in Y cells rather than X cells in both the cat and frog. A subunit based contrast network in the frog retina is also suggested by the observation that the most robust contrast

effects upon both the phase and amplitude of Y cell responses occurred when high spatial frequencies were used which presumably activate only Y cell subunits.

The distinction between frog and cat regarding the specific manifestation of contrast effects suggests that the manner in which this contrast network actually modulates the responses of ganglion cells must differ. Contrast effects in frog Y cells appear to depend, to a large extent, upon whether the linear or the nonlinear component is dominant. There are at least two possible explanations for this observation. Two separate mechanisms might mediate contrast effects in the linear and nonlinear components of the frog Y cell. Alternatively, one mechanism might be involved which is strongly activated when subunits' frequency doubling is most robust but only weakly when subunits are not directly responsive. Neither of these possibilities, however, explains why subunit contrast gain should affect the linear component of Y cells differently from the linear X cells.

One final point regarding the differences observed between frog and cat deserves mention. Many of the findings reported by Shapley and Victor (1978, 1979) were obtained using the sum of sinusoids method previously described (section 1.6). It could therefore be argued that the differences between frog and cat stemmed from the difference in stimuli between the present study and those

of Shapley and Victor. However, Shapley and Victor (1978) have also employed a single sinusoid, as in this study, and found no difference between the effectiveness of the two techniques in cells not displaying strong contrast effects. However, for cells which had shown a significant effect of contrast when a single sinusoid was used, the combined presentation of a number of sinusoids resulted in a much greater, but not a qualitatively different, effect. The effectiveness of the sum of sinusoids method illustrates that responsiveness is dependent upon the total strength of all input frequencies, not to just one Fourier component of a complex stimulus, even if the response is predominantly modulated according to only one input frequency.

4.3 Relationship of Linear vs Nonlinear Summation Distinction to Other Categorizations.

Numerous attempts have been made to categorize X and Y cells according to specific dimensions of responding unrelated to processes of spatial integration. Cleland, Dubin and Levick (1971), for example, have proposed that the essential distinction between X and Y cells is in the duration of their response to standing contrast. Thus, the terms "sustained" and "transient" have been used by these and other investigators (eg.,Ikeda and Wright, 1972) as synonymous with X and Y classes, respectively. Based on general differences in temporal responsiveness, W cells

have been termed "sluggish" to distinguish them from the "brisk" X and Y cells (Cleland and Levick, 1974). Fukada (1971), focusing upon the frequency doubling of Y cells, has assumed a connection between 'on-off' responses (Type I) and Y cells.

The utility of each of these distinctions as an index of a cell's integration processes is extremely limited. In the cat, both 'sustained' and 'transient' responses characterize cells responses to standing contrast for both X and Y classes (Hochstein and Shapley, 1976a). Similarly, frog X and Y cells did not differ, in the present study, in terms of the duration of their responses to a wide variety of stimuli. This suggests, therefore, that the 'sustained' vs 'transient' distinction is not comparable to the X vs Y distinction in the frog.

Regarding the brisk vs sluggish distinctions, informal observations made during this study suggest that the temporal responsiveness of a cell is not a reliable index of its spatial summation processes. While the majority of $\overline{X}$ cells displayed a preference for slower stimulus rates, there were a substantial number which responded best to moderate rates. A more consistent temporal preference was observed in Y cells which, with few exceptions, responded optimally when moderate to fast rates were used. X cells varied widely from cells which preferred only the slowest rate to the cell, noted previously, which was exclusively

responsive to the fastest rate used during the null test and full field stimulation.

Finally, as discussed earlier, there was no clear one-to-one correspondence between the Hartline groups and the X and Y classes. $\overline{X}$ cells, however, were more frequently related to a particular Hartline type - 'on-off' cells - with only a few representative of 'on' and 'off' types. X and Y cells in the cat are also not specifically related to a given center response type (Hochstein and Shapley, 1976a). Furthermore, Hochstein and Shapley have found that both X and Y cells produced 'on-off' responses to diffuse light thereby challenging Fukada's (1971) conclusion that 'on-off' responses (type I) were characteristic of 'transient' or Y cells and only 'on' or 'off' responses (type II) corresponded to 'sustained' or X cells.

Because so many of the cells in the frog retina produce 'on-off' responses (Hartline, 1938), a few points regarding the generation of 'on-off' responses should be made. Most importantly, it is unlikely that subunit frequency doubling is responsible for generating 'on-off' responses in many frog Y cells. Recall that subunit activity in frog Y cells was not apparent until moderately high spatial frequencies were used. Following from this, it is highly improbable that the subunits would be responsive to full field stimulation, much less capable of generating the strong bursts of impulses noted at light

onset and offset. Furthermore, in cat Y cells where subunit generated frequency doubling is observed at low spatial frequencies, 'on-off' responses to diffuse light should be more closely associated with the Y class if these responses were indeed the result of subunit activity. As noted above, however, this is not the case. 'On-off' responses can be generated in a number of ways, many of which do not necessarily indicate nonlinear spatial summation (eg., Rodieck and Stone (1965) in the cat; Nye and Naka (1971), in the frog). The 'on-off' responses of a few Y2 cells, for example, could be attributed to antagonistic center and flanking responses. Similar interactions between concentric 'on' and 'off' regions possessing equivalent strength may explain X cells' 'on-off' responses. The mechanism by which 'on-off' responses are generated in $\overline{X}$ cells, as suggested by Gordon and Shapley's model (1978), represents another, albeit nonlinear, way.

4.4 What Does the Frog's Eye Really Tell the Frog's Brain?

As noted in the Introduction, it has long been held that the functions of anuran ganglion cells are, in some essential way, qualitatively different from those of mammalian ganglion cells. This difference was conceptualized as a distinction between a purely "password" function in the frog and a "redundancy reduction" function

in the mammal (Barlow, 1961, 1966). Thus, the Lettvin, Maturana, McCulloch and Pitts (1959) scheme emphasizes the password transmitted by each of five ganglion cell classes in the frog. By using the same stimuli and analytic techniques employed in the analysis of ganglion cell function in the cat, however, the present study has demonstrated that many functional properties of the anuran retinal network are conspicuously similar to those described in the cat. Given similar observations in other nonmammalian vertebrates (eel, (Gordon and Shapley, 1978), mudpuppy (Tuttle and Scott, 1978), goldfish (Levine and Shefner, 1979; Bilotta and Abramov, 1989)) it is likely that these functional properties represent characteristic features of the vertebrate retina.

The findings presented herein are inconsistent with the notion that the anuran retina functions solely to transmit "password" information. Rather, a given cell is capable of transmitting information regarding a wide range of stimulus features: its relative phase, its spatial and temporal frequencies, contrast, and so forth. The range of information transmission is further increased in Y cells because of the dual modes of responding dependent upon spatial frequency. Furthermore, there are the complex interactions between contrast and temporal frequency which indicate an emphasis upon stimulus 'change'. A similar point was emphasized by Gordon and Hood (1976) regarding

the Lettvin et al. classes: the critical element detected by each class represents some change in the stimulus.

As noted by Hood and Gordon (1981), the idea of a 'feature detecting' cell requires the cell's responsiveness to be narrowly tuned so that its activity signals the presence of a highly specific stimulus configuration. The vast majority of ganglion cells examined in the present study typically displayed broadly tuned responses for a variety of stimulus parameters. In a few instances cells were narrowly tuned for one stimulus parameter, temporal frequency for example, but were broadly tuned for all other parameters.

It should be emphasized that a classification based upon integration processes is not necessarily incompatible with or intended to supplant the Lettvin et al. scheme. Rather, the distinctions emphasized by each classification have different merits. The Lettvin et al. scheme approaches the retinal network as a 'means to an end' and thus attempts to explain how environmental demands are met at the sensory level. Unfortunately, the Lettvin et al. scheme falls short of generating useful hypotheses regarding the mechanisms by which each class might detect specific features of the stimulus. Alternatively, the quantitative methods employed to identify spatial summation processes emphasize underlying mechanisms and may, in turn, prove useful in identifying the processes which could give

rise to the selectivity putatively demonstrated by each of the Lettvin et al. classes.

Direct comparisons between X, Y and $\overline{X}$ classes and the five Lettvin et al. groups were not attempted in the present study. There is reason to believe, however, that many of the cells examined in this study would represent classes III, IV and possibly V of the Lettvin et al. scheme. This is based on the fact that the full field responses of these classes are similar to Hartline's 'on-off' cells (class III) and 'off' cells (class IV and perhaps V). The Lettvin et al. classes I and II were probably encountered infrequently, if at all, given that these cells do not respond to uniform intensity changes used in this study to locate cells. Because X, Y and $\overline{X}$ cells were identified in both 'on-off' and 'off' classes, it can be safely concluded that at least two of the Lettvin et al. classes may be further divided into subgroups based on spatial summation processes. As noted earlier, direct evidence has been provided by Stirling and Merrill (1987) that class IV cells can, indeed, be further differentiated into linear and nonlinear summating cells. One of the shortcomings, noted by Grusser and Grusser-Cornehls (1976), of the Lettvin et al. scheme was that the number of functional classes was about half that of the number of morphological types among anuran ganglion cells reported by Cajal. If one assumes, however, that many of the Lettvin et

al. classes can be further subdivided into X, Y and $\overline{X}$ cells, then the range of functional types becomes more commensurate with the number of morphological types.

4.5 Suggestions for Future Research

As with most research, the findings obtained in this project raise a number of additional questions.

1. There is the issue of frequency doubling in X cells. More X cells need to be examined at high spatial frequencies to determine whether or not isolated frequency doubling is common in frog X cells. Furthermore, similar analyses should be performed in cat X cells to establish whether or not this behavior is specific only to X cells in the frog. The mechanism by which frequency doubling is generated in X cells also needs to be investigated. Changing the location of a high spatial frequency grating relative to the X cell's RF might establish the locus of this mechanism. By simultaneously recording from X and Y cell pairs, similar to that done in the cat by Mastronarde (1983), it can be determined whether or not subunit activity in a neighboring Y cell is correlated with frequency doubling in the X cell.

2. There is the problem of the mid-spatial frequency response depression in Y1 cells. What retinal elements are responsible and why is there such a high degree of spatial frequency selectivity for this depression?

3. More detailed analyses are required of contrast effects than was possible in the present study. More cells, from each class, need to be examined. Wider ranges of temporal frequency and contrast need to be employed. Furthermore, the issue of the different effects of contrast in Y cells, dependent upon spatial frequency, requires further investigation. Perhaps an examination of the effect of higher contrasts at a number of spatial frequencies can pinpoint a frequency at which amplitude as well as phase changes occur with contrast. The use of the sum of sinusoids method might indicate whether the inability of higher contrasts to enhance response amplitude at low spatial frequencies is simply a question of 'weak' contrast effects or the involvement of a different mechanism.

4. Cells in the Lettvin et al. classes I and II must be analyzed in terms of integration processes. In order to locate these cells the specific stimuli, deemed optimal for each class according to Lettvin et al., must be used.

5. Morphological analyses of X, Y and $\overline{X}$ cells in the frog need to be performed in order to provide a basis of comparison with similar investigations in the cat (Kolb, 1979; Watanabe,Fukada, Hsiao and Ito, 1985). This would provide a starting point for correlating functional differences between cat and frog cells with structural differences.

The above suggestions represent only a partial list. It is hoped that the findings reported herein will stimulate research into anuran retinal functions which is commensurate with that performed in the cat.

REFERENCES

Adrian, E.D., & Matthews, R. (1972). The discharge of impulses in the optic nerve and its relation to the electric changes in the retina. Journal of Physiology, 63, 378 - 414.

Barlow, H.B. (1953a). Action potentials from the frog's retina. Journal of Physiology, 119, 58-68.

Barlow, H.b. (1953b). Summation and inhibition in the frog's retina. Journal of Physiology, 119, 69-88.

Barlow, H.B. (1961). Possible principles underlying the transformations of sensory messages. In W.A. Rosenblith (ed), Sensory Communication. Cambridge, Ma: MIT Press.

Barlow, H.B. (1966). The coding of sensory messages. In W.H. Thorpe and O.L. Zangwill (eds), Current Problems in Animal Behavior. Cambridge: University Press.

Barlow, H.B., Fitzhugh, R., & Kuffler, S.W. (1957). Change of organization in the receptive fields of the cat's retina during dark adaptation. Journal of Physiology, 137, 338-354.

Belgum, J.H., Dvorak, D.R., & McReynolds, J.S. (1982). Light-evoked sustained inhibition in mudpuppy retinal ganglion cells. Vision Research, 22, 257-260.

Bilotta, J., & Abramov, I. (1989). Spatial properties of goldfish ganglion cells. Journal of General Physiology, 93, 1147-1169.

Bullock, T.H. (1984). Comparative neuroscience holds promise for quiet revolutions. Science, 225, 473-478.

Burkhardt, D.A. (1970). Proximal negative response of frog retina. Journal of Neurophysiology, 33, 405-420.

Cajal, S. R. (1893). 'La retine des vertebres'. translated by D. Maguire & R.W. Rodieck. In R.W. Rodieck's (1973): The Vertebrate Retina. San Francisco: W. H. Freeman & Co.

Campbell, F.W. (1969). Trends in physiological optics.

In Proceedings of the International School of Physics <<Enrico Fermi>>. New York: Academic Press.

Campbell, F.W., & Robson, J.G. (1968). Application of Fourier analysis to the visibility of gratings. Journal of Physiology, 197, 551-566.

Chung, S.-H., Raymond, S.A., & Lettvin, J.Y. (1970). Multiple meaning in single visual units. Brain, Behavior and Evolution, 3, 72-101.

Citron, M.C., Kroeker, J.P., & McCann, G.D. (1981). Non-linear interactions in ganglion cell receptive fields. Journal of Neurophysiology, 46(6), 1161-1176.

Cleland, B.G., Dubin, M.W., & Levick, W.R. (1971). Sustained and transient neurones in the cat's retina and lateral geniculate nucleus. Journal of Physiology, 217, 473-496.

Cleland, B.G., & Levick, W.R. (1974). Properties of rarely encountered types of ganglion cell in the cat's retina and an overall classification. Journal of Physiology, 240, 457-492.

Dawis, S., Shapley, R., Kaplan, E., & Tranchina, D. (1984). The receptive field organization of X-cells in the cat: Spatiotemporal coupling and asymmetry. Vision Research, 24(6), 549-564.

Derrington, A. M. & Lennie, P. (1982). The influence of temporal frequency and adaptation level on receptive organization of retinal ganglion cells in cat. Journal of Physiology, 333, 343-366.

Donner, K. & Gronholm, M-L. (1984). Center and surround excitation in the receptive fields of frog retinal ganglion cells. Vision Research, 24(12), 1807-1819.

Dowling, J.E. (1968). Synaptic organization of the frog retina: an E.M. analysis comparing the retinas of frog and primates. Proceedings of the Royal Society of London - Series B (biological sciences), 170, 205-228.

Dowling, J.E. (1976). Physiology and morphology of the retina. In R. Llinas and W. Precht (eds), Frog Neurobiology, New York: Springer - Verlag.

Dubin, M.W. (1970). The inner plexiform layer of the vertebrate retina; a quantitative and comparative electron microscopic analysis. Journal of Comparative

Neurology, 140(4), 479-505.

Enroth-Cugell, C., & Robson, J.G. (1966). The contrast sensitivity of retinal ganglion cells of the cat. Journal of Physiology, 187, 517-552.

Fukada, Y. (1971). Receptive field organization of cat optic nerve fibers with special reference to conduction velocity. Vision Research, 11, 209-226.

Fukada, Y., & Stone, J. (1974). Retinal distribution and central projections of Y, X-, and W- cells of the cat's retina. Journal of Neurophysiology, 37, 749-772.

Gaze, R.M., & Jacobsen, M. (1963). Convexity detectors in the frog's visual system. Proceedings of the Physiological Society, 169, 1-3.

Gordon, J., & Graham, N. (1973). Early light and dark adaptation in frog on-off retinal ganglion cells. Vision Research, 13, 647-659.

Gordon, J., & Hood, D.C. (1976). Anatomy and physiology of the frog retina. In K.V. Fite (ed), The Amphibian Visual System. New York: Academic Press.

Gordon, J., & Shapley, R.M. (1978). Contrast sensitivity and spatial summation in frog and eel retinal ganglion cells. In J.C. Armington, J. Krauskopf, & B.R. Wooten (eds), Visual Psychophysics and Physiology. New York: Academic Press.

Gronholm, M.-L., & Reuter, T. (1981). Disinhibitory action of strychnine on ganglion cells in the retina of the frog. Vision Research, 21, 1649-1652.

Grusser, O. -J., & Grusser-Cornehls, U. (1968). Neurophysiologische Grundlagen visueller angeborener Auslosemechanismen beim Frosch. Zeitschrift fur Vergleichende Physiologie, 59, 1-24.

Grusser, O.-J., & Grusser-Cornehls, U. (1976). Neurophysiology of the anuran visual system. In R. Llinas & W. Precht (eds.), Frog Neurobiology. New York: Springer Verlag.

Grusser, O.-J., Grusser-Cornehls, U. & Licker, M.D. (1968). Further studies on the velocity function of movement detecting class-2 neurons in the frog retina. Vision Research, 8, 1173-1185.

Grusser-Cornehls, U., & Saunders, R. McD. (1981). Chromatic subclasses of frog retinal ganglion cells: studies using black stimuli moving on a monochromatic background. Vision research, 21, 469-478.

Grusser-Cornehls, U., Grusser, O.-J., & Bullock, T.H. (1963). Unit responses in the frog's tectum to moving and non-moving visual stimuli. Science, 141, 820-822.

Hartline, H.K. (1938). The response of single optic nerve fibers of the vertebrate eye to illumination of the retina. American Journal of Physiology, 121(2), 400-415.

Hartline, H.K. (1940a). The effects of spatial summation in the retina on the excitation of the fibers of the optic nerve. American Journal of Physiology, 130(4), 700-711.

Hartline, H.K. (1940b). The receptive fields of optic nerve fibers. American Journal of Physiology, 130(4), 690-699.

Henn, V., & Grusser, O.-J. (1968). The summation of excitation in the receptive field of movement sensitive neurons of the frog's retina. Vision Research, 9, 57-69.

Hochstein, S., & Shapley, R.M. (1976a). Quantitative analysis of retinal ganglion cell classifications. Journal of Physiology, 262, 237-264.

Hochstein, S., & Shapley, R.M. (1976b). Linear and nonlinear spatial subunits in Y cat retinal ganglion cells. Journal of Physiology, 262, 265-284.

Hood, D. C. & Gordon, J. (1981). The frog ganglion cell: not a feature detector and not a monkey cortical cell. Perception, 10, 421-422.

Hubel, D.H., & Wiesel, T.N. (1960). Receptive fields of optic nerve fibers in the spider monkey. Journal of Physiology, 154, 572-580.

Hughes, G.W., & Maffei, L. (1966). Retinal ganglion cell response to sinusoidal light stimulation. Journal of Neurophysiology, 29(3), 333-346.

Kaplan, E., Marcus, S., & So, Y. T. (1979). Effects of dark adaptation on spatial and temporal properties of receptive fields in cat lateral geniculate nucleus. Journal of Physiology, 294, 561-580.

Kaplan, E. & Shapley, R. M. (1982). X and Y cells in the LGN of macaque monkeys. Journal of Physiology, 330, 125-143.

Ikeda, H., & Wright, M.J. (1972). Receptive field organization of 'sustained' and 'transient' retinal ganglion cells which subserve different functional roles. Journal of Physiology, 227, 769-800.

Ingle, D. (1968). Visual releasers of prey-catching behavior in frogs and toads. Brain, Behavior and Evolution, 1, 500-518.

Ingle, D. (1971). Discrimination of edge orientation by frogs. Vision Research, 11, 1365-1367.

Katz, B., & Miledi, R. (1967). A study of synaptic transmission in the absence of nerve impulses. Journal of Physiology, 192, 407-436.

Kaufman, L. (1974). Sight and Mind: An Introduction to Visual Perception. New York: Oxford University Press.

Kolb, H. (1979). The inner plexiform layer in the retina of the cat: electron microscopic observations. Journal of Neurocytology, 8, 295-329.

Kolb, H., & Famiglietti, E.V. (1974). Rod and cone bipolar connections in the inner plexiform layer of the cat retina. Science, 186, 47-49.

Kolb, H., & Nelson, R. (1981). Amacrine cells of the cat retina. Vision Research, 21, 1625-1633.

Kolb, H., Nelson, R., & Mariani, A. (1981). Amacrine cells, bipolar cells and ganglion cells of the cat retina: a Golgi study. Vision Research, 21, 1081-1114.

Kuffler, S.W. (1953). Discharge patterns and functional organization of mammalian retina. Journal of Neurophysiology, 16, 37-68.

Lennie, P. (1980). Parallel visual pathways: a review. Vision Research, 20, 561-594.

Lettvin, J.Y., Maturana, H.R., McCulloch, W.S., & Pitts, W.H. (1959). What the frog's eye tells the frog's brain. Proceedings of the Institute of Radio Engineers, 47, 1940-1951.

Lettvin, J.Y., Maturana, H.R., Pitts, W.H., & McCulloch, W.S. (1961). Two remarks on the visual system of the frog. In W.A. Rosenblith (ed), Sensory Communication. New York: Wiley.

Levine, M.W., & Shefner, J.M. (1979). X-like and not X-like cells in goldfish retina. Vision Research, 19, 95-97.

Linsenmeier, R.H., Frishman, L.J., Jakiela, H.G., & Enroth-Cugell, C. (1982). Receptive field properties of X and Y cells in the cat retina derived from contrast sensitivity measurements. Vision Research, 22, 1173-1183.

Maffei, L., & Fiorentini, A. (1973). The visual c s a spatial frequency analyzer. Vision Research, 1255-1267.

Mastronarde, D. N. (1983). Correlated firing of cat retinal ganglion cells. I. Spontaneously active inputs to X- and Y- cells. Journal of Neurophysiology, 49(2), 303-324.

Maturana, H.R., & Frenk, S. (1963). Directional movement and horizontal edge detectors in the pigeon retina. Science, 142, 977-979.

Maturana, H.R., Lettvin, J.Y., McCulloch, W.S., & Pitts, W.H., (1960). Anatomy and physiology of vision in the frog (Rana pipiens). Journal of General Physiology, 43, 129-175.

Milkman, N., Shapley, R.M., & Schick, G. (1978). Experimental applications: a microcomputer-based visual stimulator. Behavior Research Methods and Instrumentation, 10(4), 539-545.

Moore, B.C.J. (1982). An Introduction to the Psychology of Hearing. (2nd ed). New York: Academic Press.

Muntz, W.R.A. (1962). Effectiveness of different colors of light in releasing positive phototactic behavior of frogs and a possible function of the retinal projection to the diencephalon. Journal of Neurophysiology, 25, 712-720.

Muntz, W.R.A. (1977). The visual world of the amphibia. In F. Crescitelli (ed), Handbook of Sensory Physiology (vii/5) - the Visual System in Vertebrates. New York: Springer-Verlag.

Nye, P.W., & Naka, K.-I. (1971). The dynamics of inhibitory interaction in a frog receptive field: a paradigm of paracontrast. Vision Research, 11, 377-392.

Orlans, F.B. (1977). Animal Care from Protozoa to Small Mammals. Menlo Park, Ca.: Addison-Wesley.

Pickles, J.O. (1988). An Introduction to the Physiology of Hearing. London: Academic Press.

Pomeranz, B. (1972). Metamorphosis of frog vision: changes in ganglion cell physiology and anatomy. Experimental Neurology, 34, 187-199.

Pomeranz, B., & Chung, S.-H. (1970). Dendritic tree anatomy codes form-vision physiology in tadpole retina. Science, 170, 983-984.

Reid, R.C., & Shapley, R.M. (1988). Complex temporal stimuli increase relative sensitivity of cat striate cortical neurons to high temporal frequencies. Investigative Ophthalmology and Visual Science, 29 (Suppl), 11.

Reuter, T., & Virtanen, K. (1972). Border and color coding in the retina of the frog. Nature, 239, 260-263.

Robson, J.G. (1975). Receptive fields: neural representation of the spatial and intensive attributes of the visual image. In E.C. Carterette and M.P. Friedman (eds), Handbook of Perception - Seeing. New York: Academic Press.

Rodieck, R.W., & Stone, J. (1965). Analysis of receptive fields of cat retinal ganglion cells. Journal of Neurophysiology, 28, 833-849.

Shapley, R.M., & Gordon, J. (1978). The eel retina: ganglion cell and spatial mechanisms. Journal of General Physiology, 71, 139-155.

Shapley, R.M., & Victor, J.D. (1978). The effect of contrast on the transfer properties of cat retinal ganglion cells. Journal of Physiology, 285, 275-298.

Shapley, R.M., & Victor, J.D. (1979). Nonlinear spatial summation and the contrast gain control of cat retinal ganglion cells. Journal of Physiology, 290, 141-161.

Shapley, R.M., & Victor, J.D. (1981). How the contrast gain control modifies the frequency responses of cat retinal ganglion cells. Journal of Physiology, 318, 161-179.

Stark, L., & Sherman, P.M. (1957). A servoanalytic study to consensual pupil reflex to light. Journal of Neurophysiology, 20, 17-26.

Stirling, R.V., & Merrill, E.G. (1987). Functional morphology of frog retinal ganglion cells and their central projections: The dimming detectors. The Journal of Comparative Neurology, 258, 477-495.

Stone, J., & Fukada, Y. (1974). Properties of cat retinal ganglion cells: a comparison of W-cells with X- and Y-cells. Journal of Neurophysiology, 37, 722-748.

Stone, J., & Hoffman, K.-P. (1972). Very slow conducting ganglion cells in the cat's retina: a major, new functional type? Brain Research, 43, 610-616.

Sur, M., & Sherman, M. (1982). Linear and nonlinear W cells in C-laminae of the cat's LGN. Journal of Neurophysiology, 47(5), 869-884.

Toyoda, J.-I. (1974). Frequency characteristics of retinal neurons in the carp. Journal of General Physiology, 63, 214-234.

Toyoda, J.-I., Hashimoto, H., & Ohtsue, K. (1973). Bipolar-amacrine transmission in the carp retina. Vision Research, 13, 295-307.

Tranchina, D. (1981). Systems analysis of the spatial and temporal properties of horizontal cells in the turtle retina. Unpublished doctoral dissertation, The Rockefeller University: New York.

Tranchina, D., Gordon, J., Shapley, R.M., & Toyoda, J.-I. (1981). Linear information processing in the retina : a study of horizontal cell responses. Proceedings of the National Academy of Science of the United States of America, 78(10), 6540-6542.

Tuttle, J.R., & Scott, L.C. (1978). X-like and Y-like ganglion cells in the necturus retina (tech report. no.78-2). University of Rochester, Center for Visual Sciences.

Victor, J.D., & Shapley, R.M. (1979). The nonlinear pathway of Y ganglion cells in the cat retina.

Journal of General Physiology, 74, 671-689.

Watanabe, M., Fukuda, Y., Hsiao, C.-F., & Ito, H. (1985). Electron microscopic analysis of amacrine and bipolar cell inputs on Y-, X-, and W-cells in the cat retina. Vision Research, 358, 229-240.

Werblin, F.S. (1972). Lateral interactions at inner plexiform layers of vertebrate retina: antagonistic responses to change. Science, 175, 1008-1010.

Werblin, F.S., & Copenhagen, D.R. (1974). Control of retinal sensitivity. III. Lateral interactions at the inner plexiform layer. Journal of General Physiology, 63, 88-110.

Werblin, F.S., & Dowling, J.E. (1969). Organization of the vertebrate retina: II. Intracellular recordings. Journal of Neurophysiology, 32, 339-355.